EFFICIENCY MEASURES OF SUPERABSORBENT POLYMERS AS INTERNAL CURING OF CEMENT PASTE

EFFICIENCY MEASURES OF SUPERABSORBENT POLYMERS AS INTERNAL CURING OF CEMENT PASTE

By
Sylvia Nicole Mihaljevic
M.Sc.

A Thesis Submitted to the School of Graduate
Studies in Partial Fulfilment of the Requirements for
the Degree

Doctor of Philosophy

McMaster University
Hamilton, Ontario, Canada
June 2021

Doctor of Philosophy (2021) (Civil Engineering)

McMaster University Hamilton, Ontario

TITLE:	Efficiency Measures of Superabsorbent Polymers as Internal Curing of Cement Paste
AUTHOR:	Sylvia Nicole Mihaljevic, M.Sc.
SUPERVISOR:	Dr. Samir E. Chidiac, PhD PEng FCSCE
NUMBER OF PAGES:	xvi, 150

Abstract

Mixes with lower water to cement (w/c) ratio and supplementary cementing materials produce strong and durable concrete. The consequence of lowering w/c is an increase in autogenous shrinkage (AS), which contributes to concrete cracking. Internal curing (IC) is shown to mitigate AS, however improper dosing of IC material can negatively affect the concrete properties. The effectiveness of IC material, such as superabsorbent polymer (SAP), depends on the 1) amount of water stored, 2) particle distribution, and 3) ability to deliver water. The objective of this research is to quantify the in-situ efficiency of SAP by investigating its effect on the cement chemical reaction using non-destructive testing methods, specifically isothermal calorimetry and nuclear magnetic resonance (NMR).

IC was tested with varying quantities of SAP in plain cement paste using white Portland cement and three w/c (0.30, 0.32, 0.35). Overdosing of the SAP material was found to significantly affect the hydration reaction and reduce the efficiency of the material. The initial porosity of the paste influences the ability of IC to provide water. However, the extra porosity provided by SAP needs to be considered when calculating the degree of hydration. Particle agglomeration occurs when the mass of SAP to IC water is greater than 5% and is the main factor causing loss of efficiency. A new geometric model was developed to estimate the SAP distribution within the cement paste. The model employs the SAP absorption determined by NMR and assumes that the SAP particles are spherical, of equal diameter, and individual particles absorb the same amount of pore solution. The results reveal that particle spacing increases with agglomeration and reduces the IC efficiency.

A hybrid 1-D finite element transient flow model was developed to reverse engineer the effective diffusion coefficient from the NMR water distribution. The gel solid volume fraction and its impedance to water transfer were accounted for through the cement degree of hydration and tortuosity factor, respectively. Model results reveal that the effective water diffusion coefficient depends on w/c, gel volume fraction, and tortuosity once the cement

gel fractions start to connect, i.e., after 20% cement degree of hydration. The diffusion length quantifies the distance water can transfer from the SAP to the cement paste.

Acknowledgements

I would like to thank my supervisor Dr. Samir Chidiac for the years of support and guidance. Thank you for all your patience and encouragement during this very long process. Without your expertise, mentorship, and inspiration I would never have reached this stage of my academic career. Thank you for seeing my potential and encouraging me to achieve it, even when I drove you crazy.

Thank you to my supervisory committee, Dr. Dieter Stolle and Dr. Michael Thompson, for your patience and guidance. I would like to acknowledge Dr. Gillian Goward of the Department of Chemistry and Chemical Biology for her generosity and expertise. My sincere gratitude to Dr. Sergey Krachkovskiy for his willingness to share his knowledge with me. I am very fortunate that you were so enthousiastic in assisting me with my experimental work. I would also like to thank the technical staff of the Applied Dynamics Laboratory, Kent Wheeler and Paul Heerema, for their assistance. To my fellow gradute students in the Department of Civil Engineering, thank you for the support and friendship. A special thank you to Mouna Reda for proofreading this thesis.

I would like thank the Natural Science and Engineering Research Council of Canada and the McMaster University Centre for Effective Design of Structures for the financial support. Also, thank you to BASF Construction Solutions, Germany for providing the SAP material.

Finally, I would like to express my love and deepest gratitude to my parents, Ane and Ranko, and my brother, Mark, for their endless support and encouragement. Without your love and guidance, I would not be the person I am today. To my late mother, I wish you were here to see my accomplishments and I hope I have made you proud.

Publication List

This thesis consists of the following papers:

Paper I

Mihaljevic, S.N., & Chidiac, S.E. (2021). Quantification of Internal Curing Efficiency – A Critical Review. To be submitted for publication.

Paper II

Chidiac, S.E., Mihaljevic, S.N., Krachkovskiy, S.A., & Goward, G.R. (2020). Characterizing the effect of superabsorbent polymer content on internal curing process of cement paste using calorimetry and nuclear magnetic resonance methods, Journal of Thermal Analysis and Calorimetry, 145(2), 437-449, doi:10.1007/s10973-020-09754-0.

Paper III

Chidiac, S.E. , Mihaljevic, S.N., Krachkovskiy, S.A., & Goward, G.R. (2021). Efficiency measure of SAP as internal curing for cement using NMR & MRI, Construction and Building Materials, 278 122365, doi:10.1016/j.conbuildmat.2021.122365.

Paper IV

Mihaljevic, S.N., & Chidiac, S.E. (2021). Effective free water diffusion coefficient of cement paste internally cured with superabsorbent polymers. Submitted to Journal of Building Engineering, Manuscript Number: JBE-D-21-02428

Co-Authorship

This thesis has been prepared in accordance with the regulations for a "Sandwich" thesis format or a compilation of papers stipulated by the Faculty of Graduate Studies at McMaster University and has been co-authored.

Chapter 2: Quantification of internal curing efficiency – A critical review
by S.N. Mihaljevic and S.E. Chidiac

S.N. Mihaljevic: Conceptualization of study; Investigation; Formal analysis; Writing original draft and editing. **S.E. Chidiac:** Conceptualization of study; Writing, reviewing & editing; Resources; Supervision.

Chapter 3: Characterizing the effect of superabsorbent polymer content on internal curing process of cement paste using calorimetry and nuclear magnetic resonance methods
S.E. Chidiac, S.N. Mihaljevic, S.A. Krachkovskiy, and G.R. Goward

S.E. Chidiac: Conceptualization of study and models development; Methodology for experimental program and analytical investigation; Writing, reviewing & editing; Resources; Supervision. **S.N. Mihaljevic:** Conceptualization of study and Methodology; Carried out the experimental work and data analysis; Formal analysis; Investigation; Model development; Writing original draft and editing. **S.A. Krachkovskiy:** Methodology: designed and carried out the NMR and MRI portion of the experimental work including data generation and analysis; Reviewed manuscript. **G.R. Goward:** Contributed to the development of the project; Reviewed manuscript; Resources.

Chapter 4: Efficiency measure of SAP as internal curing for cement using NMR & MRI
S.E. Chidiac, S.N. Mihaljevic, S.A. Krachkovskiy, and G.R. Goward

S.E. Chidiac: Conceptualization of study and models development; Methodology for experimental program and analytical investigation; Writing, reviewing & editing;

Resources; Supervision. **S.N. Mihaljevic:** Conceptualization of study and Methodology; Carried out the experimental work and data analysis; Model development; Writing original draft and editing. **S.A. Krachkovskiy:** Designed and carried out the NMR and MRI portion of the experimental work including data generation and analysis; Reviewed manuscript. **G.R. Goward:** Contributed to the development of the project; Reviewed manuscript; Resources.

Chapter 5: Effective free water diffusion coefficient of cement paste internally cured with superabsorbent polymers

by S.N. Mihaljevic and S.E. Chidiac

S.N. Mihaljevic: Conceptualization of study and Methodology; Model development; Validation; Writing original draft and editing. **S.E. Chidiac:** Conceptualization of study and models development; Methodology for analytical investigation; Writing, reviewing & editing; Resources; Supervision.

Table of Contents

List of Tables

List of Figures

1 Thesis Summary

1.1 Introduction

Owing to its strength, versatility, and durability, concrete is the most used construction material. Mehta and Monteiro [1] define durability as the "service life of a material under given environmental conditions" meaning that durable concrete must resist chemical attack, weathering, abrasion, cracking, and other forms of damage. Concerns for the durability of concrete structures have increased over the last two decades as the cost of maintenance and repair of existing structures during their lifetime now requires an additional investment of 40% of the total construction budget in developed countries [1]. Additionally, growing awareness of the environmental impact of mining natural resources and producing Portland cement for new concrete requires the production of durable concrete [1]. Since the 1970s, increased durability of concrete was achieved by the reduction of the water to cement ratio (w/c), development of chemical admixtures, and use of supplementary cementing materials (SCM) leading to the production of concrete with high strength and low permeability [1].

The unforeseen consequence of reducing the w/c, to increase strength and decrease porosity, resulted in concrete with the potential for autogenous shrinkage and associated cracking, which severely impairs the performance and longevity of the concrete [2–5]. Internal curing (IC) is the method with the greatest potential to reduce and/or prevent autogenous shrinkage; by providing water to the hydrating cement paste so that it does not experience self-desiccation [6–8]. For IC to achieve its full potential, the amount of water that can be stored and delivered by the IC material must be quantified and incorporated into the concrete in such a way that its efficiency can be measured.

This chapter outlines the impetus for the research and the objective of the thesis, followed by a brief description of the background information necessary for understanding this topic, focusing on the mechanism for autogenous shrinkage and internal curing, and the methods

to gauge the efficacy of the IC material. Additionally, the key contributions of each published paper are summarized, the main findings from this research study are highlighted and suggestions for future research are provided.

1.2 Impetus of Research

Internal curing is the most effective method in preventing early-age cracking of concrete caused by autogenous shrinkage [6–8]; however improper dosing of IC materials can have negative consequences on concrete's mechanical and durability properties [9,10]. Furthermore, when superabsorbent polymers (SAP) are used for IC, it is imperative that their absorption properties are determined for the specific conditions in which they will be used. The pore solution of hydrating cement paste has a variable concentration of ions in the first 48 h, which makes quantifying SAP absorption difficult [11]. The effectiveness of IC depends on three factors: the amount of water available [12–14], the distribution of IC material [15,16], and the ability of water to move from the IC material to the hydrating cement paste [16–18]. Additionally, agglomeration of SAP particles greatly reduces their ability to provide IC water, but it has not been establish to what extent [15,16]. Water desorption and water transport distance from SAP have not been fully quantified, both because of the difficulty in testing concrete at early stages of hydration and the SAP's sensitivity to the environment into which it is embedded [19]. A method to quantify the amount of water absorbed by SAP and its ability to release the water to the hydrating cement paste would allow more effective design of internally cured concrete. Furthermore, the water effective diffusion coefficient for early age cement paste with SAP and the corresponding average diffusion length can provide an estimate for how well IC material will perform.

1.3 Objective and Scope of Research

The primary goal of this research is to develop a method to quantify the in-situ efficiency of the IC of concrete through non-destructive testing methods. The efficiency of IC is quantified based on two primary factors: 1) effect of the internal curing on the hydration

reaction kinetics, and 2) the distance water can be transported from the internal curing material to the hydrating cement paste. Furthermore, the in-situ absorption and desorption properties of the SAP is used to quantify the appropriate dosage of the IC material. SAP particles tend to agglomerate which needs to be addressed to gauge the true efficiency of the material.

This research is limited to internal curing with one type of polyacrylate SAP in plain cement paste using white Portland cement and three total w/c ratios (0.30, 0.32, 0.35). Isothermal calorimetry and nuclear magnetic resonance (NMR) are employed as non-destructive test methods.

1.4 Background

1.4.1 Evolution of Concrete

The main factor for the development of concrete strength and durability is the w/c as it controls the porosity of the cement paste [1]. According to Powers' [20,21], full hydration of cement is obtained at w/c of 0.42. However, in traditional concrete excess water is needed to provide adequate workability of the concrete. In the 1970s, the development of the first generation of superplasticizer allowed for the reduction in the w/c closer to 0.42, which increased the strength of the concrete. At that time, any concrete with a compressive strength over 40 MPa was considered high strength concrete [1]. Since then, the production of more effective superplasticizer, the use of finer and more reactive cements, and the introduction of SCMs, especially silica fume, have allowed modern concretes to be produced with w/c as low as 0.25 and compressive strength greater than 100 MPa [22]. Concrete with a w/c of 0.45 can achieve a 28-day compressive strength of 38 MPa, while a concrete with a water to cementing material ratio (w/cm) of 0.31 and 10% silica fume can achieve a compressive strength of 83 MPa at 28-days [22]. Furthermore, porosity can be considered the controlling factor for durability, as it controls the ingress of water, aggressive ions, and carbon dioxide, which result in damage to the concrete from effects such as corrosion of reinforcement, sulfate attack, and carbonation [1]. By reducing the

w/c from 0.50 to 0.30 at 50% hydration, the capillary porosity decreases from 0.41 to 0.26 [1]. The production of high strength concrete (HSC), high performance concrete (HPC), and ultra-high-performance concrete (UHPC) has allowed for the construction of taller concrete structures, longer span concrete bridges, thinner structural elements, and better performance of structures in aggressive environments.

The consequence of reducing the w/c below 0.42 is that the pores of the cement paste are no longer saturated and quickly become disconnected, leading to self-desiccation. Self-desiccation manifests externally as autogenous shrinkage [5,23]. In traditional concrete very little autogenous shrinkage is observed, 40-60 micro-strain [24], whereas for HPC the autogenous shrinkage can be up to 1000 micro-strain for a w/c of 0.30 within the first 24 h of set [2]. Any restraint on the concrete can produce early age cracking, which leads to impaired mechanical properties, ingress of aggressive ions, and an unsightly appearance [25]. Restrained shrinkage stress showed that HPC with a w/cm of 0.33 experienced tensile stress up to 3 MPa, resulting in cracking after 6 days due to autogenous shrinkage [26].

1.4.2 Autogenous Shrinkage

The American Concrete Institute (ACI) defines autogenous shrinkage as the “change in volume due to the chemical process of hydration of cement, exclusive of effects of applied load and change in either thermal condition or moisture content” [27]. The chemical reaction between Portland cement and water is referred to as a hydration reaction that results in products with a smaller volume than the reactants. Chemical shrinkage produces the pore structure of the cement paste. When the w/c is less than 0.40, there is not enough free water to maintain saturation of the pore structure. When the saturation decreases below 100% a liquid-vapour meniscus under tension form in the pores and causes compression on the surrounding solid skeleton of the cement paste [28,29]. As the water is consumed by hydration, the internal capillary tension increases [28–30] and according to the Young-Laplace equation the capillary tension is calculated as

$$P_c = \frac{-2\gamma\cos(\theta)}{r} \quad (1.1)$$

in which P_c, γ, θ, and r are the capillary water pressure (Pa), the surface tension of pore fluid (N/m), the liquid–solid contact angle (radians), and the meniscus radius of curvature (m), respectively. The curvature of the meniscus is assumed to be equal to the radius of the largest saturated pore. As the hydration reaction proceeds, subsequently smaller pores are emptied which causes an increase in pressure [4,30]. Furthermore, Kelvin's equation relates the internal equilibrium relative humidity (RH) to the capillary pressure by

$$P_c = \frac{\ln(RH)\,RT}{V_m} \quad (1.2)$$

in which R, T and V_m are respectively, the universal gas constant (8.314 J/mol K), the temperature (°K), and the molar volume of pore solution (~18×10^{-6} m^3/mol). Under sealed conditions the RH in low w/c concrete ranges from 85 to 90% [31] and the hydration reaction stops as the RH reaches approximately 80% [32]. Assuming circular pores, Mackenzie's equation correlates the capillary pressure to autogenous shrinkage (ε) in cement paste, where

$$\varepsilon = \frac{S\Delta P}{3}\left(\frac{1}{K} - \frac{1}{K_s}\right) \quad (1.3)$$

in which S, K, and K_s are the cement paste degree of saturation, the paste bulk modulus (Pa) and the bulk modulus of the solid skeleton of the cement paste (Pa), respectively [4].

The factors that affect the mechanism of autogenous shrinkage include pore size, pore connectivity, RH, degree of hydration, and self-stress [28]. Based on Eq. (1.1) and (1.3), the autogenous shrinkage is inversely proportional to the pore size, therefore smaller pores cause higher shrinkage. As the saturation of the pores decreases the RH decreases and, according to Eq. (1.2) and (1.3), because autogenous shrinkage is proportional to ln(RH), it also increases [4,33–35].

Wu et al. [28] identified w/c, cement composition and fineness, SCM content, aggregates, chemical admixtures, and curing to be the main factors determining the extent of autogenous shrinkage. The most significant factor that affects autogenous shrinkage is the w/c. While any concrete with a w/c less than 0.40 may experience autogenous shrinkage, further reduction in w/c increases the shrinkage significantly due to the lack of available free water [5,21]. Cement with higher fineness results in higher autogenous shrinkage caused by the increase in rate of hydration which rapidly decreases the RH [2] and refines the pore microstructure [36]. SCMs, especially silica fume, significantly increase autogenous shrinkage [37–40], by refining of the pores and consuming portlandite (CH) [28].

1.4.3 Internal Curing

Capillary suction pressure develops when subsequently smaller pores are emptied as water is consumed by hydration; this pressure increase provides the driving force required to pull water out of the internal curing reservoirs. Capillary pressure empties pores of water from largest to smallest [4,30,41], according to Richard's equation [42], and simultaneously the pores size becomes smaller as hydration product forms within the pores [43,44]. Therefore, the large pores of the IC material empty first and maintain a high saturation in the cement paste minimizing capillary pressure [4].

To determine the amount of water that can be provided by internal curing, Powers' model was extended. The entrained water, $(w/c)_{IC}$, that is needed to achieve maximum hydration is: [21]

$$(w/c)_{IC} = 0.18(w/c) \qquad \text{for } w/c < 0.36 \tag{1.4}$$

$$(w/c)_{IC} = 0.42 - (w/c) \qquad \text{for } 0.36 < w/c < 0.42 \tag{1.5}$$

The theoretical maximum degree of hydration (α_{max}), when $(w/c)_{IC}$ is provided, can be estimated according to:

$$\alpha_{max} = \frac{(w/c)}{0.36} \qquad \text{for } w/c < 0.36 \tag{1.6}$$

$$\alpha_{max} = 1 \qquad \text{for } 0.36 < w/c < 0.42 \tag{1.7}$$

If the w/c is less than 0.36, complete hydration cannot be achieved because there is not enough space for more hydration product to form. The total w/c of internally cured cement paste is the original w/c plus $(w/c)_{IC}$. However, the mechanical properties should be based on the original w/c, since it determines the porosity of the paste [21].

The dosage of IC material is critical to its success as a water entraining agent. Improper dosing of the IC material may have the following consequences: loss of workability [45–47], insignificant mitigation of autogenous shrinkage [9,10], reduction in compressive strength and other mechanical properties [9,48,49], as well as difficulty in predicting the behaviour of concrete [50].

1.4.4 Internal Curing Materials

The two prevalent internal curing materials are lightweight aggregates (LWA) and superabsorbent polymers (SAP) since both materials can absorb large quantities of water and release it to the hydrating cement paste.

1.4.4.1 Lightweight aggregate

LWA are a class of aggregate with a high porosity, such as pumice. LWA are added pre-saturated to the concrete mixture and dosed according to the equation developed by Bentz and Snyder [51]:

$$M_{LWA} = \frac{c \cdot CS \cdot \alpha_{max}}{\varphi_{LWA} \cdot S} \tag{1.8}$$

where c is cement content (kg/m^3), CS is the chemical shrinkage of cement (ratio of the mass of water to the mass of cement), α_{max} is the expected maximum degree of hydration, φ_{LWA} is the amount of water absorbed by the LWA (ratio of the mass of water to the mass of dry aggregate), and S is the degree of saturation of the aggregate.

The efficiency of LWA for IC depends on the pore structure, particle size, water absorption, and paste-aggregate proximity. For these reasons, fine LWA has generally been more successful in internal curing than coarse LWA [51,52]. However, it was found that the finest LWA were not very efficient, because the pores were also smaller making it more difficult for the water to be removed. LWA with a particle size of 2 to 4 mm was found to be optimal [3,52]. One of the problems with using LWA for internal curing is that it is difficult to achieve saturated conditions. After 5 days immersion at room temperature, only 9 to 14% saturation of pumice was observed [8].

When LWA was added, the compressive strength of concrete decreased with the increase in IC content and/or size of LWA. In some cases, it was found that while the 7-day compressive strength was lower with LWA, the 28 day compressive strength was comparable to the concrete mix without LWA [8,23,53].

1.4.4.2 Superabsorbent polymers

Superabsorbent polymers (SAP) are a special class of hydrophilic polymer that can absorb and retain large quantities of water within their structure [54]. The most common SAPs are covalently cross-linked polyacrylates and copolymerized polyacrylamides/polyacrylates [54] in the size range 50 to 250 μm [55]. Osmotic pressure is the driving force for SAP absorption, so absorption is highly dependent on the ionic concentration of a solution [54]. As the ionic concentration increases the ability for SAP to absorb the solution decreases [54]. In particular for cement pore solution, SAP is sensitive to the presence of calcium ions [19,56]. The concentration of anionic functional groups and the density of the covalent crosslinks in the SAP structural matrix determine its ability to imbibe water [57]. For SAP, the internal curing dosage is determined by:

$$ {}^{w}/_{c} = ({}^{w}/_{c})_{p} + ({}^{w}/_{c})_{IC} = ({}^{w}/_{c})_{p} + K\left({}^{SAP}/_{c}\right) \quad (1.9) $$

Where K is the average absorption of SAP and the total amount of water for the reaction consist of the initial water in the paste with IC, $({}^{w}/_{c})_{p}$, and the entrained water in the SAP, $({}^{w}/_{c})_{IC}$ [13,46].

Due to their fast absorption capability, SAP are generally added dry to the concrete mixture, so that they absorb part of the mixing water [46,58]. The amount of water that can be absorbed during mixing is often difficult to quantify and current standards for natural aggregates do not apply [59]. It is difficult to estimate the absorption capacity of SAP in concrete owing to their sensitivity to ions and the high and variable ion concentration of cement pore solution. Incorrect dosage can result in the misinterpretation of the results. Overestimation of the amount of water absorbed from the mix water results in a higher w/c ratio of the concrete leading to lower strength. Underestimation results in too much water being absorbed from the concrete mixture, thereby reducing the workability [59].

The complete elimination of autogenous shrinkage was observed with a SAP addition of 0.6% by weight of cement for a w/c of 0.30 [58,60]. For concrete with w/c of 0.34 and silica fume the demand for IC increased to 0.5 and 0.7% SAP by weight of cement; however shrinkage was still observed because of silica fume, which makes the paste denser [61]. Monnig and Lura [62] found no difference in compressive strength with 0.4% SAP, however the tensile strength decreased as much as 20%. At a SAP content of 0.7% the compressive strength was 12% lower than for the concrete without SAP. Jones and Weiss [63] found comparable strength between the reference and the SAP concrete, although the SAP concrete had a slightly lower strength. From these results it can be concluded that with SAP replacement values greater than 0.4% by weight of cement there will be some reduction in the strength of concrete.

Some problems that have been identified with SAP are: segregation [58], agglomeration when SAP is added pre-wetted [46], an increased need for superplasticizer [62], and decrease in strength, especially tensile strength. Moreover, it is difficult to quantify the amount of water that is absorbed by SAP [59].

1.4.5 Nuclear Magnetic Resonance

NMR has shown potential as a non-destructive method to analyze water distribution in cement paste [64–66]. For testing cement paste the hydrogen atom is excited and the spin-spin relaxation time, T_2, and its corresponding intensity are recorded. T_2 measurements allow for the classification of different water phases in the cement paste, where chemically and physically bound water have shorter relaxation time than capillary water [11]. For Portland cement, NMR signal is differentiated for four types of water: capillary water with $T_2 \cong 0.9$ ms, gel water with $T_2 \cong 0.25$ ms, interlayer water with $T_2 \cong 0.09$ ms, and CSH solid with $T_2 \cong 0.015$ ms [67]. When IC is added to the mixture, an additional signal was observed for the SAP water with T_2 ranging from 100 to 1000 ms [68]. NMR relaxometry tests on IC with SAP have shown that the release of water from the IC material correlates with an increase in the cement hydration over 2 days [11,69]. Another study found that, for the first 30 min, SAP absorbs water from the cement paste then begins to release water 5 h later [70]. Of particular interest is the possibility of using NMR to analyse the water transport of IC water. Preliminary work by Friedemann et al. [11] found that the self-diffusion coefficient of cement paste with 0.3 w/c was $5x10^{-10}$ m^2/s after 10 h and they estimate an average diffusion length of 5 mm.

1.4.6 Efficiency of SAP as Internal Curing

Internal curing is considered effective if it mitigates autogenous shrinkage [49], however there is no consensus about how much SAP IC material produces the best concrete. While an IC material may be able to eliminate autogenous shrinkage, it may have unintended consequences such as reduced compressive strength and loss of workability [46,58]. Therefore, efficient dosage of SAP must eliminate autogenous shrinkage without compromising the mechanical properties of cement while minimizing the amount of IC material needed. Three factors have been identified to determine the efficiency of SAP IC: 1) the amount of water it can provide, 2) its ability to release water, and 3) its distribution throughout the paste [71]. Absorption is determined based on the SAP material properties, specifically the concentration of covalent crosslinking density and concentration of anionic

functional groups [57], which determine the SAPs ability to swell and sensitivity to ions in the pore solution. Testing the absorption is difficult because of variable concentration of ions in the cement pore solution and interstitial water between SAP particles, however methods exist to determine the absorption in simulated pore solution [72,73]. The desorption of SAP is both a property of the SAP anion concentration [56] and pore size and connectivity of capillary pores in the cement paste [19]. The desorption is more difficult to effectively quantify as it must be observed continuously and because it depends on the behaviour of the cement paste and the nature of the SAP [11,57]. Some work with NMR has shown how SAP water content varies with time [11]. The distribution of SAP and the water transport from the SAP has not been quantified, but would provide a good measure of how well SAP is able to provide water to all locations in the hydrating cement paste [11,71].

1.5 Summary of Papers

Paper I: Quantification of Internal Curing Efficiency – A Critical Review

(To be submitted for publication)

In this paper the factors affecting the autogenous shrinkage are related to the properties that determine effective internal curing of HPC. The mechanism of autogenous shrinkage can be quantified based on the theory of capillary tension [28,29]. It is governed by pore size, pore connectivity, RH, degree of hydration, and self-stress [28]. The properties of the concrete mix design which influence the amount of autogenous shrinkage potential have been identified as w/c, cement composition and fineness, SCM content, aggregates, chemical admixtures, and curing [28]. Internal curing is the main method used to limit or eliminate autogenous shrinkage. IC works on the basis that the first pores to empty are large pores, so the pores that are emptied are in the IC material. By ensuring a higher degree of saturation in the pores of the cement paste the capillary tension is limited [4,30,41]. Three key factors to effective IC are: 1) the amount of water available in the IC material [12–14], 2) the distribution of IC material [15,16], and 3) the ability of water to move from the IC material to the hydrating cement paste [16–18]. The first factor depends on the

absorption kinetics of the IC material and, especially, in the case of SAP may be difficult to quantify. The second factor is highly dependent on the agglomeration of SAP particles, which can be significant for SAP, especially if they are added pre-saturated to the concrete mixture. Agglomeration of SAP leads to uneven distribution of IC water [15,16]. While agglomeration is of great concern there is little information in the literature about how to prevent or quantify it. The third factor is the most critical, yet it is not fully quantified due to the difficulty of continuously testing the hydrating cement paste [19]. Non-destructive testing, such as NMR, appears promising in increasing the knowledge about water movement through cement pastes.

Paper II: Characterizing the effect of superabsorbent polymer content on internal curing process of cement paste using calorimetry and nuclear magnetic resonance methods

(Published in Journal of Thermal Analysis and Calorimetry, May 2020)

In this paper the effect of IC with SAP on the kinetics of the cement hydration reaction are characterized using isothermal calorimetry. Furthermore, the amount of water SAP can provide for IC, which has been an ongoing area of research, is quantified by comparing the behaviour of cements with and without SAP using isothermal calorimetry and NMR. Extensive statistical analysis was performed to determine the effect of SAP dosage on the kinetics of the hydration reaction. Improper dosage of SAP is of critical concern. Overdosing results in a significant decrease in the heat of hydration (HOH) of the reaction, which is directly proportional to the degree of hydration of the cement and the strength development of the paste. Providing more SAP at the same water content does not provide more efficient internal curing. The total w/c of IC pastes is determined by $^{w}/_{c} = (^{w}/_{c})_{p} + (^{w}/_{c})_{IC} = (^{w}/_{c})_{p} + K(^{SAP}/_{c})$. Where the w/c of the paste, $(^{w}/_{c})_{p}$, is critical for determining the kinetics to the hydration reaction. There was no statistically significant correlation between the HOH and w/c. A strong linear relationship exists between HOH and initial porosity, which is a function of $(^{w}/_{c})_{p}$. The rate of the reaction is linearly related to the total w/c since the reaction is dependent on the total amount of water available

from both the paste and SAP. The amount of entrained water was found to be proportional to the resulting HOH and the initial porosity of the paste. The efficiency of the SAP IC was calculated based on idealized spacing and w/c of the paste. No improvement to the reaction was observed with more SAP particles, which suggests that there is agglomeration of SAP thereby increasing the spacing between the particles. The amount and behaviour of agglomerated particles is not readily available in the literature and is identified as a critical factor that needs further study.

Paper III: Efficiency measure of SAP as internal curing for cement using NMR & MRI

(Published in Construction and Building Materials, April 2021)

In this paper NMR with magnetic resonance imaging (MRI) was used to quantify the absorbed and desorbed water by SAP and the efficiency of SAP as internal curing. NMR T_2 time was used to characterize the water within the cement paste into three phases: gel water, capillary water, and IC water within the SAP. NMR water signal intensity was related to isothermal calorimetry data to provide a method to quantify the degree of hydration. It was determined that as SAP releases water and shrinks it provides extra porosity for the formation of hydration product. The extra porosity needs to be considered when calculating the degree of hydration of cement paste internally cured with SAP. From this study, a geometric model was developed to estimate the efficiency of SAP as IC in cement paste. The model assumes that the SAP particles are spherical, of equal diameter, and that all particles absorb the same amount of pore solution. The distribution of SAP particles was determined based on the signal intensity of the SAP water. The amount of SAP was then used to determine the efficiency of the IC based on the spacing and potential for SAP particle agglomeration. Theoretically, as the distance between the SAP decreases, the degree of hydration should increase because cement particles have a shorter access distance to the IC water. SAP particle agglomeration results in an increase in the spacing, consequently reducing the efficiency of the IC material. Therefore, increasing the dosage

can result in a decrease in the efficiency of SAP as an IC material when the amount of entrained water is kept constant.

Paper IV: Effective free water diffusion coefficient of cement paste internally cured with superabsorbent polymers

(Submitted for publication in Journal of Building Engineering, May 2021)

The ability of SAP to act as an effective IC material depends on the distribution of the SAP and amount of the cement paste that has access to the IC water. To determine the distance IC water can travel from the IC material a model, comprised of analytical and phenomenological components, was developed to estimate the free water diffusion coefficient. The diffusion coefficient was then used to calculate an average diffusion length. The hybrid model employs a 1-D finite element transient flow model using the temporal and spatial distribution of water from NMR-MRI experiments to reverse engineer the effective diffusion coefficient of the paste. The model inputs are the free and chemically bound water content. It is assumed that SAP particles are spherical, water transport is diffusion controlled, transport is spherically symmetric perfect contact between the SAP and the cement paste, boundary halfway between SAP particles does not allow water transfer, and water movement is impeded by cement gel hydrate formation. A tortuosity factor accounts for the impedance to water mobility created by the formation of hydration products. It is a function of the solid volume fraction, which is a function of degree of hydration and w/c. As the gel structure begins to connect, at approximately 20% degree of hydration, the ability of the water to move through the cement paste is hindered. The effective diffusion coefficient is a function of the paste w/c. The paste with a lower w/c has a lower diffusion coefficient. The effective diffusion coefficient is equal to the free water diffusion coefficient multiplied by the tortuosity factor. The diffusion length, $l_d = \sqrt{D_w^e t}$, is an effective way to determine the distance IC water can be transferred to the cement paste. The diffusion length shows that the paste with the higher w/c can provide water to a larger amount of the cement paste. It agrees with Powers' model stating that there is a limit to the amount of curing that can be provided based on the porosity of the paste. As noted

in paper II and III, agglomeration is critical in determining the efficiency of SAP as an IC material. This paper considered agglomeration by comparing the diffusion length and the spacing between particle with and without agglomeration.

1.6 Conclusions

Paper I characterizes the factors that affect autogenous shrinkage and internal curing. A critical review of the parameters influencing the efficiency of internal curing revealed the following:

1. The amount of autogenous shrinkage concrete will experience depends on the pore size, pore connectivity, RH, degree of hydration, and self-stress. These factors are a direct consequence of the concrete mix design (w/c, cement composition and fineness, SCM content, aggregates, and chemical admixtures).
2. Effective IC depends on 1) the amount of water in the IC material, 2) the distribution of IC material, and 3) the ability of water to move from the IC material.
3. The amount of IC water in SAP depends on the water absorption kinetics and efficiency. The absorption of SAP depends on the SAP's covalent crosslinking density and concentration of anionic functional groups as well as the concentration of ions in the pore solution of the cement paste.
4. SAP particles are susceptible to agglomeration which greatly reduces their efficiency. Agglomeration has not been quantified in the literature.
5. SAP water desorption is a function of the anion concentration in the SAP, the size and interconnectivity of the cement paste pores, and the interface between the SAP and cement paste.
6. The water desorption and distance water can travel from IC material has not been fully quantified.

Paper II compares cement pastes internally cured with varying doses of SAP. The following conclusions can be drawn:

7. The higher the amount of IC the more susceptible the cement paste became to SAP overdosing, which is characterized by a decrease in the total heat of hydration.

8. The HOH of the cement paste with IC was not equal to that of the reference paste even if the ideal SAP dosage was used.
9. The HOH is linearly related to the w/c for the reference pastes. There is no correlation between the total w/c and the HOH of the IC pastes.
10. The HOH is related to the w/c of the paste with IC. The initial porosity of the paste significantly influences the ability of IC to provide water.
11. A significant loss of IC efficiency is observed when the SAP is overdosed, and it is especially detrimental at higher levels of IC. This highlights the critical need to accurately estimate SAP water absorption.
12. SAP particle agglomeration occurs when the mass of SAP to that of entrained water is greater than 5%. Agglomeration is a key factor that needs to be addressed when evaluating the efficiency of IC with SAP.

Paper III compares the efficiency of SAP IC using NMR-MRI. The study revealed the following:

13. At constant w/c, the desorption rate decreases with increasing SAP content.
14. Water desorption and desorption rate for SAP were quantified using $e^{I_{SAP}} = Ct^A$ and $\dot{I}_{SAP} = A/t$, respectively.
15. The well-known cement hydration rate equation fits the rate of gel formation for cement paste with SAP IC: $I_{gel} = I_{gel_u} exp\left[-(\tau/t)^{\beta}\right]$.
16. After 48 h of casting, the capillary pore structure of mixes with SAP was statistically different than for mixes without SAP, which confirms that SAP content affects the pore structure.
17. Increasing the amount of SAP, while keeping the total w/c constant, prolongs the availability of SAP water, however the distribution and quantity are substantially inconsistent along the height of the sample.
18. The postulated geometric model affords the quantification of:
    a. Number of particles: $N_i = \frac{I_{SAP} V_{w_i} V_{layer}}{\frac{\pi}{6} \varphi_{sat}{}^3}$,
    b. Particle spacing: $s_i = \sqrt[3]{\frac{V_{layer}}{N_i}}$,

c. Efficiency of SAP as IC: $\eta_{IC} = \frac{\alpha_i/N_i}{\alpha_{ideal}/N_{ideal}}$,

d. Efficiency of SAP with particle agglomeration: $\eta_{agg} = \frac{N_{i_{effective}}}{N_i}$

Paper IV A hybrid model was developed to quantify the effective diffusion coefficient of cement pastes with SAP internal curing by way of NMR-MRI measurements. Accordingly, the following conclusions are drawn for this study:

19. The free water diffusion coefficient, D_o, depends on the w/c once the cement gel fractions start to connect, i.e., after 20% cement degree of hydration.
20. The effective water diffusion coefficient, D_w^e, depends on the w/c, cement gel volume fraction, and tortuosity once the cement gel fractions start to connect, i.e., after 20% cement degree of hydration.
21. The equation developed for SAP is given by $D_w^e = f_\tau D_o = [3(1-V_s)^2/(3-V_s)]D_o$.
22. Values of D_w^e confirm that water's ability to flow from the SAP particles to the cement paste depends on the porosity and tortuosity of the paste.
23. The SAP water diffusion length, $l_d = \sqrt{D_w^e t}$, provides a useful method to quantify the ability of IC to provide water in cement paste.
24. The results support Powers' model that the amount of water available for internal curing is limited by the porosity of the paste.
25. The effect of agglomeration is characterized by the amount of cement paste with access to IC water. The paste volume with accessible SAP water was severely reduced with SAP particle agglomeration.

The work of this research project shows that the porosity, as a function of the paste w/c, is a critical factor for water transfer from the SAP to the hydrating cement paste. Furthermore, this work provides a tool to determine the efficiency of SAP based on its effect on the degree of hydration, heat of hydration, and/or the water diffusion length. Agglomeration has been determined to be a key factor in the efficacy of SAP to provide IC water and it is a factor that will need to be addressed in practice when this material is used. It must be

emphasized that the experimental data and conclusions are specific to the type and size of SAP, as well to the cement paste mix composition.

1.7 Suggestions for Future Work

- This study employed one type and size of SAP particle; further research is needed into the efficiency of different SAP types as the properties of different SAP types can vary greatly.
- The models could be expanded to account for varying sizes and amount of water absorbed per SAP particle.
- SCMs reduce the porosity of the cement paste and are an important constituent of HPC. Therefore, a study on the effect of SCM on the efficiency of IC is needed using the water diffusion length.
- Agglomeration has been shown to significantly affect the efficiency of IC, however further study is needed to determine methods to prevent or reduce agglomeration of SAP in cement paste.
- The porosity of the paste is a significant factor in the ability of water to transfer through the cement paste. Experimental analysis using MIP to determine the pore size distribution would greatly enhance the predictive capacity of the diffusive length model.
- The NMR-MRI technique is a very promising approach to quantify the distance water distributes from an internal curing source. Refinement of the technique would reduce the variability observed in the results. Improvement of the technique would require shorter time intervals between data collection and thinner paste layers. Furthermore, resolving the image into two dimensions would allow for a more accurate representation of the SAP distribution.
- A study of the techniques presented here needs to be combined with measurements of autogenous shrinkage and other imaging techniques to fully quantify the efficacy of the IC material.

- A comprehensive study of the internal curing in concrete is needed to assess the added tortuosity instilled by the addition of fine and coarse aggregate.

References

[1] P.K. Mehta, P.J.M. Monteiro, Concrete: Microstructure, Properties, and Materials (4th Edition), McGraw-Hill Education, New York, 2014. https://www.accessengineeringlibrary.com/content/book/9780071797870 (accessed May 19, 2021).

[2] E. ichi Tazawa, S. Miyazawa, Influence of cement and admixture on autogenous shrinkage of cement paste, Cem. Concr. Res. 25 (1995) 281–287. doi:10.1016/0008-8846(95)00010-0.

[3] B. Akcay, M.A. Tasdemir, Optimisation of using lightweight aggregates in mitigating autogenous deformation of concrete, Constr. Build. Mater. 23 (2009) 353–363. doi:10.1016/j.conbuildmat.2007.11.015.

[4] R. Henkensiefken, D. Bentz, T. Nantung, J. Weiss, Volume change and cracking in internally cured mixtures made with saturated lightweight aggregate under sealed and unsealed conditions, Cem. Concr. Compos. 31 (2009) 427–437. doi:10.1016/j.cemconcomp.2009.04.003.

[5] P.C. Aïtcin, The durability characteristics of high performance concrete: A review, Cem. Concr. Compos. (2003). doi:10.1016/S0958-9465(02)00081-1.

[6] D.M. Al Saffar, A.J.K. Al Saad, B.A. Tayeh, Effect of internal curing on behavior of high performance concrete: An overview, Case Stud. Constr. Mater. 10 (2019) e00229. doi:10.1016/j.cscm.2019.e00229.

[7] D.P. Bentz, W.J. Weiss, Internal Curing : A 2010 State-of-the- Art Review, Gaithersburg: US Department of Commerce. National Institute of Standards and Technology, 2011.

[8] P. Lura, D.P. Bentz, D.A. Lange, K. Kovler, A. Bentur, Pumice aggregates for internal water curing, in: Int. RILEM Symp. Concr. Sci. Eng. A Tribut. to Arnon Bentur, 2004: pp. 137–151.

[9] G.R. de Sensale, A.F. Goncalves, Effects of fine LWA and SAP as internal water curing agents, Int. J. Concr. Struct. Mater. 8 (2014) 229–238. doi:10.1007/s40069-014-0076-1.

[10] D. Shen, X. Wang, D. Cheng, J. Zhang, G. Jiang, Effect of internal curing with super absorbent polymers on autogenous shrinkage of concrete at early age, Constr. Build. Mater. 106 (2016) 512–522. doi:10.1016/j.conbuildmat.2015.12.115.

[11] K. Friedemann, F. Stallmach, J. Kärger, NMR diffusion and relaxation studies during cement hydration-A non-destructive approach for clarification of the mechanism of internal post curing of cementitious materials, Cem. Concr. Res. 36 (2006) 817–826. doi:10.1016/j.cemconres.2005.12.007.

[12] L. Montanari, P. Suraneni, W.J. Weiss, Accounting for Water Stored in Superabsorbent Polymers in Increasing the Degree of Hydration and Reducing the Shrinkage of Internally Cured Cementitious Mixtures, Adv. Civ. Eng. Mater. 6 (2017) 20170098. doi:10.1520/ACEM20170098.

[13] S.E. Chidiac, S.N. Mihaljevic, S.A. Krachkovskiy, G.R. Goward, Characterizing the effect of superabsorbent polymer content on internal curing process of cement paste using calorimetry and nuclear magnetic resonance methods, J. Therm. Anal. Calorim. (2020) 1–13. doi:10.1007/s10973-020-09754-0.

[14] S.-H.H. Kang, S.-G.G. Hong, J. Moon, Absorption kinetics of superabsorbent polymers (SAP) in various cement-based solutions, Cem. Concr. Res. 97 (2017) 73–83. doi:10.1016/j.cemconres.2017.03.009.

[15] S. Mönnig, Superabsorbing additions in concrete: applications, modelling and comparison of different internal water sources, Institut für Werkstoffe im Bauwesen der Universität Stuttgart, 2009.

[16] S.E. Chidiac, S.N. Mihaljevic, S.A. Krachkovskiy, G.R. Goward, Efficiency measure of SAP as internal curing for cement using NMR & MRI, Constr. Build. Mater. 278 (2021) 122365. doi:10.1016/j.conbuildmat.2021.122365.

[17] M. Wyrzykowski, P. Lura, F. Pesavento, D. Gawin, Modeling of Water Migration during Internal Curing with Superabsorbent Polymers, J. Mater. Civ. Eng. 24 (2012)

1006–1016. doi:10.1061/(ASCE)MT.1943-5533.0000448.

[18] D. Snoeck, L. Pel, N. De Belie, The water kinetics of superabsorbent polymers during cement hydration and internal curing visualized and studied by NMR, Sci. Rep. 7 (2017) 1–14. doi:10.1038/s41598-017-10306-0.

[19] P. Lura, K. Friedemann, F. Stallmach, S. Mönnig, M. Wyrzykowski, L.P. Esteves, Kinetics of water migration in cement-based systems containing superabsobent polymers, in: Appl. Super Absorbent Polym. Concr. Constr., Springer Netherlands, Dordrecht, 2012: pp. 21–37. doi:10.1007/978-94-007-2733-5_4.

[20] T.C. Powers, A discussion of cement hydration in relation to the curing of concrete, in: Proc. Twenty-Seventh Annu. Meet. Highw. Res. Board, Highway Research Board, Washington, D.C., 1948: pp. 178–188.

[21] O.M. Jensen, P.F. Hansen, Water-entrained cement-based materials: I. Principles and theoretical background, Cem. Concr. Res. 31 (2001) 647–654. doi:10.1016/S0008-8846(01)00463-X.

[22] A.M. Neville, Properties of Concrete (5th edition), (2012).

[23] D. Cusson, T. Hoogeveen, Internal curing of high-performance concrete with pre-soaked fine lightweight aggregate for prevention of autogenous shrinkage cracking, Cem. Concr. Res. 38 (2008) 757–765. doi:10.1016/j.cemconres.2008.02.001.

[24] K. Van Breugel, N. Van Tuan, Autogenous shrinkage of HPC and ways to mitigate it, in: Key Eng. Mater., Trans Tech Publications Ltd, 2015: pp. 3–20. doi:10.4028/www.scientific.net/KEM.629-630.3.

[25] P. Lura, O.M. Jensen, J. Weiss, Cracking in cement paste induced by autogenous shrinkage, Mater. Struct. Constr. 42 (2009) 1089–1099. doi:10.1617/s11527-008-9445-z.

[26] A. Bentur, S.I. Igarashi, K. Kovler, Prevention of autogenous shrinkage in high-strength concrete by internal curing using wet lightweight aggregates, Cem. Concr. Res. 31 (2001) 1587–1591. doi:10.1016/S0008-8846(01)00608-1.

[27] ACI Standards, ACI, ACI Concrete Terminology, Farmington Hills, 2013. www.concrete.org.

[28] L. Wu, N. Farzadnia, C. Shi, Z. Zhang, H. Wang, Autogenous shrinkage of high performance concrete: A review, Constr. Build. Mater. 149 (2017) 62–75. doi:10.1016/j.conbuildmat.2017.05.064.

[29] P. Lura, O.M. Jensen, K. van Breugel, Autogenous shrinkage in high-performance cement paste: An evaluation of basic mechanisms, Cem. Concr. Res. 33 (2003) 223–232. doi:10.1016/S0008-8846(02)00890-6.

[30] H. Ye, A. Radlińska, A review and comparative study of existing shrinkage prediction models for Portland and non-Portland cementitious materials, Adv. Mater. Sci. Eng. 2016 (2016) 1–13. doi:10.1155/2016/2418219.

[31] D.P. Bentz, P. Lura, J.W. Roberts, Mixture proportioning for internal curing, Concr. Int. 27 (2005) 35–40.

[32] K. Kovler, S. Zhutovsky, Overview and future trends of shrinkage research, in: Mater. Struct. Constr., 2006. doi:10.1617/s11527-006-9114-z.

[33] J. Zhang, D. Hou, Y. Han, Micromechanical modeling on autogenous and drying shrinkages of concrete, Constr. Build. Mater. 29 (2012) 230–240. doi:10.1016/j.conbuildmat.2011.09.022.

[34] H. Chen, M. Wyrzykowski, K. Scrivener, P. Lura, Prediction of self-desiccation in low water-to-cement ratio pastes based on pore structure evolution, Cem. Concr. Res. 49 (2013) 38–47. doi:10.1016/j.cemconres.2013.03.013.

[35] J.-K.K. Kim, C.-S.S. Lee, Moisture diffusion of concrete considering self-desiccation at early ages, Cem. Concr. Res. 29 (1999) 1921–1927. doi:10.1016/S0008-8846(99)00192-1.

[36] D.P. Bentz, O.M. Jensen, K.K. Hansen, J.F. Olesen, H. Stang, C.J. Haecker, Influence of cement particle-size distribution on early age autogenous strains and stresses in cement-based materials, J. Am. Ceram. Soc. 84 (2001) 129–135. doi:10.1111/j.1151-2916.2001.tb00619.x.

[37] M.H. Zhang, C.T. Tam, M.P. Leow, Effect of water-to-cementitious materials ratio and silica fume on the autogenous shrinkage of concrete, Cem. Concr. Res. 33 (2003) 1687–1694. doi:10.1016/S0008-8846(03)00149-2.

[38] E. Ghafari, S.A. Ghahari, H. Costa, E. Júlio, A. Portugal, L. Durães, Effect of supplementary cementitious materials on autogenous shrinkage of ultra-high performance concrete, Constr. Build. Mater. 127 (2016) 43–48. doi:10.1016/j.conbuildmat.2016.09.123.

[39] Y. Li, J. Bao, Y. Guo, The relationship between autogenous shrinkage and pore structure of cement paste with mineral admixtures, Constr. Build. Mater. 24 (2010) 1855–1860. doi:10.1016/j.conbuildmat.2010.04.018.

[40] I. Maruyama, A. Teramoto, Temperature dependence of autogenous shrinkage of silica fume cement pastes with a very low water-binder ratio, Cem. Concr. Res. 50 (2013) 41–50. doi:10.1016/j.cemconres.2013.03.017.

[41] G.W. Scherer, Theory of Drying, J. Am. Ceram. Soc. 73 (1990) 3–14. doi:10.1111/j.1151-2916.1990.tb05082.x.

[42] L.A. Richards, Capillary conduction of liquids through porous mediums, Physics (College. Park. Md). 1 (1931) 318–333. doi:10.1063/1.1745010.

[43] Z.C. Grasley, D.A. Lange, M.D. D'Ambrosia, Internal relative humidity and drying stress gradients in concrete, Mater. Struct. 39 (2006) 901–909. doi:10.1617/s11527-006-9090-3.

[44] J.K. Kim, C.S. Lee, Moisture diffusion of concrete considering self-desiccation at early ages, Cem. Concr. Res. 29 (1999) 1921–1927. doi:10.1016/S0008-8846(99)00192-1.

[45] J. Justs, M. Wyrzykowski, D. Bajare, P. Lura, Internal curing by superabsorbent polymers in ultra-high performance concrete, Cem. Concr. Res. 76 (2015) 82–90. doi:10.1016/j.cemconres.2015.05.005.

[46] S. Mönnig, Water saturated super-absorbent polymers used in high strength concrete, Otto-Graf-Journal. 16 (2005) 193–202.

[47] J. Kočí, J. Fořt, M. Mildner, R. Černý, Effect of incorporated superabsorbent polymers on workability and hydration process in cement-based materials, in: Int. Multidiscip. Sci. GeoConference Surv. Geol. Min. Ecol. Manag. SGEM, Albena, Bulgaria, 2019: pp. 99–106. doi:10.5593/sgem2019/6.2/S26.013.

[48] K. Farzanian, K. Pimenta Teixeira, I. Perdigão Rocha, L. De Sa Carneiro, A. Ghahremaninezhad, The mechanical strength, degree of hydration, and electrical resistivity of cement pastes modified with superabsorbent polymers, Constr. Build. Mater. 109 (2016) 156–165. doi:10.1016/j.conbuildmat.2015.12.082.

[49] F.C.R. Almeida, A.J. Klemm, Efficiency of internal curing by superabsorbent polymers (SAP) in PC-GGBS mortars, Cem. Concr. Compos. 88 (2018) 41–51. doi:10.1016/j.cemconcomp.2018.01.002.

[50] J. Castro, I.D. Varga, J. Weiss, Using isothermal calorimetry to assess the water absorbed by fine LWA during mixing, J. Mater. Civ. Eng. 24 (2012) 996–1005. doi:10.1061/(ASCE)MT.1943-5533.0000496.

[51] D.P. Bentz, K.A. Snyder, Protected paste volume in concrete, Cem. Concr. Res. 29 (1999) 1863–1867. doi:10.1016/S0008-8846(99)00178-7.

[52] S. Zhutovsky, K. Kovler, A. Bentur, Autogenous curing of high-strength concrete using pre-soaked pumice and perlite sand, Third Int. Res. Semin. Lund,. (2002).

[53] M. Golias, J. Castro, J. Weiss, The influence of the initial moisture content of lightweight aggregate on internal curing, Constr. Build. Mater. 35 (2012) 52–62. doi:10.1016/j.conbuildmat.2012.02.074.

[54] O.M. Jensen, P.F. Hansen, Autogenous deformation and RH-change in perspective, Cem. Concr. Res. 31 (2001) 1859–1865. doi:10.1016/S0008-8846(01)00501-4.

[55] L.P. Esteves, P. Cachim, V.M. Ferreira, Mechanical properties of cement mortars with superabsorbent polymers, in: Adv. Constr. Mater. 2007, Springer Verlag, 2007: pp. 451–462. doi:10.1007/978-3-540-72448-3_45.

[56] C. Schröfl, V. Mechtcherine, M. Gorges, Relation between the molecular structure and the efficiency of superabsorbent polymers (SAP) as concrete admixture to mitigate autogenous shrinkage, Cem. Concr. Res. 42 (2012) 865–873. doi:10.1016/j.cemconres.2012.03.011.

[57] Q. Zhu, C.W. Barney, K.A. Erk, Effect of ionic crosslinking on the swelling and mechanical response of model superabsorbent polymer hydrogels for internally cured concrete, Mater. Struct. 48 (2015) 2261–2276. doi:10.1617/s11527-014-

0308-5.

[58] O.M. Jensen, P.F. Hansen, Water-entrained cement-based materials: II. Experimental observations, Cem. Concr. Res. 32 (2002) 973–978. doi:10.1016/S0008-8846(02)00737-8.

[59] N.A. Johansen, M.J. Millard, A. Mezencevova, V.Y. Garas, K.E. Kurtis, New method for determination of absorption capacity of internal curing agents, Cem. Concr. Res. 39 (2009) 65–68. doi:10.1016/j.cemconres.2008.10.004.

[60] M. Geiker, D. Bentz, O. Jensen, Mitigating autogenous shrinkage by internal curing, ACI Spec. Publ. (2004) 143–54.

[61] F. Wang, Y. Zhou, B. Peng, Z. Liu, S. Hu, Autogenous shrinkage of concrete with super-absorbent polymer, ACI Mater. J. 106 (2009) 123–127.

[62] S. Mönnig, P. Lura, Superabsorbent polymers - An additive to increase the freeze-thaw resistance of high strength concrete, in: Adv. Constr. Mater. 2007, Springer Verlag, 2007: pp. 351–358. doi:10.1007/978-3-540-72448-3_35.

[63] W.A. Jones, W.J. Weiss, Freeze thaw durability of internally cured concrete made using superabsorbent polymers, in: Proc. 4th Int. Conf. Durab. Concr. Struct. ICDCS 2014, Purdue University Libraries Scholarly Publishing Services, West Lafayette, Indiana, 2014: pp. 3–11. doi:10.5703/1288284315376.

[64] A. Valori, P.J. McDonald, K.L. Scrivener, The morphology of C-S-H: Lessons from 1H nuclear magnetic resonance relaxometry, Cem. Concr. Res. 49 (2013) 65–81. doi:10.1016/j.cemconres.2013.03.011.

[65] V.I. Bakhmutov, NMR Spectroscopy in Liquids and Solids, CRC Press, 2015. doi:10.1201/b18341.

[66] T.C. Pochapsky, S.S. Pochapsky, Nuclear Magnetic Resonance Spectroscopy, in: Mol. Biophys. Life Sci., Springer New York, New York, NY, 2013: pp. 113–173. doi:10.1007/978-1-4614-8548-3_5.

[67] R. Holly, E.J. Reardon, C.M. Hansson, H. Peemoeller, Proton spin-spin relaxation study of the effect of temperature on white cement hydration, J. Am. Ceram. Soc. 90 (2007) 570–577. doi:10.1111/j.1551-2916.2006.01422.x.

[68] J. Yang, Z. Sun, Y. Zhao, Y. Ji, B. Li, The water absorption-release of superabsorbent polymers in fresh cement paste: An NMR study, J. Adv. Concr. Technol. 18 (2020) 139–145. doi:10.3151/jact.18.139.

[69] N. Nestle, A. Kühn, K. Friedemann, C. Horch, F. Stallmach, G. Herth, Water balance and pore structure development in cementitious materials in internal curing with modified superabsorbent polymer studied by NMR, Microporous Mesoporous Mater. 125 (2009) 51–57. doi:10.1016/j.micromeso.2009.02.024.

[70] M. Fourmentin, P. Faure, S. Rodts, U. Peter, D. Lesueur, D. Daviller, P. Coussot, NMR observation of water transfer between a cement paste and a porous medium, Cem. Concr. Res. 95 (2017) 56–64. doi:10.1016/j.cemconres.2017.02.027.

[71] L. Yang, C. Shi, J. Liu, Z. Wu, Factors affecting the effectiveness of internal curing: A review, Constr. Build. Mater. 267 (2021) 121017. doi:10.1016/j.conbuildmat.2020.121017.

[72] C. Schröfl, D. Snoeck, V. Mechtcherine, A review of characterisation methods for superabsorbent polymer (SAP) samples to be used in cement-based construction materials: report of the RILEM TC 260-RSC, Mater. Struct. Constr. 50 (2017) 1–19.

[73] D. Snoeck, K. Van Tittelboom, S. Steuperaert, P. Dubruel, N. De Belie, Self-healing cementitious materials by the combination of microfibres and superabsorbent polymers, J. Intell. Mater. Syst. Struct. 25 (2014) 13–24. doi:10.1177/1045389X12438623.

2 Quantification of Internal Curing Efficiency – A Critical Review

Abstract

The development of concrete with lower water to cement ratio (w/c) has led to high autogenous shrinkage. Autogenous shrinkage is affected by the pore size, degree of hydration, and internal relative humidity of concrete, all of which are functions of the mix design. Of all the factors affecting autogenous shrinkage w/c is the most influential. Below 0.40 there is a strong linear relationship between autogenous shrinkage and w/c. Internal curing (IC) is the most effective method to mitigate autogenous shrinkage. To provide effective IC, material must absorb and store water, then release it as cement paste hydrates. Furthermore, the IC material must be distributed throughout so that all regions of concrete have access to water. Lightweight aggregate (LWA) in the size range of 2-4 mm and fine aggregate replacement less than 20% provides adequate IC. Superabsorbent polymers (SAP) are effective IC at 0.3-0.5% by cement weight, in the size range of 100 to 150 μm. Providing $(w/c)_{IC}$ is in the range of 0.05 to 0.075 is optimal to mitigate autogenous shrinkage and maintain adequate compressive strength.

Keywords: Autogenous shrinkage, internal curing, self-desiccation, lightweight aggregate, superabsorbent polymers

2.1 Introduction

Advances in concrete materials, such as the production of finer cement, the increased use of supplementary cementing materials (SCM), and the development of superplasticizers, have allowed for the production of high-strength concrete (HSC), high-performance concrete (HPC) and ultra-high performance concrete (UHPC) [1–4]. These types of concrete have very high strength and low porosity compared to conventional concrete. The benefits instilled by reducing the water to cement ratio (w/c) and using SCMs may be compromised by the increased susceptibility of this type of concrete to autogenous

shrinkage [5–8]. Autogenous shrinkage can produce early age cracking, which severely impairs the performance and longevity of the concrete [7,9].

The American Concrete Institute (ACI) defines autogenous shrinkage as the "change in volume due to the chemical process of hydration of cement, exclusive of effects of applied load and change in either thermal condition or moisture content" [10]. Autogenous shrinkage occurs consequently to the chemical reaction of cement which results in a product with a lower volume than the reactants. When the amount of water is insufficient to maintain complete saturation of the pores, that is a w/c less than 0.42, self-desiccation occurs. In normal concrete (w/c>0.42) the self-desiccation occurs in large capillaries so the stress in the meniscus of the pore fluid is low resulting in very little shrinkage (40-60 μm/m) [11]. In concrete with w/c less than 0.42 the self-desiccation occurs in much finer pores resulting in higher shrinkage [8,12]. For a w/c of 0.30 the autogenous shrinkage can be as high as 1000 μm/m within 24h after set [5]. This type of shrinkage is of particular concern because it occurs in very young concrete which has not developed the strength to endure this strain and consequently may crack within the first 12 h to 24 h of casting [11,13].

Self-desiccation can be prevented by maintaining high saturation of the pores through internal curing (IC) [14–17]. First identified by Philleo [18], IC provides a distributed source of water within the concrete, ideally producing concrete with all the strength and durability benefits of low w/c concrete without the adverse effect of autogenous shrinkage [12]. Materials that have the ability of store large amounts of water within their structure then release it as the cement hydration reaction consumes water are required for IC. Lightweight aggregate (LWA) [6,19–22] and superabsorbent polymers (SAP) [12,23–28] are most commonly used materials for IC. Other IC material include: rise husk ash [29,30], cenospheres [31,32], recycled concrete aggregate [33–35], and porous ceramic waste [36,37].

Autogenous shrinkage and mitigation methods have been a research subject for almost thirty years, yet the problem of high early-age shrinkage and associated cracking persists. This paper addresses pertinent research findings required to quantify the efficiency of internal curing. For completeness, the mechanisms of autogenous shrinkage and internal curing and their effects on the properties of concrete are presented. The experimental findings from the literature are analysed to determine the effect of IC water on the autogenous shrinkage of concrete and the corresponding mechanical properties.

2.2 Autogenous shrinkage

2.2.1 Mechanism

Autogenous shrinkage may be considered analogous to drying shrinkage. Simplistically, it is internal self-drying instead of drying caused by external environmental action. Lack of free water in the capillary pore structure produces a liquid-vapour meniscus. Capillary tension is generally accepted as the driving force for autogenous shrinkage [13,38]. The fluid which is under tension from capillary depression, causes compression on the surrounding solid structure of the pores [39]. As water is consumed by hydration, the internal pressure within cement paste pores increases [13,38,40] and according to the Young-Laplace equation the capillary tension is calculated as

$$P_c = \frac{-2\gamma\cos(\theta)}{r} \tag{2.1}$$

in which P_c, P_v, γ, θ, and r are the capillary water pressure (Pa), the water vapour pressure (Pa), the surface tension of pore fluid (N/m), the liquid–solid contact angle (radians), and the meniscus radius of curvature (m), respectively. The curvature of the meniscus is assumed to be equal to the radius of the largest saturated pore. As the hydration reaction proceeds, subsequently smaller pores are emptied which causes an increase in pressure [7,40,41]. Furthermore, Kelvin's equation relates the internal equilibrium relative humidity (RH) to the capillary pressure by

$$P_c = \frac{\ln(RH)\,RT}{V_m} \tag{2.2}$$

in which R, T and V_m are respectively, the universal gas constant (8.314 J/mol K), the temperature (^oK) and the molar volume of pore solution (~$18x10^{-6}$ m^3/mol). Assuming circular pores, Mackenzie's equation correlates the capillary pressure to autogenous shrinkage (ε) in cement paste, where

$$\varepsilon = \frac{S\Delta P}{3}\left(\frac{1}{K} - \frac{1}{K_s}\right) \tag{2.3}$$

in which *S*, *K*, and K_s are the cement paste degree of saturation, the paste bulk modulus (Pa) and the bulk modulus of the solid skeleton of the cement paste (Pa), respectively [7].

Zhang et al. [42] proposed a micro-mechanical model for shrinkage strain in concrete accounting for both drying and self-desiccation of the concrete. They expanded Eq. (2.3) to include multiple pores of various radii through a pore influence factor, v_p,

$$\varepsilon_{as} = -\frac{S v_p \rho_w RT}{3M}\left(\frac{1}{K} - \frac{1}{K_s}\right)\ln(RH) \tag{2.4}$$

$$v_p = 1 - \exp(k_0 \beta r) \tag{2.5}$$

Where k_0 is a constant and β relates the pore volume to the degree of hydration. Since autogenous shrinkage does not occur unless the RH is less than 100%, the following formula was proposed to account for any shrinkage that occurs prior to the RH reduction.

$$\varepsilon = \begin{cases} \eta\left[1 - \sqrt[3]{1 - (V_{ch} - V_{ch0})}\right] & for\ RH = 1 \\ \eta\left[1 - \sqrt[3]{1 - (V_{ch} - V_{ch0})}\right] + \varepsilon_{as} & for\ RH < 1 \end{cases} \tag{2.6}$$

Where the initial strain is related to the chemical shrinkage, V_{ch}, and a stiffness influence factor, η [42].

2.2.2 Factors Influencing Autogenous Shrinkage

Wu et al. [13] identified w/c, cement composition and fineness, SCM content, aggregates, chemical admixtures, and curing to be the main factors determining the extent of autogenous shrinkage. The most significant factor that affects autogenous shrinkage is the w/c. While any concrete with a w/c less than 0.40 may experience autogenous shrinkage,

further reduction in w/c increases the shrinkage significantly due to the lack of available free water [8,12]. Decreasing the w/c from 0.35 to 0.30 increased the 7-day autogenous shrinkage from 42 µm/m to 90 µm/m [43]. Fig. 2.1 presents the relation of autogenous shrinkage to w/c compiled from the data presented in Appendix A. The results show that there is a strong linear relationship (R^2 of 90% at 7 days) between w/c and autogenous shrinkage.

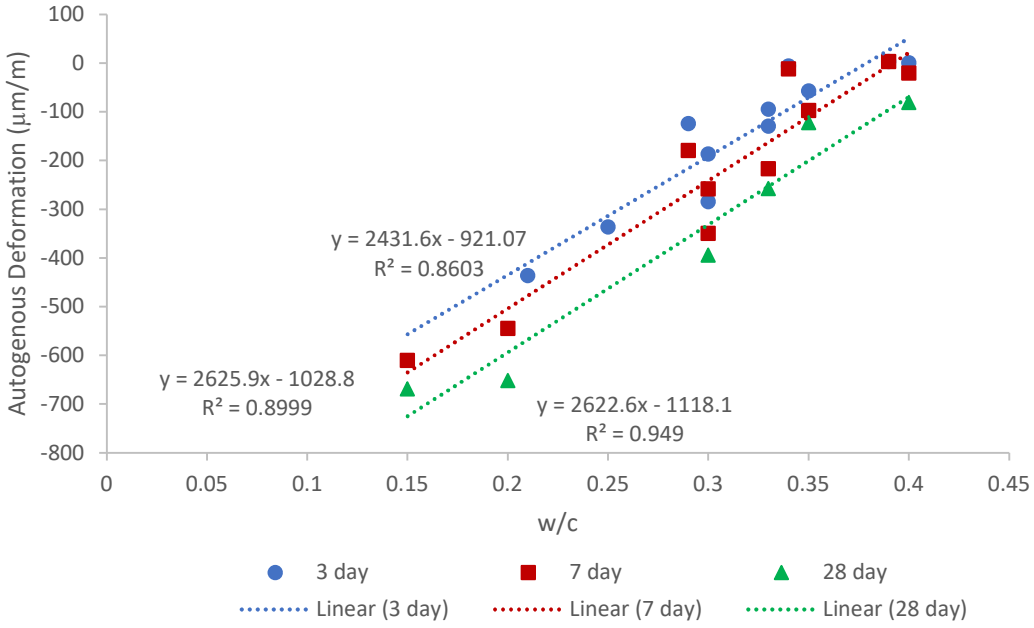

Fig. 2.1 The effect of w/c on the autogenous deformation

Cement with higher fineness results in higher autogenous shrinkage due to the increase in rate of hydration, which rapidly decreases the RH [5] and refines the pore microstructure [44]. Under sealed conditions the RH in low w/c concrete ranges from 85 to 90% [45] and the hydration reaction stops as the RH reaches approximately 80% [46]. As the saturation of the pores decreases the RH decreases and, according to Eq. (2.2) and (2.3), the autogenous shrinkage is proportional to ln(RH) so it also increases. Studies on the relation of autogenous shrinkage and RH have shown that the autogenous shrinkage increases as

the RH decreases and the w/c of the concrete is govern how the RH decreases [7,42,47,48]. This especially evident in the first 14 days of hydration.

SCMs, especially silica fume, significantly increase autogenous shrinkage [43,49–51], by refining the pores, consuming portlandite (CH), and increasing the rate of hydration [13]. For concrete with w/c of 0.35, the autogenous shrinkage strain was 42 μm/m. However, by replacing 10% of the cement with silica fume the strain increased to 110 μm/m. While the plain Portland cement concrete shrinkage only increased slightly after 7 days (shrinkage of 45 μm/m at 28 days), the silica fume concrete continued to experience autogenous shrinkage ever after 28 days (195 μm/m) [43]. However, when fly ash is used as SCM it slows the rate of hydration, therefore resulting in less autogenous shrinkage [49,52]. Snoeck et al. [53] found that both fly ash and blast furnace slag cement replacement resulted in less early-age autogenous shrinkage than the w/c 0.30 Portland cement concrete. However, they found that the rate of autogenous shrinkage with SCMs increased after 7 days compared to the reference concrete [53].

The presence of aggregates increases the cracking tendency from autogenous shrinkage as it provides restraint to the cement paste matrix [5,54]. Restrained HPC with a w/cm of 0.33 has developed tensile stresses of 3 MPa from autogenous shrinkage and cracked withing 6 days of casting [55]. However, steel or synthetic fibers can suppress shrinkage in HPC by restraining shrinkage [56]. Chemical admixture, such as expansive admixtures and shrinkage-reducing admixtures (SRA), have had limited success in reducing autogenous shrinkage and a loss of early strength [57]. External curing has a limited effect on autogenous shrinkage, because of the fine and disconnected pores characteristic of HPC. Internal curing has proven to be a more effective curing alternative.

2.3 Internal curing

External curing is effective in preventing the formation of a liquid vapour meniscus in the pores if the capillaries are interconnected. However, with HPC the dense microstructure

does not allow water penetration from an external source [8]. This has led to the development of IC as the method for curing HPC. This section discusses the mechanism of IC and the two most prevalent internal curing materials, i.e. lightweight aggregates (LWA) and superabsorbent polymers (SAP).

2.3.1 Mechanism

Capillary suction pressure develops when subsequently smaller pores are emptied as water is consumed by hydration. The pressure increase provides the driving force required to pull water out of the internal curing reservoirs, from largest to smallest pore [7,40,41]. Therefore, the large pores of the IC material empty first and maintain a high saturation in the small cement paste pores minimizing capillary pressure [7].

To determine the amount of water that can be provided by internal curing, Powers' model was extended. The entrained water, $(w/c)_{IC}$, that is needed to achieve maximum hydration is: [12]

$$(w/c)_{IC} = 0.18(^{w}/_{c})_{p} \qquad \text{for } (^{w}/_{c})_{p} < 0.36 \tag{2.7}$$

$$(w/c)_{IC} = 0.42 - (^{w}/_{c})_{p} \qquad \text{for } 0.36 < (^{w}/_{c})_{p} < 0.42 \tag{2.8}$$

The theoretical maximum degree of hydration (α_{max}), when $(w/c)_{IC}$ is provided, can be estimated according to:

$$\alpha_{max} = \frac{(^{w}/_{c})_{p}}{0.36} \qquad \text{for } (^{w}/_{c})_{p} < 0.36 \tag{2.9}$$

$$\alpha_{max} = 1 \qquad \text{for } 0.36 < (^{w}/_{c})_{p} < 0.42 \tag{2.10}$$

If the w/c is less than 0.36, complete hydration cannot be achieved because there is not enough space for more hydration product to form. The total w/c of internally cured cement paste is the original w/c plus $(w/c)_{IC}$. Since the w/c of the paste determines the porosity of the paste, the mechanical properties should depend on the original w/c [12].

Research has shown that, in addition to reduction in autogenous shrinkage, IC increases the degree of hydration [58], refines the interfacial transition zone [59] and produces adequate freeze-thaw resistance [34,60]. The dosage of IC material is critical to its success as a water entraining agent. Improper dosing of the IC material may have the following consequences: loss of workability [26,61,62], insignificant mitigation of autogenous shrinkage [63,64], reduction in compressive strength and other mechanical properties [63,65,66], as well as difficulty in predicting the behaviour of concrete [67].

2.3.2 Lightweight aggregate

The most used internal curing material is saturated lightweight aggregate (LWA). The IC water in LWA is physically bound in the porous microstructure of the LWA. For effective IC, LWA must have open, coarse pores, and a high porosity [16]. Examples of LWA include pumice [16], perlite, Leca (expanded clay) [68], and expanded shale [69]. The LWA is saturated by spraying it with water [6], leaving it submerged in water [7], or by vacuum saturation [16,20].

Bentz and Snyder [70] developed the following equation for the dosage of LWA:

$$M_{LWA} = \frac{c \cdot CS \cdot \alpha_{max}}{\varphi_{LWA} \cdot S} \tag{2.11}$$

where c is cement content (kg/m^3), CS is the chemical shrinkage of cement (ratio of the mass of water to the mass of cement), α_{max} is the expected maximum degree of hydration, φ_{LWA} is the amount of water absorbed by the LWA (ratio of the mass of water to the mass of dry aggregate), and S is the degree of saturation of the aggregate. It has been noted that not all the water in the LWA is available for IC due to the pores being too fine to release water and the spacing between LWA being too large [71]. The difference between the estimated water and the actual water needed can be compensated by an efficiency factor determined by trial and error [71]. Furthermore, one of the problems with using LWA for internal curing is that it is difficult to achieve saturated conditions. After 5 days of immersion at room temperature, only 9 to 14% saturation of pumice was observed [16].

The efficiency of LWA for IC depends on the pore structure, particle size, water absorption, and paste-aggregate proximity. For these reasons, fine LWA has generally been more successful in internal curing than coarse LWA [70,72]. However, it was found that the finest LWA were not very efficient, because the pores were also smaller making it more difficult for the water to be removed. In the literature, good IC had been obtained with LWA with particles in the range of 2 to 4 mm [72], 3.13 mm [6], and 0.59 to 4.76 mm [73]. For most LWA the optimum particle size is 2 to 4 mm.

The goal of the IC is to eliminate the autogenous shrinkage. However, often it is more important to control this shrinkage to an acceptable limit, especially for very low w/c ratios. For example, a 67% reduction in autogenous shrinkage was obtained for a 20% saturated LWA substitution of normal weight fine aggregate at a w/c of 0.20 [73]. A concrete with silica fume and w/cm of 0.33 has been observed to experience over 200 μm/m strain from autogenous shrinkage, while the same concrete with 25% LWA experienced only expansion [55]. Fig. 2.2 summaries the data compiled in Table A.1 and shows the relation between LWA aggregate content and autogenous deformation. LWA aggregate, as fine aggregate replacement in the range of 15 to 20%, provides adequate reduction in autogenous shrinkage. LWA content greater than 20% does not provide any additional benefit and may reduce compressive strength.

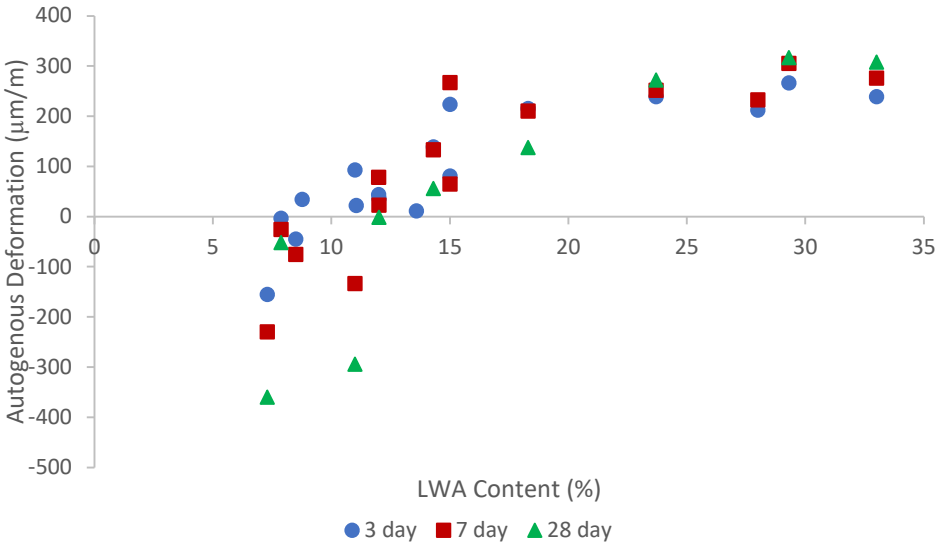

Fig. 2.2 Autogenous deformation versus LWA content

When LWA was added, the compressive strength of concrete decreased with the increase in IC content and/or size of LWA. In some cases, it was found that while the 7-day compressive strength was lower with LWA, the 28-day compressive strength was comparable to the concrete mix without LWA [16,20,74]. When large quantities are required to reduce autogenous shrinkage the effect of LWA on compressive strength is significant [73]. At a w/c of 0.33 the compressive strength was not affected by IC with LWA, but at w/c of 0.25 and 0.21 it was reduced by 10 and 4%, respectively [17]. A blanket statement about the effect of LWA on compressive strength is not possible since the result depends specifically on the type of LWA used and the properties of the mix design. Fig. 2.3 summaries the data compiled in Table A.1 and shows the relation between LWA content and compressive strength. From the available data, no statistically significant effect on the compressive strength was observed as the LWA content increased. While LWA is the weakest portion of the concrete, it does not necessarily negatively impact the compressive strength below 30% LWA content, possibly because of improved hydration from IC [12].

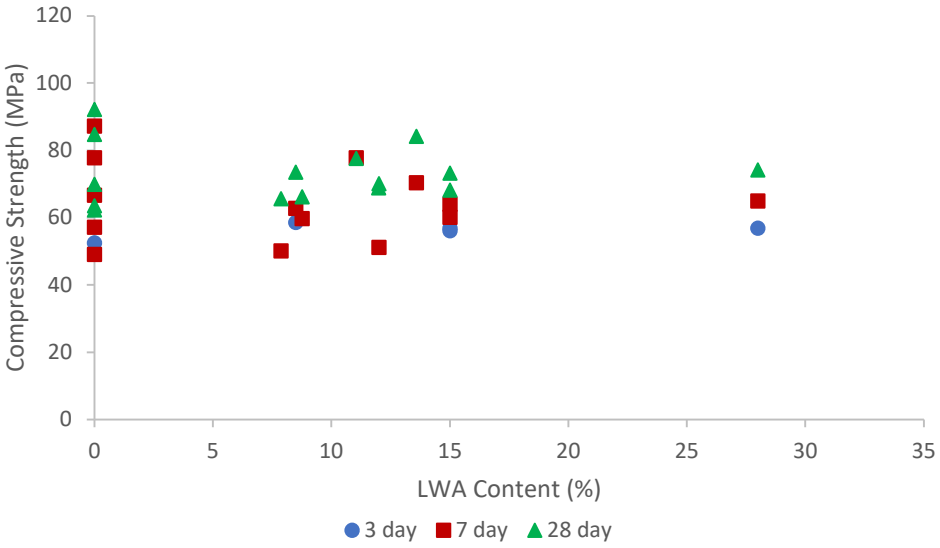

Fig. 2.3 Compressive strength versus LWA content

2.3.3 Superabsorbent polymer

Superabsorbent polymers (SAP) are a special class of hydrophilic polymer that can absorb and retain large quantities of water within their structure [75]. The most common SAPs are covalently cross-linked polyacrylates and copolymerized polyacrylamides/polyacrylates [75]. Optimal SAP has been reported to be in the size range from 100 to 150 µm and dosed as an additive at 0.3 to 0.5% by weight of cement content [76].

Osmotic pressure is the driving force for SAP absorption. The ionic concentration of the solution into which they are submerged determines their absorption capacity [75]. For cement pore solution, SAP is sensitive to the presence of calcium ions [77,78]. The concentration of anionic functional groups and the density of the covalent crosslinks in the SAP structural matrix determine its ability to imbibe water [79]. For SAP, the internal curing dosage is determined by:

$$w/c = (w/c)_p + (w/c)_{IC} = (w/c)_p + K\left(SAP/c\right) \quad (2.12)$$

Where K is the average absorption of SAP and the total amount of water for the reaction consist of the initial water in the paste with IC, $(^{w}/_{c})_{p}$, and the entrained water in the SAP, $(^{w}/_{c})_{IC}$ [28,61].

The complete elimination of autogenous shrinkage was observed with a SAP addition of 0.6% by weight of cement for a w/c of 0.30 [80,81]. For concrete with w/c of 0.34 and silica fume the demand for IC increased to 0.5 and 0.7% SAP by weight of cement; however, shrinkage was still observed because of silica fume [82]. Fig. 2.4 summaries the data compiled in Table A.2 and shows the relation between SAP content and autogenous deformation. SAP content in the range of 0.2 to 0.4% showed improvement in the autogenous shrinkage. One distinct type of SAP performed poorly at 0.25%, Fig. 2.4, which shows that not all types of SAP are suitable for IC [83]. Furthermore, testing on various types of SAP at the same IC water content showed 7-day autogenous shrinkage of 130.2 ± 343.2 µm/m, which shows the variable nature of SAP material [83].

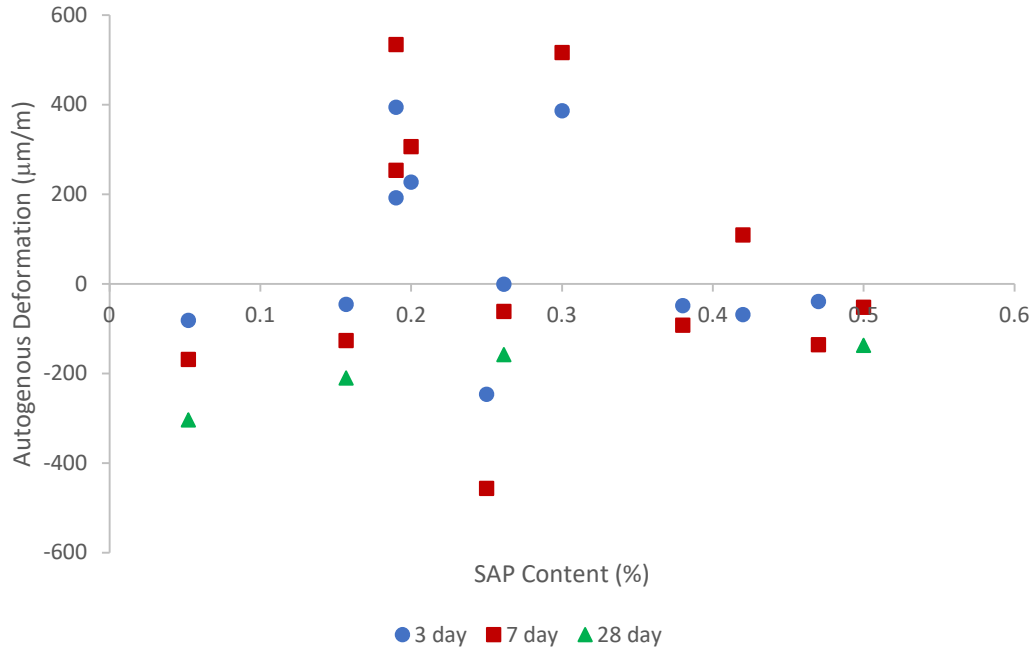

Fig. 2.4 Autogenous deformation versus SAP content

Mönnig and Lura [84] found no difference in compressive strength with 0.4% SAP; however, the tensile strength decreased as much as 20%. At SAP content of 0.7%, the compressive strength was 12% lower than the concrete without SAP. Jones and Weiss [60] found comparable strength between the reference and the SAP concrete, although the SAP concrete had a slightly lower strength. From these results it can be concluded that with SAP replacement values greater than 0.4% by weight of cement there will be some reduction in the strength of concrete. As shown in Fig. 2.5, from the data in Table A.2, there is no significant difference in compressive strength between 0.2 and 0.5 % SAP content, although there is a decrease in compressive strength compared to the control concrete for the 7-day compressive strength.

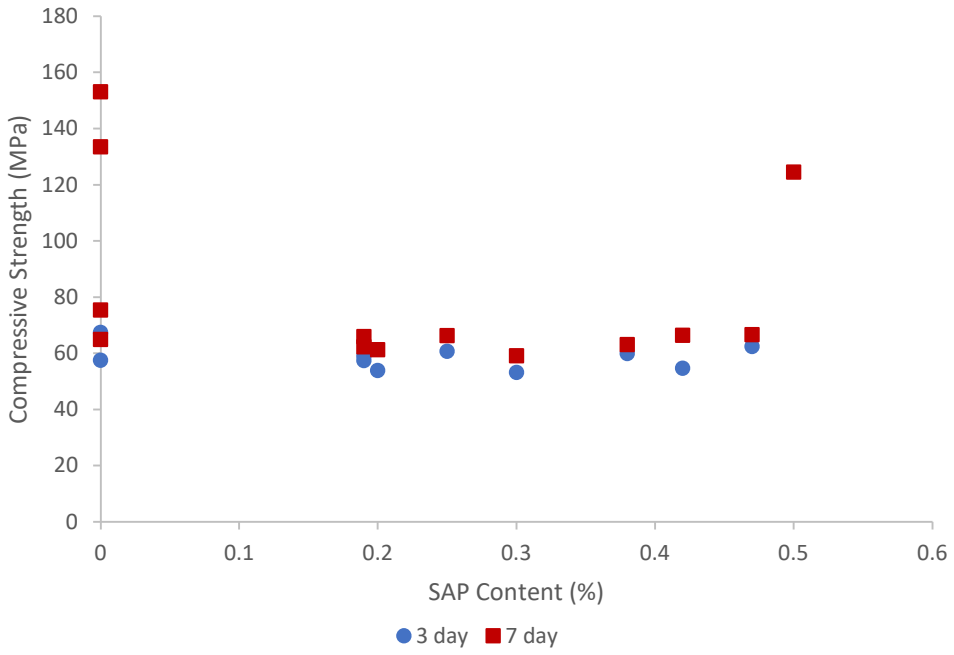

Fig. 2.5 Compressive strength versus SAP content

Jensen and Hansen [12] postulated improvements in concrete durability with SAP as IC. Mönnig and Lura [84] tested the salt scaling resistance of concrete with SAP and reported 40% reduction in scaling. They attributed the scaling resistance to improved pore structure. The results presented by Jones and Weiss [60] and later confirmed by Mechtcherine et al.

[85], revealed that SAP in concrete does not provide adequate freeze-thaw protection without air entrainment. The air content due to SAP was in the range of 4% which is considerably less than the 6 to 8% required to provide freeze-thaw protection. The potential of SAP particles to prevent the ingress of water by re-swelling and sealing cracks showed promising results by Lee et al. [86].

Some problems that have been identified with SAP are: segregation [80], agglomeration when SAP is added pre-wetted [61], an increased need for superplasticizer [84], and decrease in strength, especially tensile strength. Moreover, it is difficult to quantify the amount of water that is absorbed by SAP [87].

2.4 Efficiency of Internal Curing

Internal curing is considered effective if it mitigates autogenous shrinkage [66]. However, there is no consensus about how much IC material produces the best concrete. In addition to reducing autogenous shrinkage, IC much maintain adequate workability and mechanical properties of the concrete [61,80]. Therefore, efficient dosage of IC must eliminate autogenous shrinkage without compromising the mechanical properties of cement while minimizing the amount of IC material needed. Three factors have been identified to determine the efficiency of IC: 1) amount of water absorbed and available for IC, 2) the ability to release water, and 3) distribution of the IC material through the paste [88]. Furthermore, with SAP there is also a potential for agglomeration, which affects the distribution.

2.4.1 Absorption of IC water

Both LWA and SAP provide unique challenges for determining the absorption capacity of the material. For LWA, achieving full saturation of the material is difficult and time consuming [16], while with SAP it is difficult to quantify the amount of water absorbed [89,90].

After 5 days immersion at room temperature resulted in only 9 to 14% saturation of pumice [16]. Vacuum saturation or immersion in boiling water was more effective, yet more difficult for practical applications [16]. Furthermore, vacuum saturation saturates pores they would not be emptied by the capillary forces generated in concrete [20]. Golias et al. [20] found some success by adding dry LWA to concrete to absorb mixing water. The oven-dry LWA was able to absorb approximately 55% of amount absorbed by pre-saturated LWA. This approach has the potential to make dosing LWA easier in practice.

SAP are generally added dry to the concrete mixture, so that they absorb part of the mixing water [61,80]. SAP absorption depends on the concentration of covalent crosslinking density and concentration of anionic functional groups [79], which determine the SAPs ability to swell and sensitivity to ions in the pore solution. Testing eight different SAP types of varying crosslink density and anionic functional groups, Zhong et al. [83] found that the absorption capacity after 3 min varied between 11.51 and 27.89 g/g in cement filtrate. The average absorption was 20.2 g/g with a standard deviation of 6.9 g/g. This shows that the properties of every SAP material must be tested prior to use, since the absorption capacity can vary significantly. Testing the absorption is difficult because of variable concentration of ions in the cement pore solution and interstitial water between SAP particles [89,90]. Incorrect dosage can result in misinterpretation of the results. Overestimation of the amount of water absorbed from the mix water results in a higher w/c ratio of the concrete leading to lower strength. Underestimation results in too much water being absorbed from the concrete mixture, thereby reducing the workability [87].

Standards for natural aggregates do not apply for SAP, thus a new method for testing absorption is needed [87]. Several techniques for determining the pore solution absorption have been presented. Johansen, et al. [87] compared the heat of hydration of cement pastes with SAP and reference pastes of varying w/c using isothermal calorimetry to find the amount of water absorbed. Other studies have measured the absorption based on the amount of synthetic pore solution absorbed [80]. However, this may induce errors because

of the variable nature of the pore solution in the first hours after the start of hydration. Absorption capacity may be determined gravimetrically by the "tea-bag" method, which does not distinguish between absorbed water and interstitial water. The rate of absorption and quantity absorbed varies based on particle size. Test have shown that SAP can be fully saturated in less than 7 min of submersion in synthetic pore solution. This would indicate that several minutes of mixing are sufficient to achieve fully saturation of the SAP [91]. Mönnig [92] determined the water absorbed by comparing the slump flow of concrete mixtures with SAP and reference mixtures with different w/c ratios. Using this equivalent flow methodology, Sun et al. [93] found that for w/c of 0.30 and $(w/c)_{IC}$ of 0.054, 0.5% SAP produced optimal results for workability and IC.

2.4.2 Desorption of IC water

For LWA, the main factor determining water desorption is the size of the LWA pores [72,94]. With LWA, most of the IC water is released in the RH range of 92 to 96% [7,94]. If the pores of the LWA are too fine and vacuum saturated, they will not release their stored water to the cement paste [20]. Pores finer than 100 nm can be saturated with water by vacuum saturation, yet they do not provide any IC benefit as the pressure required to empty them is too great [95]. Furthermore, the entry diameter is the most important to determine the LWA's ability to release water. It was found that smaller LWA lost more water (80%) at an RH of 85% compared to some larger LWA (50%) with more porosity, because the larger LWA had a more closed pore structure [16].

In the case of SAP, desorption is highly dependent on the SAP structure and composition [96]. Some types of SAP, based on the crosslink density and anionic concentration, do not retain water in a synthetic pore solution or within cement paste [96]. Using isothermal calorimetry to study the kinetics of the hydration reaction with IC, showed that the addition of SAP IC significantly impacts the hydration reaction initially by delaying the hydration reaction peak. Although the reaction starts sooner in plain concrete it proceeds at a slower rate [25].

2.4.3 Distribution of IC water

The effectiveness of an internal curing method can be assessed by tracking the water movement from the internal curing reservoirs. This allows for better dosing of the curing agents as well as determining the most appropriate particle size. However, experimental knowledge is lacking in this area [19,88,97].

Henkensiefken et al. [19] used X-ray absorption to determine the distance water traveled from saturated lightweight aggregate to the hydrating cement paste. With time, the cement paste was shown to become denser with the ingress of water. From 24 to 75 h, water travelled as far as 1.8 mm from the LWA into the paste [19]. From X-ray microtomography, water was found to easily travel 2 mm or more because the paste is highly permeable [98]. From image analysis, the distance that water can transfer from LWA found to be in the range of 1 to 2 mm [6,15]. Neutron radiography found that water movement can be up to 8 mm within 21 h [99], which is significantly large than found in similar studied where the transfer distance was about 3 mm [100].

As a non-destructive method nuclear magnetic resonance (NMR) can be employed to observe the movement of water from the internal curing reservoir to the hydrating cement paste. The NMR studies showed the ability of SAP particles to release water at the onset of the acceleration period of cement hydration. Water diffused 10 mm from the source from NMR studies of cement paste containing one SAP particle [97]. For cement paste with w/c of 0.3 and using pulsed field gradient NMR, the average diffusion length of 5 mm after 10 h was determine [97]. Using an optical microscope and cement paste with 0.5 w/c, the water transport distance was reported to range between 0.05 and 0.06 mm from the surface of SAP [101].

Pre-saturating SAP was found to cause particle agglomeration during mixing, which has the potential to lower the efficacy SAP IC and lower the compressive strength

[76,77,101,102]. Scanning electron microscopy (SEM) showed that large voids, approximately 300 μm, were observed in mortars containing SAP IC as a result of particle agglomeration [103]. Furthermore, testing IC with SAP in a large scale production plant showed that SAP tended to agglomerate [104]. In the mixes where agglomeration was observed, the shrinkage reduction was 36% lower than in concrete without agglomeration. Testing the air void system found that the pore sizes were significantly larger than in concrete with agglomeration (peak void size of 4000 μm) potentially compromising the compressive strength. It was found that the timing of SAP addition was critical in preventing agglomeration and that SAP should be added to the dry material [104]. However, another study found agglomeration when SAP was added dry, but no agglomeration SAP was dispersed within the mixing water [105]. Further study is needed in this area to properly assess the effect of agglomeration on the efficiency of IC with SAP.

2.4.4 Effect of w/c on IC

The w/c is the most important factor in determining the potential for concrete to experience autogenous shrinkage and is important in determining how well IC performs. The data for LWA and SAP IC, provided in Table A.1 and Table A.2, respectively, was analysed to determine the effect of the internal curing w/c, $(w/c)_{IC}$, and total w/c, $(w/c)_t$, on the autogenous shrinkage and compressive strength of concrete.

From the data available, as shown in Fig. 2.6, there is a weak relationship between $(w/c)_{IC}$ and autogenous deformation. There is evidence (R^2 of 57%) that there is an optimum amount of water that can be entrained in the range of 0.05 to 0.075 that effectively mitigates autogenous shrinkage without requiring a large amount of IC material. IC curing outside this range does not effectively mitigate autogenous shrinkage. From Fig. 2.7, as the total w/c approaches 0.40, the less autogenous shrinkage is observed. Fig. 2.8 shows that there is no statistically significant relationship between $(w/c)_{IC}$ and compressive strength and IC below $(w/c)_{IC}$ 0.15 results in adequate strength concrete. However, Fig. 2.9 shows that

compressive strength is related to the total w/c (R^2 of 73%) and that lower total w/c achieves higher strength.

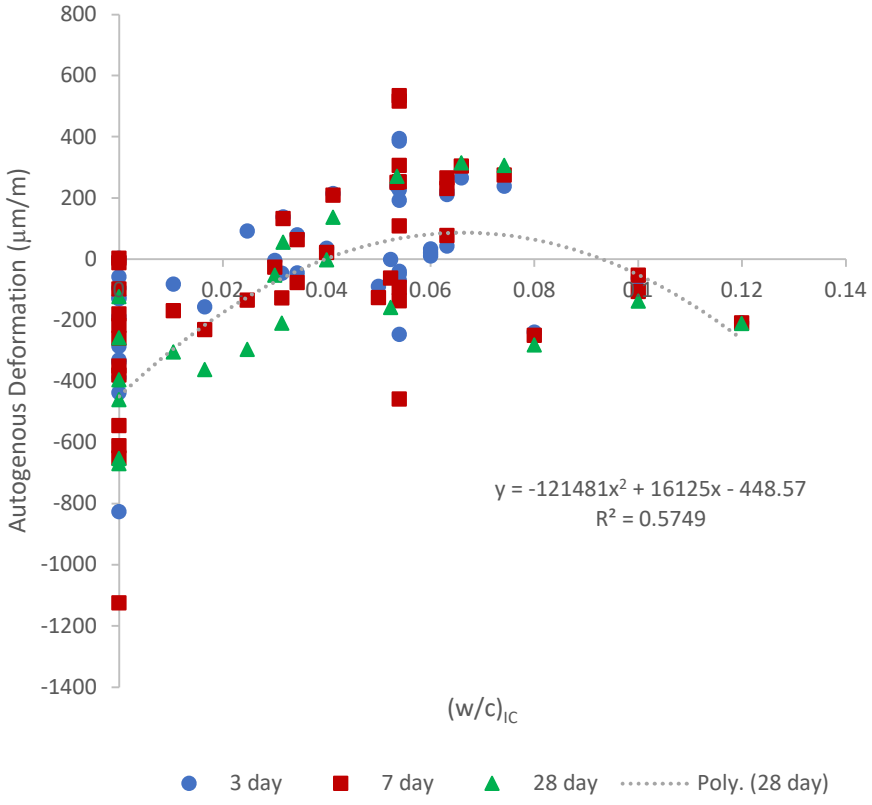

Fig. 2.6 Autogenous deformation versus w/c provided by IC

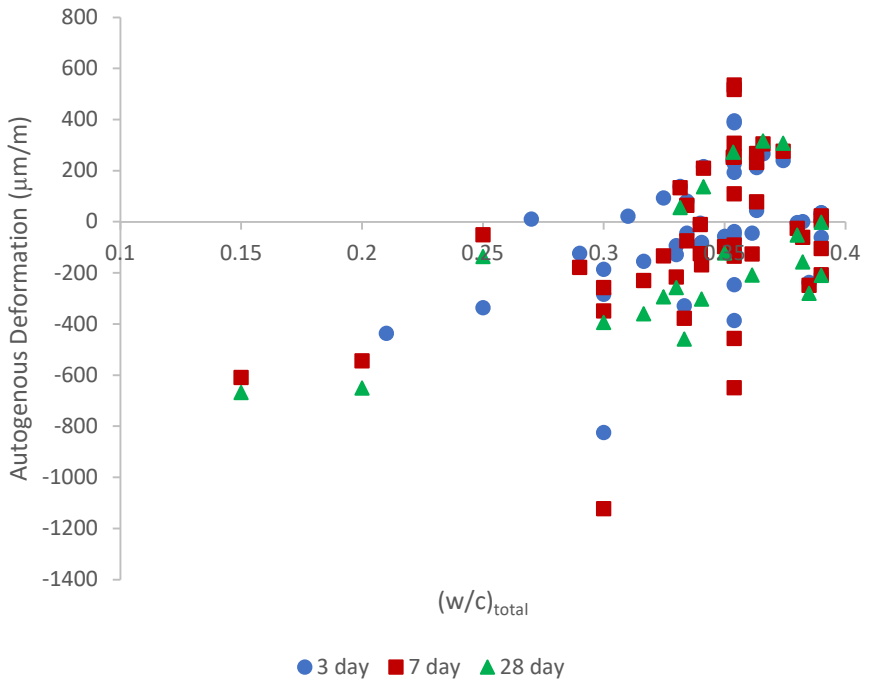

Fig. 2.7 Autogenous deformation versus total w/c

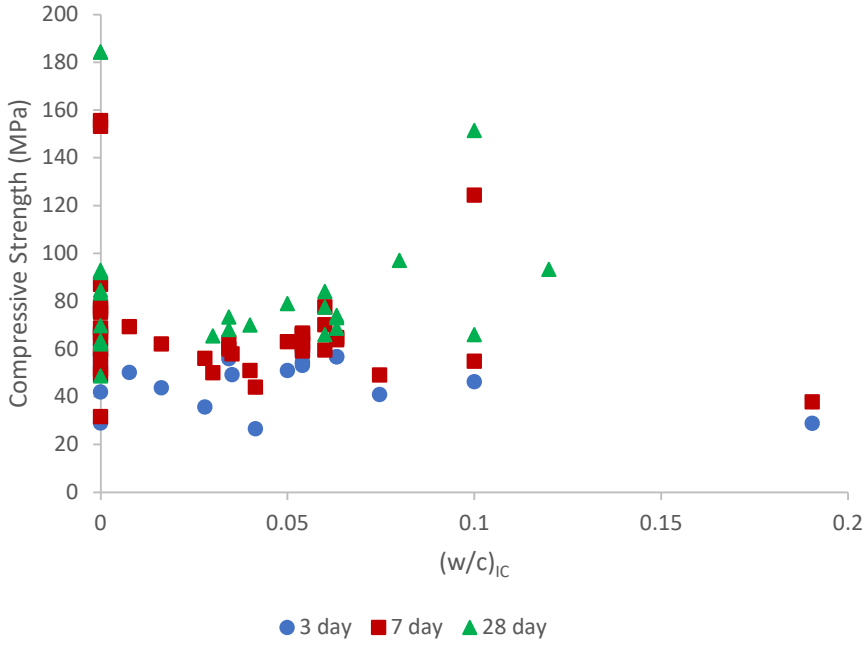

Fig. 2.8 Compressive strength versus w/c provided by IC

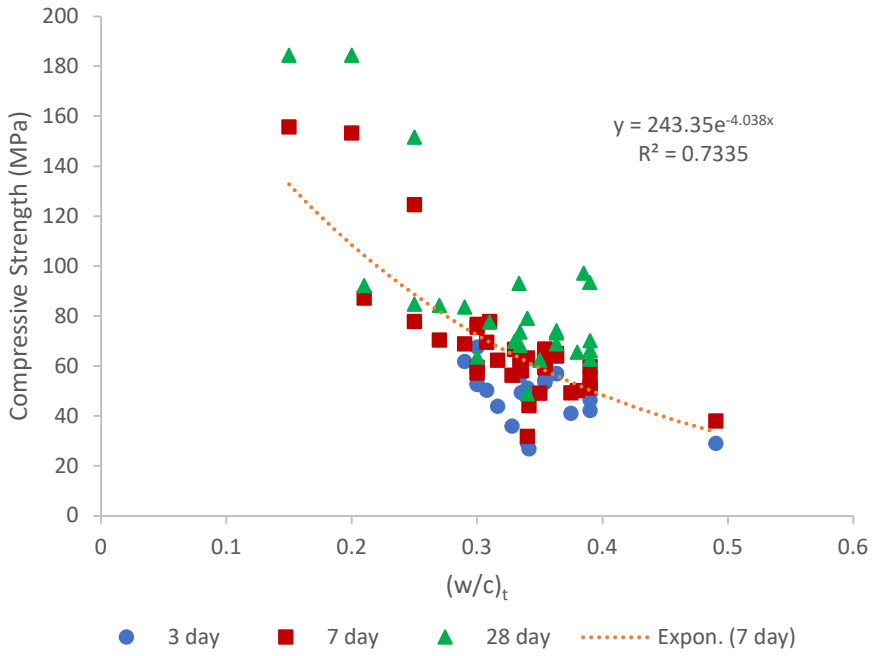

Fig. 2.9 Compressive strength versus total w/c

2.5 Conclusions

From a review of the literature the following conclusions were determined:

1. Autogenous shrinkage is a function of the pore size, pore connectivity, RH, degree of hydration, and self-stress.
2. The w/c, cement composition and fineness, SCM content, aggregates, fibers, and chemical admixtures in the mix design influence the autogenous shrinkage.
3. Effective IC depends on 1) the amount of water in the IC material, 2) the distribution of IC material, and 3) the ability of water to move from the IC material.
4. LWA in the size range of 2 to 4 mm is an effective material for internal curing when it replaces no more than 20% of regular fine aggregate.
5. SAP is effective for internal curing when used at 0.3 to 0.5% by weight of cement, yet the compressive strength decreases by about 10% compared to the control.
6. The amount of IC water in SAP depends on the water absorption kinetics and efficiency. The absorption of SAP depends on the SAP's covalent crosslinking

density and concentration of anionic functional groups as well as the concentration of ions in the pore solution of the cement paste.

7. SAP water desorption is a function of the anion concentration in the SAP, the size and interconnectivity of the cement paste pores, and the interface between the SAP and cement paste.
8. The water desorption and distance water can travel from IC material has not been fully quantified.
9. SAP particles are susceptible to agglomeration which greatly reduces their efficiency. Agglomeration has not been quantified in the literature.

Acknowledgements

The authors would like to thank NSERC for funding this research.

References

[1] S.E. Chidiac, F. Moutassem, F. Mahmoodzadeh, Compressive strength model for concrete, Mag. Concr. Res. 65 (2013) 557–572. doi:10.1680/macr.12.00167.

[2] S.E. Chidiac, M. Shafikhani, Phenomenological model for quantifying concrete chloride diffusion coefficient, Constr. Build. Mater. 224 (2019) 773–784. doi:10.1016/j.conbuildmat.2019.07.006.

[3] M. Shafikhani, S.E. Chidiac, A holistic model for cement paste and concrete chloride diffusion coefficient, Cem. Concr. Res. 133 (2020) 106049. doi:10.1016/j.cemconres.2020.106049.

[4] A. Elahi, P.A.M. Basheer, S. V. Nanukuttan, Q.U.Z. Khan, Mechanical and durability properties of high performance concretes containing supplementary cementitious materials, Constr. Build. Mater. (2010). doi:10.1016/j.conbuildmat.2009.08.045.

[5] E. ichi Tazawa, S. Miyazawa, Influence of cement and admixture on autogenous shrinkage of cement paste, Cem. Concr. Res. 25 (1995) 281–287. doi:10.1016/0008-8846(95)00010-0.

[6] B. Akcay, M.A. Tasdemir, Optimisation of using lightweight aggregates in mitigating autogenous deformation of concrete, Constr. Build. Mater. 23 (2009) 353–363. doi:10.1016/j.conbuildmat.2007.11.015.

[7] R. Henkensiefken, D. Bentz, T. Nantung, J. Weiss, Volume change and cracking in internally cured mixtures made with saturated lightweight aggregate under sealed and unsealed conditions, Cem. Concr. Compos. 31 (2009) 427–437. doi:10.1016/j.cemconcomp.2009.04.003.

[8] P.C. Aïtcin, The durability characteristics of high performance concrete: A review, Cem. Concr. Compos. (2003). doi:10.1016/S0958-9465(02)00081-1.

[9] B. Craeye, M. Geirnaert, G. De Schutter, Super absorbing polymers as an internal curing agent for mitigation of early-age cracking of high-performance concrete bridge decks, Constr. Build. Mater. 25 (2011) 1–13. doi:10.1016/j.conbuildmat.2010.06.063.

[10] ACI Standards, ACI, ACI Concrete Terminology, Farmington Hills, 2013. www.concrete.org.

[11] K. Van Breugel, N. Van Tuan, Autogenous shrinkage of HPC and ways to mitigate it, in: Key Eng. Mater., Trans Tech Publications Ltd, 2015: pp. 3–20. doi:10.4028/www.scientific.net/KEM.629-630.3.

[12] O.M. Jensen, P.F. Hansen, Water-entrained cement-based materials: I. Principles and theoretical background, Cem. Concr. Res. 31 (2001) 647–654. doi:10.1016/S0008-8846(01)00463-X.

[13] L. Wu, N. Farzadnia, C. Shi, Z. Zhang, H. Wang, Autogenous shrinkage of high performance concrete: A review, Constr. Build. Mater. 149 (2017) 62–75. doi:10.1016/j.conbuildmat.2017.05.064.

[14] D.M. Al Saffar, A.J.K. Al Saad, B.A. Tayeh, Effect of internal curing on behavior of high performance concrete: An overview, Case Stud. Constr. Mater. 10 (2019) e00229. doi:10.1016/j.cscm.2019.e00229.

[15] D.P. Bentz, W.J. Weiss, Internal Curing : A 2010 State-of-the- Art Review, Gaithersburg: US Department of Commerce. National Institute of Standards and

Technology, 2011.

[16] P. Lura, D.P. Bentz, D.A. Lange, K. Kovler, A. Bentur, Pumice aggregates for internal water curing, in: Int. RILEM Symp. Concr. Sci. Eng. A Tribut. to Arnon Bentur, 2004: pp. 137–151.

[17] S. Zhutovsky, K. Kovler, Effect of internal curing on durability-related properties of high performance concrete, Cem. Concr. Res. 42 (2012) 20–26. doi:10.1016/j.cemconres.2011.07.012.

[18] R.E. Philleo, Concrete science and reality, in: J. Skalny, S. Mindess (Eds.), Mater. Sci. Concr. II, American Ceramic Society, Westerville, Ohio, 1991: pp. 1–8.

[19] R. Henkensiefken, T. Nantung, J. Weiss, Saturated lightweight aggregate for internal curing in low w/c mixtures: Monitoring water movement using x-ray absorption, Strain. 47 (2011) e432–e441. doi:10.1111/j.1475-1305.2009.00626.x.

[20] M. Golias, J. Castro, J. Weiss, The influence of the initial moisture content of lightweight aggregate on internal curing, Constr. Build. Mater. 35 (2012) 52–62. doi:10.1016/j.conbuildmat.2012.02.074.

[21] J.T. Kevern, Q.C. Nowasell, Internal curing of pervious concrete using lightweight aggregates, Constr. Build. Mater. 161 (2018) 229–235. doi:10.1016/j.conbuildmat.2017.11.055.

[22] A. Paul, S. Murgadas, J. Delpiano, P.A. Moreno-Casas, M. Walczak, M. Lopez, The role of moisture transport mechanisms on the performance of lightweight aggregates in internal curing, Constr. Build. Mater. 268 (2021) 121191. doi:10.1016/j.conbuildmat.2020.121191.

[23] J. Liu, Z. Ou, J. Mo, Y. Wang, H. Wu, The effect of SCMs and SAP on the autogenous shrinkage and hydration process of RPC, Constr. Build. Mater. 155 (2017) 239–249. doi:10.1016/j.conbuildmat.2017.08.061.

[24] S.E. Chidiac, S.N. Mihaljevic, S.A. Krachkovskiy, G.R. Goward, Efficiency measure of SAP as internal curing for cement using NMR & MRI, Constr. Build. Mater. 278 (2021) 122365. doi:10.1016/j.conbuildmat.2021.122365.

[25] J. Justs, M. Wyrzykowski, F. Winnefeld, D. Bajare, P. Lura, Influence of

superabsorbent polymers on hydration of cement pastes with low water-to-binder ratio, J. Therm. Anal. Calorim. 115 (2014) 425–432. doi:10.1007/s10973-013-3359-x.

[26] J. Justs, M. Wyrzykowski, D. Bajare, P. Lura, Internal curing by superabsorbent polymers in ultra-high performance concrete, Cem. Concr. Res. 76 (2015) 82–90. doi:10.1016/j.cemconres.2015.05.005.

[27] L. Montanari, P. Suraneni, M.T. Chang, C. Villani, J. Weiss, Absorption and desorption of superabsorbent polymers for use in internally cured concrete, Adv. Civ. Eng. Mater. 7 (2018) 20180008. doi:10.1520/ACEM20180008.

[28] S.E. Chidiac, S.N. Mihaljevic, S.A. Krachkovskiy, G.R. Goward, Characterizing the effect of superabsorbent polymer content on internal curing process of cement paste using calorimetry and nuclear magnetic resonance methods, J. Therm. Anal. Calorim. (2020) 1–13. doi:10.1007/s10973-020-09754-0.

[29] N. Van Tuan, G. Ye, K. Van Breugel, Internal curing of ultra-high performance concrete by using rice husk ash, in: Int. RILEM Conf. Mater. Sci. – MATSCI, 2010: pp. 265–274. http://rilem.net/publication/publication/81?id_papier=3511 (accessed May 5, 2021).

[30] V.-T.-A. Van, C. Rößler, D.-D. Bui, H.-M. Ludwig, Mesoporous structure and pozzolanic reactivity of rice husk ash in cementitious system, Constr. Build. Mater. 43 (2013) 208–216. doi:10.1016/j.conbuildmat.2013.02.004.

[31] F. Liu, J. Wang, X. Qian, J. Hollingsworth, Internal curing of high performance concrete using cenospheres, Cem. Concr. Res. 95 (2017) 39–46. doi:10.1016/j.cemconres.2017.02.023.

[32] P. Chen, J. Wang, F. Liu, X. Qian, Y. Xu, J. Li, Converting hollow fly ash into admixture carrier for concrete, Constr. Build. Mater. 159 (2018) 431–439. doi:10.1016/j.conbuildmat.2017.10.122.

[33] H. Kim, D.P. Bentz, Internal curing with crushed returned concrete aggregates, NRMCA Concr. Technol. Forum Focus Sustain. Dev. (2008) 1–12.

[34] S.T. Yildirim, C. Meyer, S. Herfellner, Effects of internal curing on the strength,

drying shrinkage and freeze-thaw resistance of concrete containing recycled concrete aggregates, Constr. Build. Mater. 91 (2015) 288–296. doi:10.1016/j.conbuildmat.2015.05.045.

[35] A. Gonzalez-Corominas, M. Etxeberria, Effects of using recycled concrete aggregates on the shrinkage of high performance concrete, Constr. Build. Mater. 115 (2016) 32–41. doi:10.1016/j.conbuildmat.2016.04.031.

[36] R. Sato, A. Shigematsu, T. Nukushina, M. Kimura, Improvement of properties of Portland blast furnace cement type B concrete by internal curing using ceramic roof material waste, J. Mater. Civ. Eng. 23 (2011) 777–782. doi:10.1061/(asce)mt.1943-5533.0000232.

[37] M. Suzuki, M. Seddik Meddah, R. Sato, Use of porous ceramic waste aggregates for internal curing of high-performance concrete, Cem. Concr. Res. 39 (2009) 373–381. doi:10.1016/j.cemconres.2009.01.007.

[38] P. Lura, O.M. Jensen, K. van Breugel, Autogenous shrinkage in high-performance cement paste: An evaluation of basic mechanisms, Cem. Concr. Res. 33 (2003) 223–232. doi:10.1016/S0008-8846(02)00890-6.

[39] C. Hua, P. Acker, A. Ehrlacher, Analyses and models of the autogenous shrinkage of hardening cement paste, Cem. Concr. Res. (1995). doi:10.1016/0008-8846(95)00140-8.

[40] H. Ye, A. Radlińska, A review and comparative study of existing shrinkage prediction models for Portland and non-Portland cementitious materials, Adv. Mater. Sci. Eng. 2016 (2016) 1–13. doi:10.1155/2016/2418219.

[41] G.W. Scherer, Theory of Drying, J. Am. Ceram. Soc. 73 (1990) 3–14. doi:10.1111/j.1151-2916.1990.tb05082.x.

[42] J. Zhang, D. Hou, Y. Han, Micromechanical modeling on autogenous and drying shrinkages of concrete, Constr. Build. Mater. 29 (2012) 230–240. doi:10.1016/j.conbuildmat.2011.09.022.

[43] M.H. Zhang, C.T. Tam, M.P. Leow, Effect of water-to-cementitious materials ratio and silica fume on the autogenous shrinkage of concrete, Cem. Concr. Res. 33

(2003) 1687–1694. doi:10.1016/S0008-8846(03)00149-2.

[44] D.P. Bentz, O.M. Jensen, K.K. Hansen, J.F. Olesen, H. Stang, C.J. Haecker, Influence of cement particle-size distribution on early age autogenous strains and stresses in cement-based materials, J. Am. Ceram. Soc. 84 (2001) 129–135. doi:10.1111/j.1151-2916.2001.tb00619.x.

[45] D.P. Bentz, P. Lura, J.W. Roberts, Mixture proportioning for internal curing, Concr. Int. 27 (2005) 35–40.

[46] K. Kovler, S. Zhutovsky, Overview and future trends of shrinkage research, in: Mater. Struct. Constr., 2006. doi:10.1617/s11527-006-9114-z.

[47] H. Chen, M. Wyrzykowski, K. Scrivener, P. Lura, Prediction of self-desiccation in low water-to-cement ratio pastes based on pore structure evolution, Cem. Concr. Res. 49 (2013) 38–47. doi:10.1016/j.cemconres.2013.03.013.

[48] J.-K.K. Kim, C.-S.S. Lee, Moisture diffusion of concrete considering self-desiccation at early ages, Cem. Concr. Res. 29 (1999) 1921–1927. doi:10.1016/S0008-8846(99)00192-1.

[49] E. Ghafari, S.A. Ghahari, H. Costa, E. Júlio, A. Portugal, L. Durães, Effect of supplementary cementitious materials on autogenous shrinkage of ultra-high performance concrete, Constr. Build. Mater. 127 (2016) 43–48. doi:10.1016/j.conbuildmat.2016.09.123.

[50] Y. Li, J. Bao, Y. Guo, The relationship between autogenous shrinkage and pore structure of cement paste with mineral admixtures, Constr. Build. Mater. 24 (2010) 1855–1860. doi:10.1016/j.conbuildmat.2010.04.018.

[51] I. Maruyama, A. Teramoto, Temperature dependence of autogenous shrinkage of silica fume cement pastes with a very low water-binder ratio, Cem. Concr. Res. 50 (2013) 41–50. doi:10.1016/j.cemconres.2013.03.017.

[52] P. Termkhajornkit, T. Nawa, M. Nakai, T. Saito, Effect of fly ash on autogenous shrinkage, Cem. Concr. Res. 35 (2005) 473–482. doi:10.1016/j.cemconres.2004.07.010.

[53] D. Snoeck, O.M. Jensen, N. De Belie, The influence of superabsorbent polymers on

the autogenous shrinkage properties of cement pastes with supplementary cementitious materials, Cem. Concr. Res. 74 (2015) 59–67. doi:10.1016/j.cemconres.2015.03.020.

[54] P. Lura, O.M. Jensen, J. Weiss, Cracking in cement paste induced by autogenous shrinkage, Mater. Struct. Constr. 42 (2009) 1089–1099. doi:10.1617/s11527-008-9445-z.

[55] A. Bentur, S.I. Igarashi, K. Kovler, Prevention of autogenous shrinkage in high-strength concrete by internal curing using wet lightweight aggregates, Cem. Concr. Res. 31 (2001) 1587–1591. doi:10.1016/S0008-8846(01)00608-1.

[56] Z. Wu, C. Shi, K.H. Khayat, Investigation of mechanical properties and shrinkage of ultra-high performance concrete: Influence of steel fiber content and shape, Compos. Part B Eng. 174 (2019) 107021. doi:10.1016/j.compositesb.2019.107021.

[57] M. José Oliveira, A.B. Ribeiro, F.G. Branco, Combined effect of expansive and shrinkage reducing admixtures to control autogenous shrinkage in self-compacting concrete, Constr. Build. Mater. 52 (2014) 267–275. doi:10.1016/j.conbuildmat.2013.11.033.

[58] B.E. Byard, A.K. Schindler, R.W. Barnes, Early-age cracking tendency and ultimate degree of hydration of internally cured concrete, J. Mater. Civ. Eng. 24 (2012) 1025–1033. doi:10.1061/(asce)mt.1943-5533.0000469.

[59] D.P. Bentz, Influence of internal curing using lightweight aggregates on interfacial transition zone percolation and chloride ingress in mortars, Cem. Concr. Compos. 31 (2009) 285–289. doi:10.1016/j.cemconcomp.2009.03.001.

[60] W.A. Jones, W.J. Weiss, Freeze thaw durability of internally cured concrete made using superabsorbent polymers, in: Proc. 4th Int. Conf. Durab. Concr. Struct. ICDCS 2014, Purdue University Libraries Scholarly Publishing Services, West Lafayette, Indiana, 2014: pp. 3–11. doi:10.5703/1288284315376.

[61] S. Mönnig, Water saturated super-absorbent polymers used in high strength concrete, Otto-Graf-Journal. 16 (2005) 193–202.

[62] J. Kočí, J. Fořt, M. Mildner, R. Černý, Effect of incorporated superabsorbent

polymers on workability and hydration process in cement-based materials, in: Int. Multidiscip. Sci. GeoConference Surv. Geol. Min. Ecol. Manag. SGEM, Albena, Bulgaria, 2019: pp. 99–106. doi:10.5593/sgem2019/6.2/S26.013.

[63] G.R. de Sensale, A.F. Goncalves, Effects of fine LWA and SAP as internal water curing agents, Int. J. Concr. Struct. Mater. 8 (2014) 229–238. doi:10.1007/s40069-014-0076-1.

[64] D. Shen, X. Wang, D. Cheng, J. Zhang, G. Jiang, Effect of internal curing with super absorbent polymers on autogenous shrinkage of concrete at early age, Constr. Build. Mater. 106 (2016) 512–522. doi:10.1016/j.conbuildmat.2015.12.115.

[65] K. Farzanian, K. Pimenta Teixeira, I. Perdigão Rocha, L. De Sa Carneiro, A. Ghahremaninezhad, The mechanical strength, degree of hydration, and electrical resistivity of cement pastes modified with superabsorbent polymers, Constr. Build. Mater. 109 (2016) 156–165. doi:10.1016/j.conbuildmat.2015.12.082.

[66] F.C.R. Almeida, A.J. Klemm, Efficiency of internal curing by superabsorbent polymers (SAP) in PC-GGBS mortars, Cem. Concr. Compos. 88 (2018) 41–51. doi:10.1016/j.cemconcomp.2018.01.002.

[67] J. Castro, I.D. Varga, J. Weiss, Using isothermal calorimetry to assess the water absorbed by fine LWA during mixing, J. Mater. Civ. Eng. 24 (2012) 996–1005. doi:10.1061/(ASCE)MT.1943-5533.0000496.

[68] O.M. Jensen, P. Lura, Techniques and materials for internal water curing of concrete, in: Mater. Struct. Constr., Springer Netherlands, 2006: pp. 817–825. doi:10.1617/s11527-006-9136-6.

[69] D.P. Bentz, Internal curing of high-performance blended cement mortars, ACI Mater. J. 104 (2007) 408–414. doi:10.14359/18831.

[70] D.P. Bentz, K.A. Snyder, Protected paste volume in concrete, Cem. Concr. Res. 29 (1999) 1863–1867. doi:10.1016/S0008-8846(99)00178-7.

[71] S. Zhutovsky, K. Kovler, A. Bentur, Efficiency of lightweight aggregates for internal curing of high strength concrete to eliminate autogenous shrinkage, 2002.

[72] S. Zhutovsky, K. Kovler, A. Bentur, Autogenous curing of high-strength concrete

using pre-soaked pumice and perlite sand, Third Int. Res. Semin. Lund,. (2002).

[73] M. Şahmaran, M. Lachemi, K.M.A. Hossain, V.C. Li, Internal curing of engineered cementitious composites for prevention of early age autogenous shrinkage cracking, Cem. Concr. Res. 39 (2009) 893–901. doi:10.1016/j.cemconres.2009.07.006.

[74] D. Cusson, T. Hoogeveen, Internal curing of high-performance concrete with pre-soaked fine lightweight aggregate for prevention of autogenous shrinkage cracking, Cem. Concr. Res. 38 (2008) 757–765. doi:10.1016/j.cemconres.2008.02.001.

[75] O.M. Jensen, P.F. Hansen, Autogenous deformation and RH-change in perspective, Cem. Concr. Res. 31 (2001) 1859–1865. doi:10.1016/S0008-8846(01)00501-4.

[76] L.P. Esteves, P. Cachim, V.M. Ferreira, Mechanical properties of cement mortars with superabsorbent polymers, in: Adv. Constr. Mater. 2007, Springer Verlag, 2007: pp. 451–462. doi:10.1007/978-3-540-72448-3_45.

[77] P. Lura, K. Friedemann, F. Stallmach, S. Mönnig, M. Wyrzykowski, L.P. Esteves, Kinetics of water migration in cement-based systems containing superabsobent polymers, in: Appl. Super Absorbent Polym. Concr. Constr., Springer Netherlands, Dordrecht, 2012: pp. 21–37. doi:10.1007/978-94-007-2733-5_4.

[78] C. Schröfl, V. Mechtcherine, M. Gorges, Relation between the molecular structure and the efficiency of superabsorbent polymers (SAP) as concrete admixture to mitigate autogenous shrinkage, Cem. Concr. Res. 42 (2012) 865–873. doi:10.1016/j.cemconres.2012.03.011.

[79] Q. Zhu, C.W. Barney, K.A. Erk, Effect of ionic crosslinking on the swelling and mechanical response of model superabsorbent polymer hydrogels for internally cured concrete, Mater. Struct. 48 (2015) 2261–2276. doi:10.1617/s11527-014-0308-5.

[80] O.M. Jensen, P.F. Hansen, Water-entrained cement-based materials: II. Experimental observations, Cem. Concr. Res. 32 (2002) 973–978. doi:10.1016/S0008-8846(02)00737-8.

[81] M. Geiker, D. Bentz, O. Jensen, Mitigating autogenous shrinkage by internal curing, ACI Spec. Publ. (2004) 143–54.

[82] F. Wang, Y. Zhou, B. Peng, Z. Liu, S. Hu, Autogenous shrinkage of concrete with super-absorbent polymer, ACI Mater. J. 106 (2009) 123–127.

[83] P. Zhong, M. Wyrzykowski, N. Toropovs, L. Li, J. Liu, P. Lura, Internal curing with superabsorbent polymers of different chemical structures, Cem. Concr. Res. 123 (2019) 105789. doi:10.1016/j.cemconres.2019.105789.

[84] S. Mönnig, P. Lura, Superabsorbent polymers - An additive to increase the freeze-thaw resistance of high strength concrete, in: Adv. Constr. Mater. 2007, Springer Verlag, 2007: pp. 351–358. doi:10.1007/978-3-540-72448-3_35.

[85] V. Mechtcherine, C. Schröfl, M. Wyrzykowski, M. Gorges, P. Lura, D. Cusson, J. Margeson, N. De Belie, D. Snoeck, K. Ichimiya, S.I. Igarashi, V. Falikman, S. Friedrich, J. Bokern, P. Kara, A. Marciniak, H.W. Reinhardt, S. Sippel, A. Bettencourt Ribeiro, J. Custódio, G. Ye, H. Dong, J. Weiss, Effect of superabsorbent polymers (SAP) on the freeze–thaw resistance of concrete: results of a RILEM interlaboratory study, Mater. Struct. Constr. 50 (2017) 1–19. doi:10.1617/s11527-016-0868-7.

[86] H.X.D. Lee, H.S. Wong, N.R. Buenfeld, Potential of superabsorbent polymer for self-sealing cracks in concrete, Adv. Appl. Ceram. 109 (2010) 296–302. doi:10.1179/174367609X459559.

[87] N.A. Johansen, M.J. Millard, A. Mezencevova, V.Y. Garas, K.E. Kurtis, New method for determination of absorption capacity of internal curing agents, Cem. Concr. Res. 39 (2009) 65–68. doi:10.1016/j.cemconres.2008.10.004.

[88] L. Yang, C. Shi, J. Liu, Z. Wu, Factors affecting the effectiveness of internal curing: A review, Constr. Build. Mater. 267 (2021) 121017. doi:10.1016/j.conbuildmat.2020.121017.

[89] C. Schröfl, D. Snoeck, V. Mechtcherine, A review of characterisation methods for superabsorbent polymer (SAP) samples to be used in cement-based construction materials: report of the RILEM TC 260-RSC, Mater. Struct. Constr. 50 (2017) 1–19.

[90] D. Snoeck, K. Van Tittelboom, S. Steuperaert, P. Dubruel, N. De Belie, Self-healing

cementitious materials by the combination of microfibres and superabsorbent polymers, J. Intell. Mater. Syst. Struct. 25 (2014) 13–24. doi:10.1177/1045389X12438623.

[91] L.P. Esteves, On the absorption kinetics of superabsorbent polymers, in: Int. RILEM Conf. Use Superabsorbent Polym. Other New Addit. Concr. 15-18 August, RILEM publications SARL, 2010: pp. 77–84.

[92] S. Mönnig, Water saturated super-absorbent polymers used in high strength concrete, Otto-Graf-Journal. 16 (2005) 71–82.

[93] B. Sun, H. Wu, W. Song, Z. Li, J. Yu, Design methodology and mechanical properties of Superabsorbent Polymer (SAP) cement-based materials, Constr. Build. Mater. 204 (2019) 440–449. doi:10.1016/j.conbuildmat.2019.01.206.

[94] X. Ma, J. Liu, C. Shi, A review on the use of LWA as an internal curing agent of high performance cement-based materials, Constr. Build. Mater. (2019). doi:10.1016/j.conbuildmat.2019.05.126.

[95] V. Mechtcherine, M. Wyrzykowski, C. Schröfl, D. Snoeck, P. Lura, N. De Belie, A. Mignon, S. Van Vlierberghe, A.J. Klemm, F.C.R. Almeida, J.R. Tenório Filho, W.P. Boshoff, H.-W. Reinhardt, S.-I. Igarashi, Application of super absorbent polymers (SAP) in concrete construction—update of RILEM state-of-the-art report, Mater. Struct. 54 (2021) 80. doi:10.1617/s11527-021-01668-z.

[96] C. Schroefl, V. Mechtcherine, P. Vontobel, J. Hovind, E. Lehmann, Sorption kinetics of superabsorbent polymers (SAPs) in fresh Portland cement-based pastes visualized and quantified by neutron radiography and correlated to the progress of cement hydration, Cem. Concr. Res. (2015). doi:10.1016/j.cemconres.2015.05.001.

[97] K. Friedemann, F. Stallmach, J. Kärger, NMR diffusion and relaxation studies during cement hydration-A non-destructive approach for clarification of the mechanism of internal post curing of cementitious materials, Cem. Concr. Res. 36 (2006) 817–826. doi:10.1016/j.cemconres.2005.12.007.

[98] D.P. Bentz, Four-dimensional X-ray microtomography study of water movement during internal curing, in: Concr. Int. Des. Constr., 2006: pp. 11–20.

doi:10.1617/2351580052.002.

[99] I. Maruyama, M. Kanematsu, T. Noguchi, H. Iikura, A. Teramoto, H. Hayano, Evaluation of water transfer from saturated lightweight aggregate to cement paste matrix by neutron radiography, (2009). doi:10.1016/j.nima.2009.01.138.

[100] P. Trtik, B. Münch, W.J. Weiss, A. Kaestner, I. Jerjen, L. Josic, E. Lehmann, P. Lura, Release of internal curing water from lightweight aggregates in cement paste investigated by neutron and X-ray tomography, in: Nucl. Instruments Methods Phys. Res. Sect. A Accel. Spectrometers, Detect. Assoc. Equip., 2011: pp. 244–249. doi:10.1016/j.nima.2011.02.012.

[101] S. Mönnig, Superabsorbing additions in concrete: applications, modelling and comparison of different internal water sources, Institut für Werkstoffe im Bauwesen der Universität Stuttgart, 2009.

[102] H. Ding, L. Zhang, P. Zhang, Factors influencing strength of super absorbent polymer (SAP) concrete, Trans. Tianjin Univ. 23 (2017) 245–257. doi:10.1007/s12209-017-0049-y.

[103] G. Ye, K. Van Breugel, P. Lura, V. Mechtcherine, Hardening process of binder paste and microstructure development, in: Appl. Super Absorbent Polym. Concr. Constr. State-of-the-Art Rep. Prep. by Tech. Comm. 225-SAP, Springer Netherlands, Dordrecht, 2012: pp. 51–62. doi:10.1007/978-94-007-2733-5_6.

[104] J.R. Tenório Filho, D. Snoeck, N. De Belie, Mixing protocols for plant-scale production of concrete with superabsorbent polymers, Struct. Concr. 21 (2020) 983–991. doi:10.1002/suco.201900443.

[105] M. Kalinowski, P. Woyciechowski, J. Sokołowska, Effect of mechanically-induced fragmentation of polyacrylic superabsorbent polymer (SAP) hydrogel on the properties of cement composites, (2020). doi:10.1016/j.conbuildmat.2020.120135.

[106] S. Zhutovsky, K. Kovler, Influence of water to cement ratio on the efficiency of internal curing of high-performance concrete, Constr. Build. Mater. 144 (2017) 311–316. doi:10.1016/j.conbuildmat.2017.03.203.

[107] H. Zhao, J. Ding, S. Li, P. Wang, Y. Chen, Y. Liu, Q. Tian, Effects of porous shale

waste brick lightweight aggregate on mechanical properties and autogenous deformation of early-age concrete, Constr. Build. Mater. 261 (2020) 120450. doi:10.1016/j.conbuildmat.2020.120450.

[108] Y. Han, J. Zhang, Y. Luosun, T. Hao, Effect of internal curing on internal relative humidity and shrinkage of high strength concrete slabs, Constr. Build. Mater. 61 (2014) 41–49. doi:10.1016/j.conbuildmat.2014.02.060.

[109] X. ming Kong, Z. lin Zhang, Z. chen Lu, Effect of pre-soaked superabsorbent polymer on shrinkage of high-strength concrete, Mater. Struct. Constr. 48 (2015) 2741–2758. doi:10.1617/s11527-014-0351-2.

Appendix A Experimental Data from the Literature

Table A.1 Internal Curing with LWA

Reference	LWA (%)	$(w/c)_{IC}$	$(w/c)_t$	Autogenous Deformation (μm/m) 3 day	7 day	28 day	Compressive Strength (MPa) 3 day	7 day	28 day
Henkensiefken et al. [7]	0.0	0.00	0.30	-186.1	-257.3	-393.5			
	7.3	0.02	0.32	-155.1	-229.9	-360.0			
	11.0	0.02	0.32	93.1	-133.2	-294.4			
	14.3	0.03	0.33	138.7	133.2	56.1			
	18.3	0.04	0.34	215.3	209.9	137.5			
	23.7	0.05	0.35	239.1	251.8	272.0			
	29.3	0.07	0.37	266.4	304.7	316.2			
	33.0	0.07	0.37	239.1	275.5	307.4			
Golias et al.[20]	0.0	0.00	0.30	-284.0	-349.1		52.5	57.1	63.6
	28.0	0.06	0.36	212.2	232.4		56.9	64.9	74.1
	15.0	0.06	0.36	223.7	267.0		56.9	64.0	73.2
	12.0	0.06	0.36	43.7	77.8				68.9
	15.0	0.03	0.33	80.6	64.5		56.1	60.1	68.2
	8.5	0.03	0.33	-44.7	-75.2		58.6	62.8	73.5
Zutovsky & Kovler [106]	0.0	0.00	0.21	-435.9				87.2	92.2
	0.0	0.00	0.25	-335.9				77.8	84.7
	0.0	0.00	0.33	-93.7				66.6	69.9
	13.6	0.06	0.27	10.9				70.3	84.2
	11.1	0.06	0.31	21.9				77.8	77.6
	8.8	0.06	0.39	34.4				59.8	66.2
Zhao et al. [107]	0.0	0.00	0.35	-56.6	-96.7	-121.7		49.1	62.3
	7.9	0.03	0.38	-3.4	-25.8	-51.7		50.1	65.6
	12.0	0.04	0.39	35.8	22.5	-1.7		51.1	70.1
Han et al. [108]		0.00	0.33	-328.6	-377.8	-458.7			93.1
		0.08	0.39	-237.5	-248.4	-280.0			97.2
		0.12	0.39	-207.8	-207.8	-209.7			93.5

Table A.2 Internal Curing with SAP

				Autogenous Deformation (um/m)			Compressive Strength (MPa)		
	Sap (%)	$(w/c)_{IC}$	$(w/c)_t$	3 day	7 day	28 day	3 day	7 day	28 day
Zhong et al. [83]	0.00	0.00	0.30	-824.6	-1122.8		67.5	75.5	
	0.00	0.00	0.35	-386.0	-649.1		57.7	65.0	
	0.42	0.05	0.35	-68.0	109.9		54.8	66.5	
	0.19	0.05	0.35	193.0	254.4		59.2	66.0	
	0.20	0.05	0.35	228.1	307.0		54.0	61.3	
	0.19	0.05	0.35	394.7	535.1		57.5	62.4	
	0.30	0.05	0.35	387.0	517.4		53.3	59.3	
	0.25	0.05	0.35	-245.6	-456.1		60.8	66.4	
	0.47	0.05	0.35	-38.9	-134.9		62.5	66.8	
	0.38	0.05	0.35	-47.8	-91.3		60.1	63.2	
Justs et al. [26]	0.00	0.00	0.15		-609.8	-668.3		155.7	184.3
	0.00	0.00	0.20		-543.9	-651.2		153.2	184.3
	0.50	0.10	0.25		-51.2	-136.6		124.6	151.6
Kong et al. [109]		0.00	0.29	-123.4	-178.5		61.8	68.9	83.5
		0.05	0.34	-87.9	-125.2		51.2	63.2	79.1
		0.10	0.39	-60.7	-104.7		46.4	55.0	66.1
		0.00	0.34	-5.6	-11.2		29.1	31.8	48.8
		0.00	0.39	3.7	3.7		42.2	51.6	62.7
Shen et al. [64]	0.00	0.00	0.33	-129.0	-216.0	-257.0			
	0.05	0.01	0.34	-81.0	-168.0	-303.0			
	0.16	0.03	0.36	-45.0	-126.0	-209.0			
	0.26	0.05	0.38	0.0	-61.0	-157.0			
Sun et al. [93]	0.00	0.00	0.30				55.2	76.7	
	0.25	0.01	0.31				50.3	69.5	
	0.50	0.02	0.32				43.9	62.3	
	0.75	0.03	0.33				35.9	56.2	
	1.00	0.04	0.34				26.8	44.1	
	0.00	0.00	0.30				52.9	59.5	
	1.15	0.04	0.34				49.4	58.1	
	2.30	0.07	0.37				41.0	49.2	
	4.60	0.19	0.49				29.0	38.0	

3 Characterizing the effect of superabsorbent polymer content on internal curing process of cement paste using calorimetry and nuclear magnetic resonance methods

Chidiac, S.E., Mihaljevic, S.N., Krachkovskiy, S.A., & Goward, G.R. (2020). Characterizing the effect of superabsorbent polymer content on internal curing process of cement paste using calorimetry and nuclear magnetic resonance methods, Journal of Thermal Analysis and Calorimetry, 145(2), 437-449, doi:10.1007/s10973-020-09754-0.

Abstract

Internal curing (IC) is used to mitigate autogenous shrinkage in low water to cement ratio (w/c) concrete. Although, superabsorbent polymers (SAP) have been shown to work well for IC, their effects on the kinetics of the cement chemical reaction and the amount of water they provide have not been fully quantified. An experimental program was performed using isothermal calorimetry and nuclear magnetic resonance (NMR) to study the behaviour of cement paste with various level of IC using SAP. The results revealed that the higher the amount of IC the more susceptible the cement paste became to SAP overdosing resulting a significant decrease in the heat of hydration (HOH) and therefore loss of IC efficiency. The mass of SAP to entrained water greater than 5% led to particles agglomeration and a 65% decrease in its IC efficiency. The HOH is observed to be linearly proportional to the entrained w/c, and that its development is limited by the initial porosity of the paste which controls the water diffusion from the SAP. The NMR signal corresponding to IC water showed that the SAP absorbs 4 to 7% more mixing water than initially estimated, and that prewetted SAP has larger amount of entrained water in comparison to dry SAP.

Keywords: internal curing; superabsorbent polymer; heat of hydration; gel water; agglomeration; diffusion coefficient; IC efficiency

3.1 Introduction

Concrete, comprised of low water to cement ratio (w/c) and supplementary cementing materials, achieves a dense microstructure and a high risk of developing autogenous shrinkage [1–5]. Internal curing (IC) has been proposed as an effective method to mitigate autogenous shrinkage [5,6]. The initial research focussed on lightweight aggregates (LWA) as water saturated inclusions for IC [7] given the high porosity of LWA. However, the variable nature of LWA, combined with the time needed to fully water saturate the particles and the negative implications on the mechanical properties of concrete, have inhibited its application [8–10]. Superabsorbent polymers (SAP), which are covalently crosslinked polyacrylates and copolymerized polyacrylamides/polyacrylates [11–13], have emerged as an alternative IC material due to their ability to retain a large quantity of water. Although SAP as an IC agent has many advantages due to its size, shape and water absorption, quantifying the amount of absorbed water in a highly ionic cement paste environment is challenging [14,15]. Traditional methods of determining aggregate water absorption do not apply for SAP, since they cannot distinguish between absorbed water, adsorbed water on the SAP surface, and interstitial water between particles. Interstitial water tends to cause the particles to agglomerate if SAP is added pre-saturated [16], as such, SAP is mixed with the dry material and allowed to absorb a portion of the mixing water. This practice requires proper dosage of the SAP that accounts for water it can absorb during mixing. If the absorbed water is underestimated, the w/c of the paste is higher than the design value, and vice versa, both of which have consequences on the behaviour of the mortar or concrete. These consequences include: loss of workability and an increase dependence on superplasticizer [16–18], inadequate IC so autogenous shrinkage is not fully mitigated [4,10], lower strength due to more voids in the concrete [10,19,20], and difficulty in interpreting/predicting the behaviour of concrete [8].

Recognizing the ionic nature of cement paste and its adverse effect on SAP absorption, Johansen et al. [15] used isothermal calorimetry to study the relationship between cement paste with different amounts of absorbent fiber. The absorption of the material is then

estimated based on the heat evolution of plain paste. It is assumed that the IC material absorbs the mixing water, that the absorbed water is available for further curing, and that the IC water does not affect the global rate of the hydration reaction. Also, Castro et al. [8] used isothermal calorimetry to determine the water absorption of LWA, however they used the total heat of hydration (HOH) for their comparison. The rational for using heat of hydration, as opposed to the heat evolution, is that at later age the effect of admixtures is negligible. The procedure assumes that the additional heat produced is the same due to IC with dry aggregate and with pre-wetted aggregate, which is valid if the water demand of hydration is less than the total water stored in LWA pores. If the HOH was the same for the initially dry LWA and the fully saturated LWA, the dry aggregate absorbed the desired amount of mixing water.

Justs et al. [21] studied the influence of SAP on the hydration process of ultra high performance concrete (UHPC) using isothermal calorimetry. They studied cement paste with w/c of 0.20 to 0.30 and paste with SAP providing 0.033 to 0.100 w/c of internal curing to a 0.20 w/c reference paste. They found that the addition of SAP significantly impacts the initial kinetics of the hydration reaction. Initially there was a delay in the occurrence of the hydration peak compared to the reference cement paste. Compared to the cement paste with equivalent total w/c and no SAP, the cement paste with SAP initiated hydration sooner, but at a slower rate. All the cement pastes with SAP reached a higher HOH than the reference paste after 24 h, and after 3 days the HOH was similar to the plain paste without SAP with an equivalent total w/c. Additionally, the degree of hydration increased with SAP similarly to the increase achieved by a corresponding increase in w/c. Further study suggests that SAP provides additional space for hydration product so the IC pastes are able to achieve higher degree of hydration [17].

The goals of this paper are threefold: to quantify the effectiveness of SAP as an IC material, to determine the initial w/c of the paste based on the amount of mixing water absorbed by SAP and to investigate the interplay between SAP content, particle spacing, and

effectiveness of SAP as IC. Towards these goals an experimental program and an analytical study were carried out.

3.2 Experimental Program

3.2.1 Materials and Cement Paste Mix Design

White Portland cement CSA type GU-A3001 [22], SAP, superplasticizer and water were the material used for this study. Low iron cement manufactured by Federal White Cement Ltd. was used to be compatible with parallel studies carried out using nuclear magnetic resonance (NMR). The cement oxide composition is listed in Table 3.1 along with the corresponding phases calculated according to the Bogue equations [23]. The SAP, manufactured by BASF Germany, has an average particle size 126.5 μm ± 3.0 μm, as determined by laser diffraction following the procedure presented by Esteves [14] using ethanol as the dispersion liquid and assuming spherical particles. SAP cement pore solution absorption was estimated to be 25 g g^{-1} SAP using a modified filter method [24,25]. MasterGlenium 7700 superplasticizer from BASF was used at 400 mL per 100 kg of cement to achieve the desired workability.

Table 3.1 Oxide composition of white cement

Oxide	% Mass
CaO	65.10
SiO_2	21.39
Al_2O_3	6.32
Fe_2O_3	0.01
MgO	0.25
SO_3	3.25
Finesse/m^2 kg^{-1}	400
Phase	% Mass
C_3S	59.93
C_2S	16.13
C_3A	16.73
C_4AF	0.03

The mix proportions presented in Table 3.2, include 3 reference pastes with w/c of 0.30, 0.32 and 0.35, designated as Ref30, Ref32 and Ref35, respectively, and 2 levels of IC, 0.02 and 0.05. Based on the estimated absorption of 25 g g^{-1} SAP, the dosage for a 0.30+0.02 water entrained paste and a 0.30+0.05 water entrained paste corresponds to SAP08 and SAP20, respectively. Two additional mixes were added to evaluate the adequacy of 25 g g^{-1} SAP and effects of SAP dosage on the IC efficiency. Moreover, the addition method of the SAP was evaluated by using dry and pre-saturated SAP. The label "W" was added to the end of the mix designation for the mixes using pre-saturated SAP.

Table 3.2 Cement paste mix proportions

	Mix Designation	Cement/g	Water/g	SAP/g kg^{-1} cement	w/c (estimated)
1	Ref30	50	15.0	0	0.30
2	Ref32	50	16.0	0	0.32
3	Ref35	50	17.5	0	0.35
4	SAP04	50	16.0	0.4	0.30+0.02
5	SAP08	50	16.0	0.8	0.30+0.02
6	SAP12	50	16.0	1.2	0.30+0.02
7	SAP10	50	17.5	1.0	0.30+0.05
8	SAP20	50	17.5	2.0	0.30+0.05
9	SAP40	50	17.5	4.0	0.30+0.05

3.2.2 Mixing and Testing Procedure

The materials were proportioned according to the mix design and stored in the laboratory at 21±2°C for 24 h. The mixing was performed by hand as per the calorimeter manufacturer recommendations while ensuring uniform mixing of the material. The mixing procedure for dry SAP was as follow: 1) Mix SAP and cement for 10 s; 2) Add water with superplasticizer to the mixture; 3) Mix for 1 min. For pre-saturated SAP, the mixing procedure was: 1) Add entraining water to the SAP; 2) Wait for 10 min; 3) Mix cement and water for 1 min; 4) Add the saturated SAP and mix for 30 s. Immediately after mixing, the specimen was placed in the calorimeter which was set to 20.1ºC. Measurements were taken every minute for the first 24 h and then every 10 min for 66 h using isothermal calorimeter I-Cal 8000 HPC and according to ASTM C1679 [26]. Three repeats were carried out per mix.

An exploratory NMR experiment was also performed on 3 pastes: Ref30, Ref32, and SAP08. A Bruker Avance 300 MHz wide-bore spectrometer NMR was used, with a Diff50 gradient probe and 8 mm ^{1}H RF insert. Carr-Purcell-Meiboom-Gill (CPMG) pulse sequence [27] was used for transverse NMR relaxation time (T_2) determination of bulk sample. Up to 50 echoes were collected with the echo-time progressively decreased from 150 μs to 60 μs as the sample dried out; the 90° pulse length was 7.1 μs; and the relaxation

delay of 1.5 s. Obtained spectra were processed using Bruker TopSpin 3.5 software. The samples were mixed in a small mixer on high speed for 2 min, then 1 min of rest followed by an additional minute of mixing. For the mixes with SAP, the SAP was added after the cement paste was mixed then everything was mixed for an additional minute. The samples were then poured into small vials to form samples with height of approximately 10 mm and diameter of approximately 6 mm.

3.3 Results

The average exothermic HOH and heat flow results with corresponding one standard deviation are presented in Fig. 3.1 and Fig. 3.2, respectively, for the reference pastes. Up to 36 h there is no statistically significant difference between the HOH of the reference pastes, with a P-value of 0.13 at a 95% confidence level [28]. After 55 h, a significant statistical difference between the HOHs of the reference pastes was observed with a P-value of 0.02. The paste with w/c of 0.35, Ref35, has the highest heat of hydration while Ref30 has the lowest total heat of hydration at 90 h. Pastes with higher w/c will produce a higher HOH since there is more water available for the reaction to proceed, while the reaction will slow down sooner in the pastes with lower w/c as water becomes limited [17,21,29]. From the heat flow peaks of the plain pastes, Fig. 3.2, it is observed that the peak value occurs earlier in the pastes with lower w/c, which is expected as pastes with lower water content reach the critical concentration of alkalis earlier initiating the start of hydration [17,30,31].

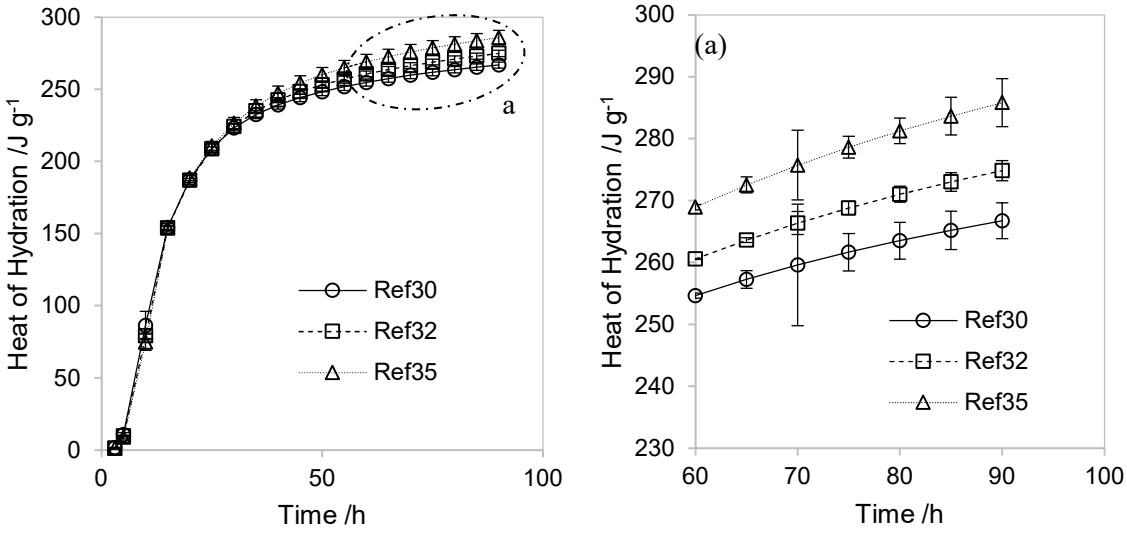

Fig. 3.1 Average heat of hydration for reference mixes with one standard deviation

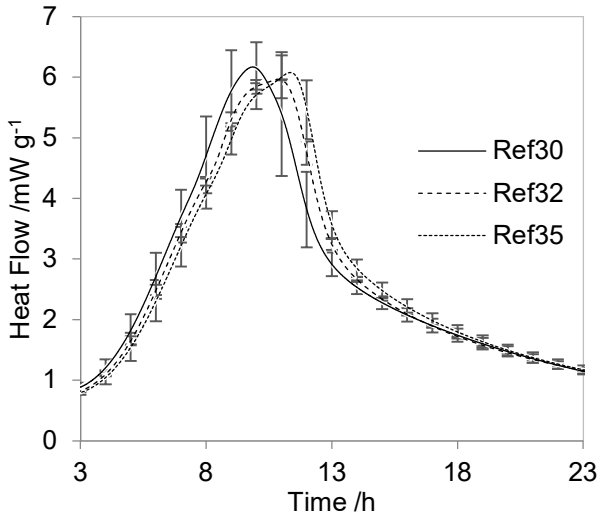

Fig. 3.2 Average heat flow of reference mixes for the first 24 h with standard deviation

The average results and standard deviation of 3 tests for the pastes mixed using dry SAP are presented in Fig. 3.3 to Fig. 3.6. For the pastes with w/c of 0.30+0.02 and three dosage levels, SAP04, SAP08 and SAP10, statistically there is no significant difference between their HOH values at 90 h with P-value equals to 0.41. These results indicate that for a low amount of IC, the hydration process is not sensitive to the range of SAP dosage tested. Fig.

3.4 shows a short delay in the development of SAP12 heat flow, however the delay does not appear to affect the overall hydration process. For the pastes with w/c of 0.30+0.05, referring to SAP10, SAP20 and SAP40, there is a visible difference in the HOH with the addition of more SAP. Statistically, the P-value is equal to 0.0002. These results reveal that the addition of excess SAP yields a significant decrease in the heat of hydration. This implies that the higher dosage of SAP is potentially causing agglomeration and thus limiting the accessibility of the IC water to the paste. Fig. 3.6 shows a significant depression of the hydration peak with SAP40. It is postulated that as the SAP content increases the likelihood of particle agglomeration increases, resulting in greater spacing between the SAP particles. Accordingly, the SAP absorbed water becomes less accessible with the reduced porosity of the cement paste.

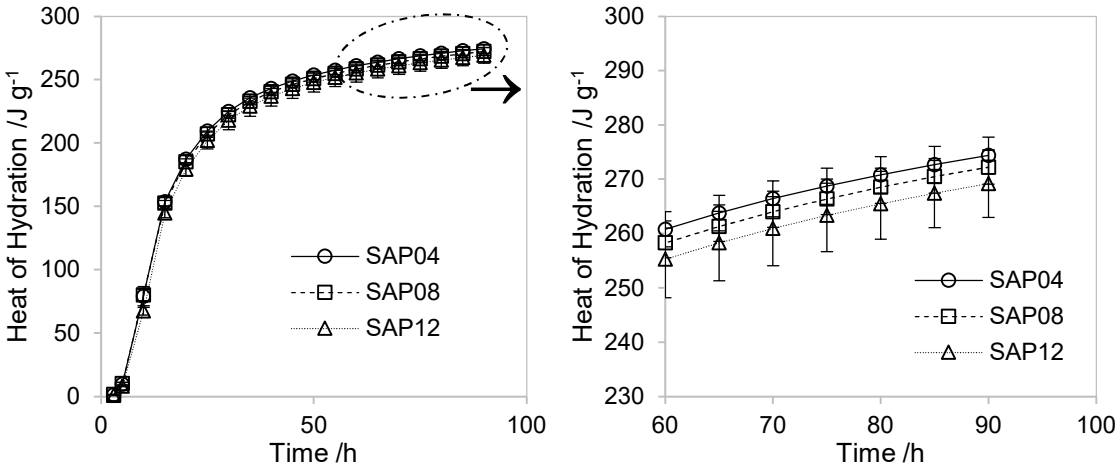

Fig. 3.3 Average heat of hydration of pastes with w/c=0.30+0.02

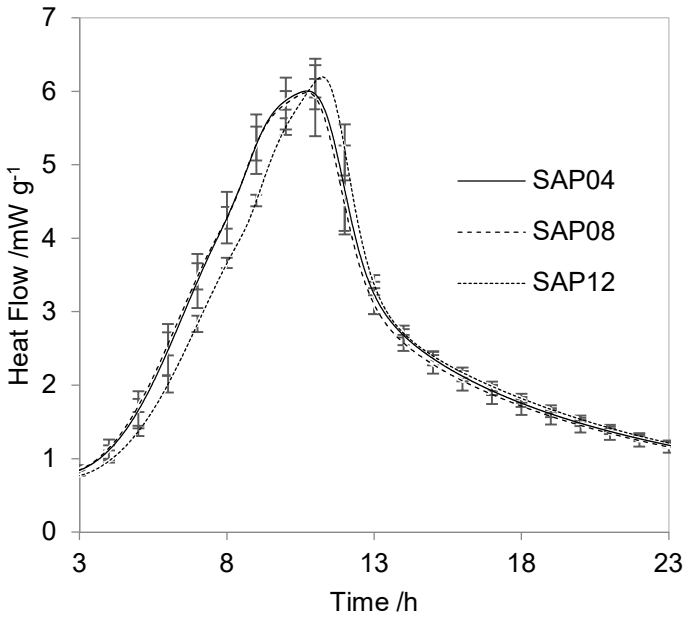

Fig. 3.4 Average heat flow of pastes with w/c=0.30+0.02

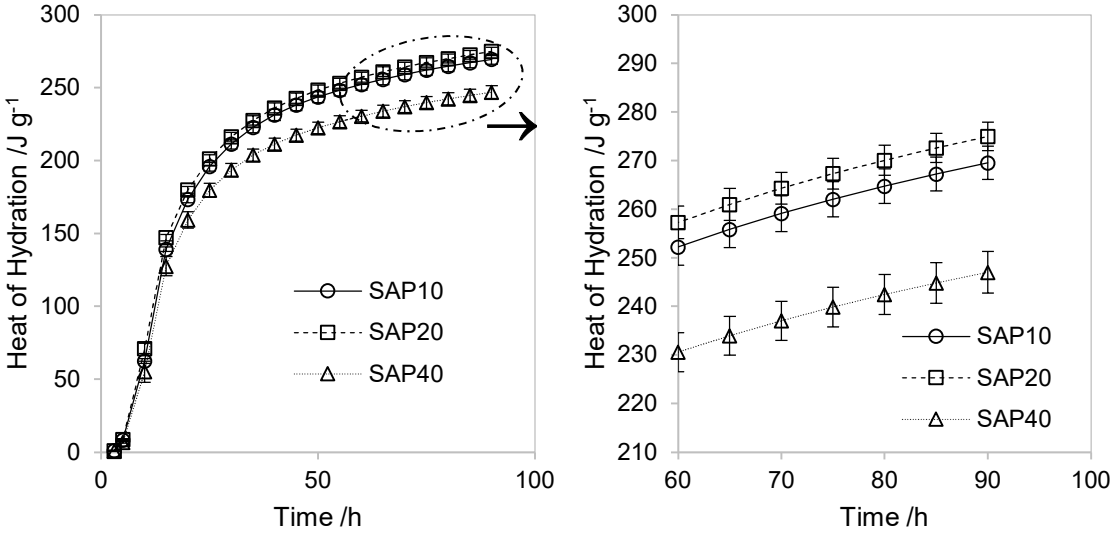

Fig. 3.5 Average heat of hydration of pastes with w/c=0.30+0.05 where SAP is added to the dry material

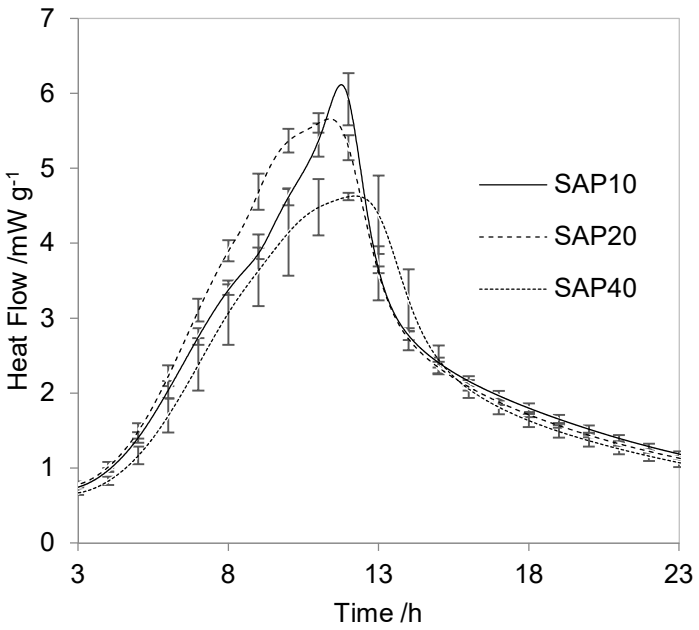

Fig. 3.6 Average heat flow of pastes with w/c=0.30+0.05

Fig. 3.7 compares the heat of hydration at 90 h based on SAP addition method. The percent difference between reference paste and addition method is given in Table 3.3. The results show that the w/c of 0.30+0.02 mixes were not affected by the addition method of SAP, however the 0.30+0.05 mixes showed a clear increase in the HOH when the SAP was added pre-saturated. It would suggest that the addition of SAP pre-saturated did not cause any significant agglomeration of the particles as previously reported [16], since no negative effects were observed. It has been hypothesized that the SAP particles absorb part of the alkalis from the cement paste pore solution, diluting the alkali content, thereby delaying the onset of cement hydration [21], so when the SAP is added wet (i.e. mostly saturated with pure water) it does not have time to absorb alkalis and no delay in the onset of hydration is observed resulting in a slightly higher HOH when the SAP is pre-wetted. When the SAP was tested with filtered pore solution it absorbed approximately 25 g g^{-1} SAP, but in distilled water it absorbed approximately 120 g g^{-1} SAP, which shows the significant effect the ionic concentration of the absorbed liquid has on the absorption capacity of the SAP. These results indicate that the difference in behaviour between the 0.30+0.02 and

0.35+0.05 is mostly caused by the ions present in water. It is postulated that at lower dosage, the uptake of water is balanced with the availability of water surrounding the SAP and with increased dosage the concentration of ions in the water surrounding the SAP increases which reduces the water uptake of the SAP. This indicates that the state of SAP added to the mix is influenced by agglomeration and the ionic concentration of surrounding water.

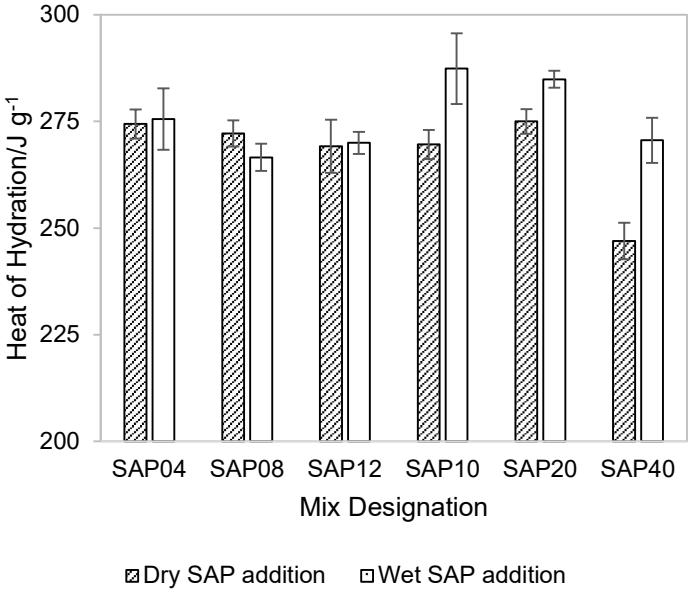

Fig. 3.7 Effect of SAP addition method of 90 h HOH

Table 3.3 Percent difference between paste with SAP and corresponding reference paste

	% Difference of 90 h HOH	
	Dry SAP addition	Wet SAP addition
SAP04	-0.2	0.3
SAP08	-1.0	-3.0
SAP12	-2.1	-1.8
SAP10	-5.7	0.6
SAP20	-3.8	-0.3
SAP40	-13.6	-5.3

From the NMR analysis, three distinct types of water can be observed for pastes with SAP. While the ^{1}H NMR spectrum of the bulk sample consists of the single peak (Fig. 3.8a), the information regarding water content in the paste was extracted by the transverse magnetization decay measurement (T_2 relaxation). As shown on Fig. 3.8b, the best fit is achieved by triple exponential decay, with well-distinct transverse relaxation times corresponding to gel, capillary and free water or water in the SAP. The greater the interaction between water and a solid structure (i.e. the finer the pore size) the shorter the T_2. Notably SAP water has relaxation time initially of about 65 ms which is much longer than the paste water but shorter than pure water (T_2>100 ms). Water, which is classified as gel water with a pore size ranging from 2.5 to 10 nm, correspond to T_2 values of 0.07 to 0.33 m. Capillary water with a pore size of 10 to 50 nm correspond to T_2 values of 1.34 to 6.7 ms [32,33].The normalized intensity of the three water phases for the pastes tested are presented in Fig. 3.8c. The signal intensity of the SAP begins to decrease as soon as the hydration reaction begins, corresponding to a decrease in the capillary water and increase in gel water. For SAP08, the SAP water signal decreases to an almost negligible amount at about 40 h, which would suggest that most of this type of water is used up by this time. From the intensity results, the initial amount of water in SAP was estimated to be 10-14% of the total water. The 0.30+0.02 paste is proportioned so that 0.02 of the water is contained within the SAP which is 6.25% of the total water. Clearly the larger SAP water signal from the NMR shows that it absorbed more water than intended. This confirms the postulation

that initially the concentration of ions in water surrounding the SAP is negligible resulting in a higher uptake than the approximated value of 25 g g^{-1} SAP.

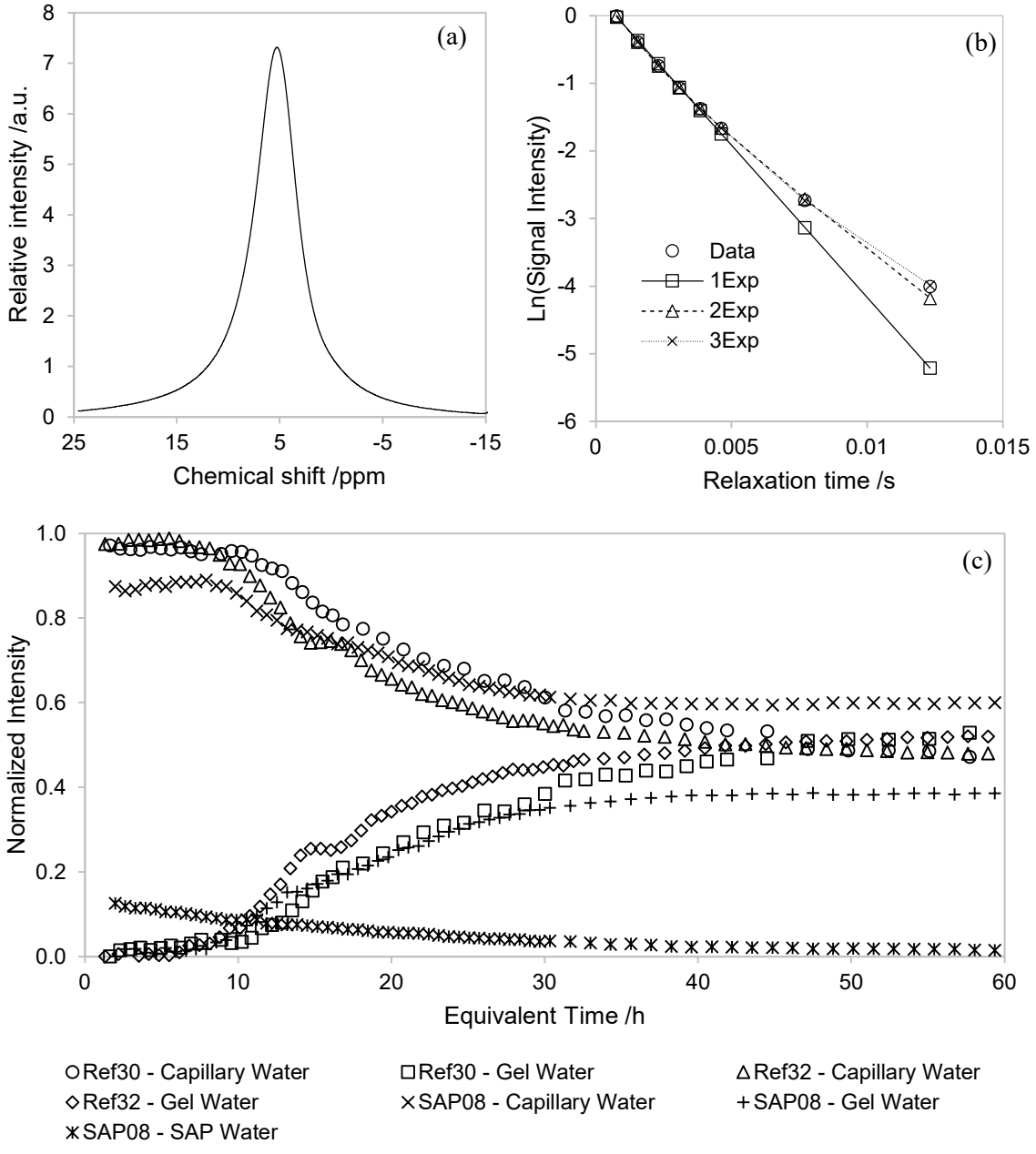

Fig. 3.8 (a) Example of ^{1}H NMR spectrum collected for Ref30 sample; (b) T_2 fit with single, double and triple exponential decay of the signal shown in panel (a); (c) relative distribution of water in the samples calculated based on NMR data

Fig. 3.9 shows the normalized NMR gel water intensity and the heat of hydration corresponding to SAP08 pastes. It is notable that the NMR water intensities begin to change at approximately the same time as the heat generation begins. Up to about 17 h, the measured reaction rate is the same for both NMR and calorimetry however, the calorimetry results thereafter indicate a decrease in the HOH rate whereas the NMR results maintain the same rate up to about 30 h after which the captured rate plateaus. The difference in the results, albeit not significant, is attributed to the resolution of the NMR ability to capture the water phases at these low concentrations [34].

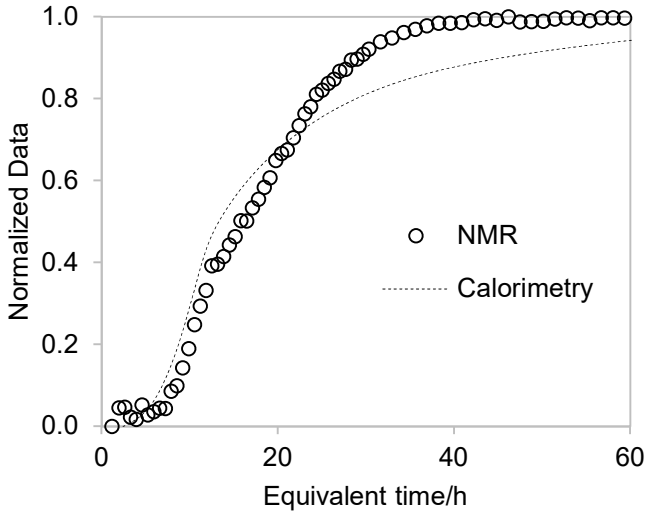

Fig. 3.9 Comparing normalized NMR intensities with normalized heat of hydration of SAP08

3.4 Analysis and Discussion

Analysis of Variance (ANOVA) with a 95% confidence shows that statistically, there is a significant difference between the means of the HOH at 90 h, with a P-value of $9x10^{-8}$. Fishers's Least significant difference (LSD) was performed as a post hoc analysis of the ANOVA to determine in which pair of tests the difference is significant [28]. LSD value greater than 6.6 implies that the difference between the compared means is statistically significant. The results, given in Table 3.4, reveal that the differences between the

0.30+0.02 pastes, namely SAP04, SAP08 and SAP10, and Ref32 paste are not statistically significant, and the difference between Ref35 paste and all the 0.30+0.05 pastes, namely SAP10, SAP20 and SAP40, are statistically different. Moreover, the difference between SAP40 paste and SAP10 and SAP20 is statistically significant. In brief, these results indicate that the chemical reaction of pastes with IC is not equivalent to a paste with the same total w/c.

Table 3.4 Post hoc analysis of ANOVA, statistically significant difference according to LSD are underlined

	Ref32	Ref35	SAP04	SAP08	SAP12	SAP10	SAP20	SAP40
Ref30	<u>8.1</u>	<u>19.1</u>	<u>7.6</u>	5.5	2.5	2.8	<u>8.2</u>	<u>19.7</u>
Ref32		<u>11.0</u>	0.5	5.6	5.6			
Ref35						<u>16.3</u>	<u>10.9</u>	<u>38.8</u>
SAP04				2.2	5.2			
SAP08					3.0	2.7		
SAP10							5.4	<u>22.5</u>
SAP20								<u>27.9</u>

For understanding the effects of IC on the cement reaction, the HOH for each mix was fitted using two straight lines corresponding to the initial rate of cement hydration between 2.4 and 15 h and the later rate of cement hydration between 36 to 90 h. Fig. 3.10 illustrates the fitting protocol using Ref30 paste as an example. The results, given in Table 3.5, show that the linear estimate is adequate with the coefficient of determination (R^2) greater than 95% for all the mixes. Statistically, the three reference pastes are found to have the same initial reaction rate and that the rate is comparatively higher after 36 h for the pastes with higher w/c. These results, which are expected according to the literature, give confidence to the approach followed for analyzing the effects of IC on the reaction rate. When comparing the results of w/c 0.30+0.02 pastes, no significant difference is observed between their initial rate of reaction and that of the reference paste. However, the initial reaction rate of w/c 0.30+0.05 pastes are found to be slower that the reference rate. The difference in the reaction rates is likely due to the water not being freely available when it is contained within the SAP. Accordingly, the assumption that the paste with internal

curing behaves just like a paste made with free water equivalent to the internal curing water plus free water [8] depends on the dosage of the SAP. The reaction rates at later time of the 0.30+0.02 pastes and 0.30+0.05 are found to correspond to Ref0.32 and Ref0.35 pastes, respectively. These results reveal that entrained water was available for the hydration reaction between 36 and 90 h. For mitigating autogenous shrinkage, the initial reaction rate is critical as the cement hardens in the first 12 h, see Fig. 3.2, Fig. 3.4 and Fig. 3.6.

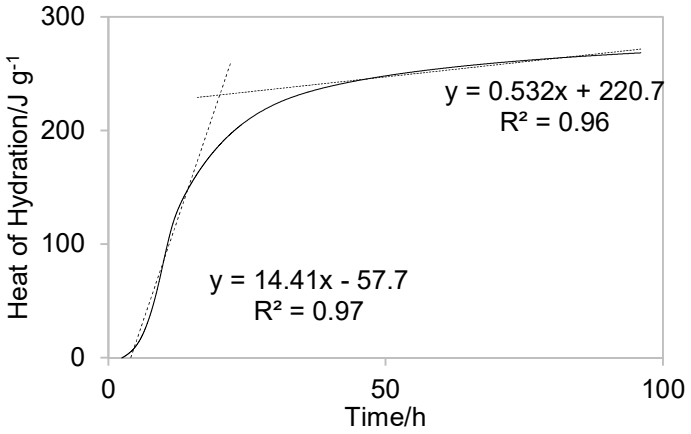

Fig. 3.10 Characterization of the HOH curve, Ref30 sample 1 for example

Table 3.5 Fitted data for HOH rate

	2.4 to 15 h			36 to 90 h		
	Heat Flow /mW g^{-1}	Standard deviation	R^2	Heat Flow /mW g^{-1}	Standard deviation	R^2
Ref30	4.05	0.11	0.97	0.147	0.003	0.96
Ref32	4.01	0.03	0.97	0.172	0.006	0.96
Ref35	4.00	0.07	0.96	0.206	0.006	0.96
SAP04	4.00	0.12	0.97	0.167	0.006	0.96
SAP08	3.96	0.08	0.97	0.169	0.006	0.96
SAP12	3.76	0.11	0.96	0.172	0.011	0.95
SAP10	3.54	0.06	0.96	0.208	0.003	0.97
SAP20	3.82	0.06	0.97	0.214	0.003	0.97
SAP40	3.19	0.25	0.96	0.194	0.003	0.97

Assuming the average absorption of SAP (K) in cement paste is 25 g g^{-1} SAP and knowing that the total amount of water for the reaction consist of the initial water in the paste with IC, $(^{w}/_{c})_{p}$, and the entrained water in the SAP, $(^{w}/_{c})_{IC}$, the corresponding w/c ratios are calculated according to [16,35]:

$$^{w}/_{c} = (^{w}/_{c})_{p} + (^{w}/_{c})_{IC} = (^{w}/_{c})_{p} + K\left(^{SAP}/_{c}\right) \quad (3.1)$$

The results, given in Table 3.6, show that the initial water decreases with increasing SAP content and supporting the computed initial cement reaction rate of Table 3.5. By plotting the HOH versus the w/c, Fig. 3.11, the results clearly show that the reference pastes are in the range tested and that the corresponding HOH is linearly related to the w/c (R^2=0.999). For the IC pastes, however, although there is no correlation between the HOH and their total w/c, results of Fig. 3.12 show a strong linear relationship between the HOH rate and the total w/c (R^2=0.92).

Table 3.6 Paste w/c and IC w/c based on Eq. (3.1)

	(w/c) paste	(w/c) IC
Ref30	0.30	0.00
Ref32	0.32	0.00
Ref35	0.35	0.00
SAP04	0.31	0.01
SAP08	0.30	0.02
SAP12	0.29	0.03
SAP10	0.33	0.03
SAP20	0.30	0.05
SAP40	0.25	0.10

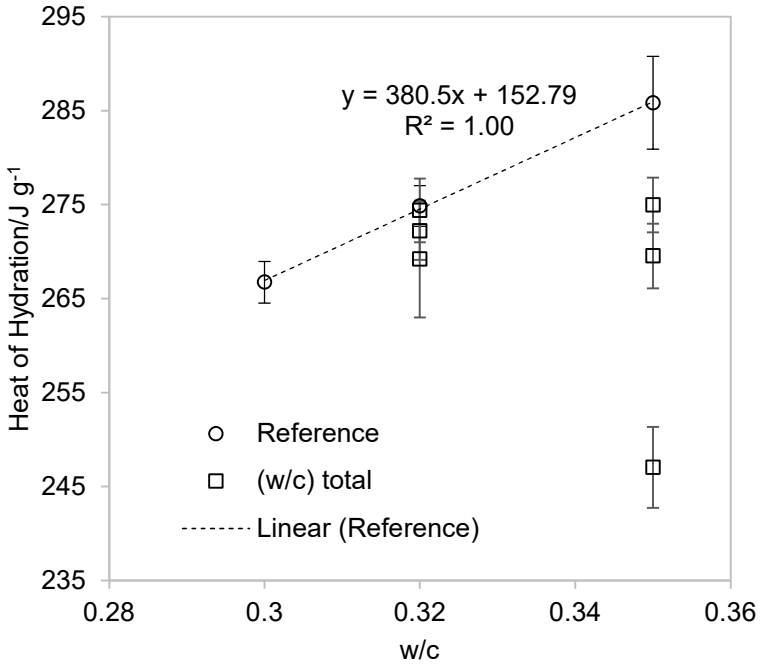

Fig. 3.11 Total w/c versus HOH at 90 h

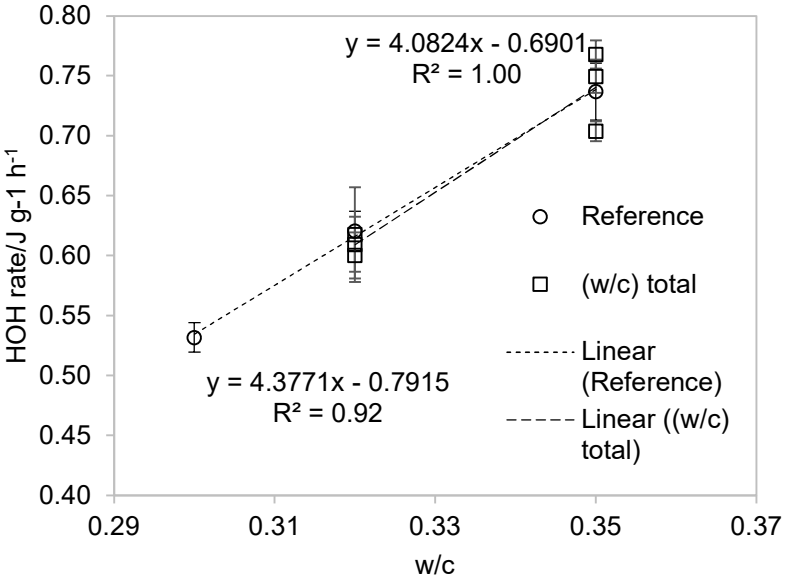

Fig. 3.12 Total and paste w/c versus HOH rate between 36 and 90 h

Using Powers' model [36], porosity of the paste, p_p is related to the $(w/c)_p$ not the total w/c according to [35]:

$$p_p = \frac{(w/c)_p}{(w/c)_p + \rho_w/\rho_c} \tag{3.2}$$

The relationship between porosity and HOH is linear with R^2 equal to 0.84 as shown in Fig. 3.13. Given that the HOH is directly related to degree of hydration, then degree of hydration is also linearly proportional to p_p when IC is used.

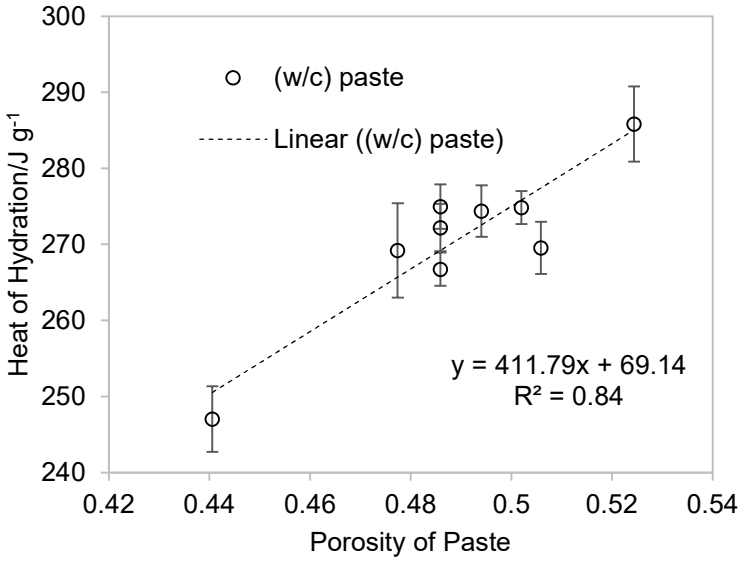

Fig. 3.13 Effect of paste porosity on HOH at 90 h

Fig. 3.14 shows schematically even distribution of SAP in cement paste. Assuming that the SAP particles are spherical, of equal size, and with the same absorption capacity, then the initial porosity of each paste is p_p according to Eq. (3.2). Consequently, p_p for the 0.30+0.02 and for the 0.30+0.05 pastes are equal to p_p of a w/c of 0.30 paste. The ability of water to diffuse from the SAP to the hydrating cement pastes depends on two factors: the porosity of the paste through which it needs to travel and the capillary pressure gradient between the SAP and the paste. Since the medium through which water needs to diffuse is

the same in both cases and the SAP spacing is spaced in a square lattice, then the diameter around each SAP particle that has efficient access to water, d, is equal for both paste (b) and paste (c) in Fig. 3.14 (i.e. $d_{0.02} = d_{0.05}$). The difference between the w/c of 0.30+0.02 paste and the 0.30+0.05 paste is then just the spacing between the particles. The spacing between the 0.30+0.02 paste SAP, $S_{0.02}$, would be higher than the spacing of the 0.30+0.05 paste, $S_{0.05}$. Theoretically, the HOH of the 0.30+0.05 paste should be higher than the 0.30+0.02 paste because a larger volume of the paste should have easier access to water. Since there is no statistically significant difference between the SAP08 and SAP10, Table 3.4, this would suggest that the SAP particles are not ideally spaced, possible due to agglomeration, thereby increasing $S_{0.05}$.

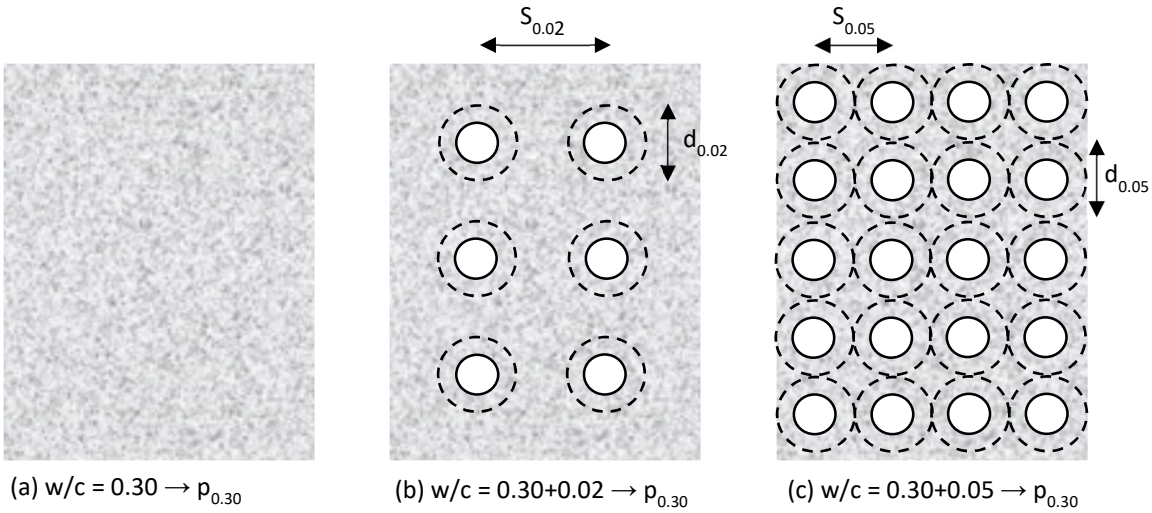

Fig. 3.14 Equal spacing of different percentage of SAP added to cement paste

The results show that the HOH of the reaction is directly dependent on the initial paste porosity, Fig. 3.13, and that providing additional water in IC does not increase the total HOH at 90 h, but the rate of the reaction increases with more IC water, Fig. 3.12. Looking at the diffusion potential from the IC material in the various pastes, the governing factor is the diffusion coefficient. In young cement paste, the diffusion coefficient is a function of the relative humidity, degree of hydration and porosity of the paste [9,37,38]. The lower

the porosity, which is a function of the degree of hydration, the shorter the distance water diffuses. From Bažant and Najjar [37] and Kim and Lee [38], the moisture diffusion coefficient can be estimated by

$$D(h) = D_1\left(m + \frac{1-m}{1+\left(\frac{1-h}{1+h_c}\right)^n}\right) \tag{3.3}$$

in which m and n are coefficients approximately equal to 0.05 and 15, respectively, h is the relative humidity, h_c is the RH when the diffusion coefficient is 50% of the initial value approximately equal to 0.80. D_1, which is the maximum D(h) when the RH is 100%, is approximated by

$$D_1 = \frac{D_{11}}{A_1 \exp(-A_2\varphi)} \tag{3.4}$$

in which φ is the capillary porosity of binder, D_{11} is 3.9×10^{-6} m^2 h^{-1}, and A_1 and A_2 are equal to 14.5 and 4.66, respectively [9]. The capillary porosity given in Eq (3.5) was modified from Wang and Park [9], which was based on the work of van Breugel [39], by incorporated the effect of IC on the porosity by means of Eq. (3.2),

$$\varphi = \frac{(w/c)_p - 0.3375\alpha}{(w/c)_p + \rho_w/\rho_c} \tag{3.5}$$

In which α is the degree of hydration, which was calculated directly using the measured HOH [40]. Accordingly, the diffusion coefficients for the pastes, calculated using Eq. (3.3) to (3.5), are plotted in Fig 3.15 and the results are summarized in Table 3.7. As shown in Fig. 3.16, good agreement is observed between HOH and the diffusion coefficient where the value of the diffusion coefficient is found to increase as the HOH increases. The results reveal that the HOH at 90 h is linearly dependent on the ability of the water to diffuse through the paste.

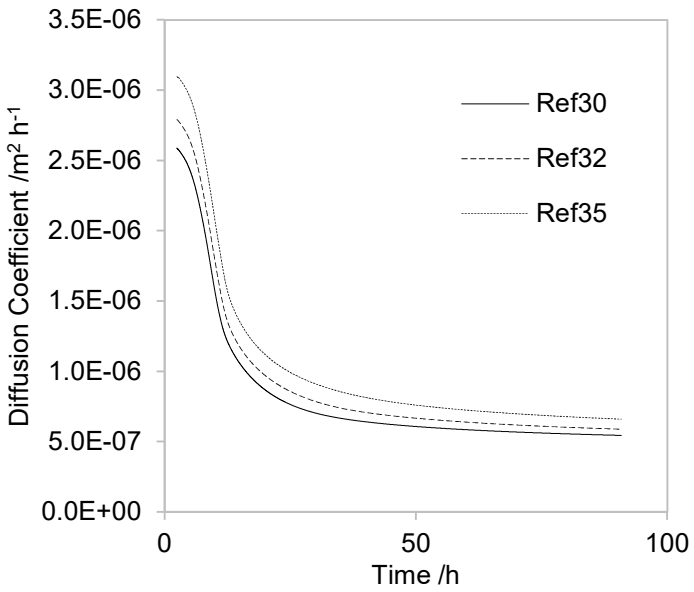

Fig 3.15 Diffusion coefficient of the reference pastes

Table 3.7 Diffusion coefficient/m^2 h^{-1}

	Initial	At 90 h
Ref30	2.6E-06	5.5E-07
Ref32	2.8E-06	5.9E-07
Ref35	3.1E-06	6.6E-07
SAP04	2.7E-06	5.6E-07
SAP08	2.6E-06	5.3E-07
SAP12	2.5E-06	5.0E-07
SAP10	2.8E-06	6.3E-07
SAP20	2.6E-06	5.2E-07
SAP40	2.1E-06	4.4E-07

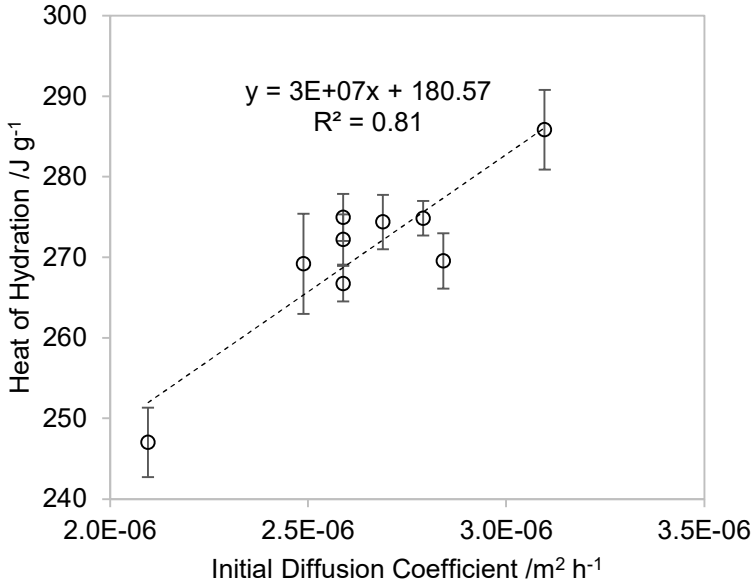

Fig. 3.16 Relation between HOH and diffusion coefficient

Modifying the spacing calculations presented by Mihaljevic et al. [35], the ideal spacing to the pastes may be determined using Eq. (3.6) and (3.7),

$$N_i = \frac{V_{SAP} V_{paste}}{\frac{\pi}{6} {\varphi_{sat}}^3} = \frac{({}^{w}/_{c})_{IC}}{{}^{w}/_{c} + {}^{\rho_w}/_{\rho_c}} \frac{V_{paste}}{\left(\frac{\pi}{6} {\varphi_{sat}}^3\right)} \tag{3.6}$$

$$s_i = \sqrt[3]{\frac{V_{paste}}{N_i}} \tag{3.7}$$

in which N_i is the ideal spacing, V_{paste} is the volume of the paste, φ_{sat} is the saturated diameter of the SAP and s_i is the ideal spacing. The spacings are presented in Fig. 3.17 versus the HOH. Since a smaller spacing did not produce a larger amount of HOH, this means that the particles agglomerated and did not adequately provide IC water to all regions of the paste.

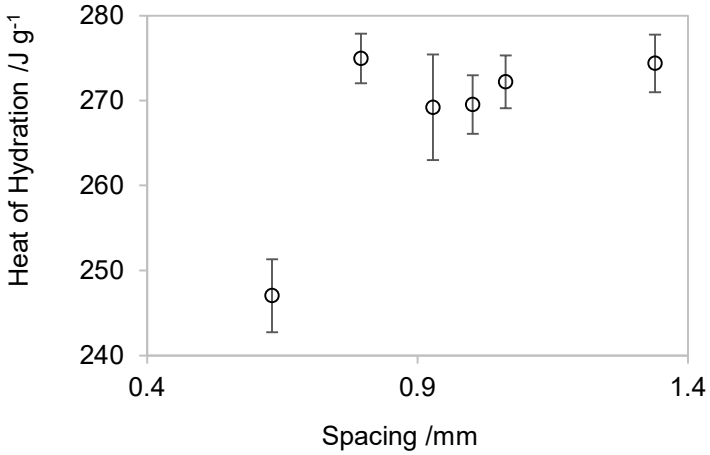

Fig. 3.17 Ideal SAP spacing versus degree of hydration

Defining the efficiency of the internal curing according to Eq. (3.8):

$$\eta_{IC} = \frac{HOH_i / N_i}{HOH_{ref} / N_{ref}} \tag{3.8}$$

Fig. 3.18 shows the efficiency of each of the IC mixes. It should be noted that N_{ref} represents the number of SAP needed to provide the exact amount of IC at ideal spacing. There is a significant loss of efficiency when the amount of SAP added exceeds the necessary amount to absorb 25 g g^{-1} SAP. For example, the efficiency of SAP12 and SAP40 is 63% and 45%, respectively, and the efficiency of SAP04 and SAP10 is almost equal to SAP08 and SAP20, respectively. Therefore, the higher dosages of SAP, which are resulting in the agglomeration of the SAP particles, are negatively affecting the efficiency. Closer analysis of the data reveals that particle agglomeration is occurring when the mass of SAP to that of entrained water is greater than 5%.

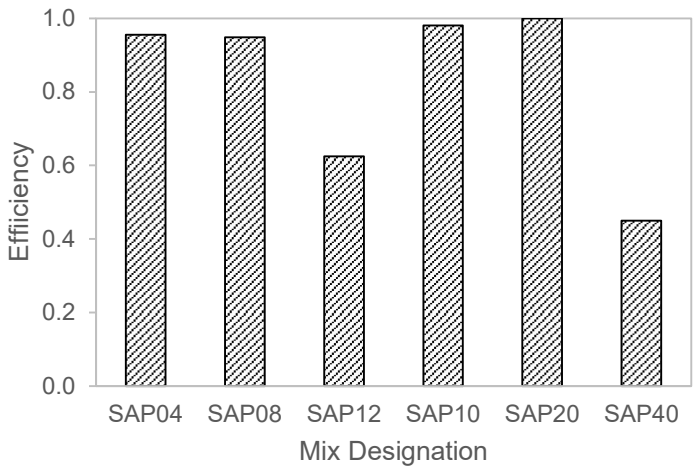

Fig. 3.18 Efficiency of IC mixes

3.5 Conclusions

From the results of isothermal calorimetry testing, the following conclusions can be drawn:

1. The higher the amount of IC the more susceptible the cement paste became to SAP overdosing.
2. Difference in the HOH between the 0.30+0.02 pastes was not statistically significant.
3. Difference in the HOH between the 0.30+0.05 pastes was statistically significant.
4. Adding pre-wetted SAP in 0.30+0.05 pastes had a higher HOH in comparison to dry SAP. NMR results confirm a larger amount of entrained water uptake when the SAP was prewetted.
5. SAP absorbs 4 to 7% more mixing water than the value estimated from of 25 g g^{-1} SAP.
6. The HOH of the cement paste with IC was not equal to that of the reference paste even if the ideal SAP dosage was used.
7. The HOH is linearly related to the w/c of the reference pastes. There is no correlation between the total w/c and the HOH of the IC pastes.
8. The HOH is related to the w/c of the paste with IC. The initial porosity of the paste significantly influences the ability of IC to provide water.

9. The HOH at 90 h is linearly dependent on the diffusion coefficient of the paste.
10. A significant loss of IC efficiency is observed when the SAP is overdosed. The efficiency dropped to 63% for SAP12 and 45% for SAP40.
11. SAP particles agglomeration occurred when the mass of SAP to that of entrained water is greater than 5%.

Acknowledgements

The authors would like to thank NSERC for funding this research and Dr. Alexander Assmann of BASF Construction Solutions GmbH, Trostberg, Germany for providing the SAP material.

References

1. Tazawa E, Miyazawa S. Influence of cement and admixture on autogenous shrinkage of cement paste. Cem Concr Res. 1995;25:281–7.

2. Akcay B, Tasdemir MA. Optimisation of using lightweight aggregates in mitigating autogenous deformation of concrete. Constr Build Mater. 2009;23:353–63.

3. Henkensiefken R, Bentz D, Nantung T, Weiss J. Volume change and cracking in internally cured mixtures made with saturated lightweight aggregate under sealed and unsealed conditions. Cem Concr Compos. 2009;31:427–37.

4. Shen D, Wang X, Cheng D, Zhang J, Jiang G. Effect of internal curing with super absorbent polymers on autogenous shrinkage of concrete at early age. Constr Build Mater. 2016;106:512–22.

5. Zhang J, Wang J, Ding X. Calculation of shrinkage stress in concrete structures with impact of internal curing. Eng Fract Mech. 2018;192:54–76.

6. Philleo RE. Concrete science and reality. In: Skalny J, Mindess S, editors. Mater Sci Concr II. Westerville, Ohio: American Ceramic Society; 1991. p. 1–8.

7. Bentz DP, Snyder KA. Protected paste volume in concrete. Cem Concr Res. 1999;29:1863–7.

8. Castro J, Varga ID, Weiss J. Using isothermal calorimetry to assess the water absorbed

by fine LWA during mixing. J Mater Civ Eng. 2012;24:996–1005.
9. Wang XY, Park KB. Analysis of the compressive strength development of concrete considering the interactions between hydration and drying. Cem Concr Res. 2017;102:1–15.
10. de Sensale GR, Goncalves AF. Effects of fine LWA and SAP as internal water curing agents. Int J Concr Struct Mater. 2014;8:229–38.
11. Jensen OM, Hansen PF. Water-entrained cement-based materials. Cem Concr Res. 2001;31:647–54.
12. Liu J, Ou Z, Mo J, Wang Y, Wu H. The effect of SCMs and SAP on the autogenous shrinkage and hydration process of RPC. Constr Build Mater. 2017;155:239–49.
13. Tu W, Zhu Y, Fang G, Wang X, Zhang M. Internal curing of alkali-activated fly ash-slag pastes using superabsorbent polymer. Cem Concr Res. 2019;116:179–90.
14. Esteves LP. Recommended method for measurement of absorbency of superabsorbent polymers in cement-based materials. Mater Struct. 2015;48:2397–401.
15. Johansen NA, Millard MJ, Mezencevova A, Garas VY, Kurtis KE. New method for determination of absorption capacity of internal curing agents. Cem Concr Res. 2009;39:65–8.
16. Mönnig S. Water saturated super-absorbent polymers used in high strength concrete. Otto-Graf-Journal. 2005;16:193–202.
17. Justs J, Wyrzykowski M, Bajare D, Lura P. Internal curing by superabsorbent polymers in ultra-high performance concrete. Cem Concr Res. 2015;76:82–90.
18. Kočí J, Fořt J, Mildner M, Černý R. Effect of incorporated superabsorbent polymers on workability and hydration process in cement-based materials. Int Multidiscip Sci GeoConference Surv Geol Min Ecol Manag SGEM. Albena, Bulgaria; 2019. p. 99–106.
19. Farzanian K, Pimenta Teixeira K, Perdigão Rocha I, De Sa Carneiro L, Ghahremaninezhad A. The mechanical strength, degree of hydration, and electrical resistivity of cement pastes modified with superabsorbent polymers. Constr Build Mater. 2016;109:156–65.
20. Almeida FCR, Klemm AJ. Efficiency of internal curing by superabsorbent polymers

(SAP) in PC-GGBS mortars. Cem Concr Compos. 2018;88:41–51.

21. Justs J, Wyrzykowski M, Winnefeld F, Bajare D, Lura P. Influence of superabsorbent polymers on hydration of cement pastes with low water-to-binder ratio. J Therm Anal Calorim. 2014;115:425–32.

22. Canadian Standards Association. Cementitious materials compendium. Toronto, ON: CSA Group; 2018.

23. Taylor HFW. Cement chemistry. 2nd ed. Thomas Telford. London; 1997.

24. Schröfl C, Snoeck D, Mechtcherine V. A review of characterisation methods for superabsorbent polymer (SAP) samples to be used in cement-based construction materials: report of the RILEM TC 260-RSC. Mater Struct Constr. 2017;50:1–19.

25. Snoeck D, Van Tittelboom K, Steuperaert S, Dubruel P, De Belie N. Self-healing cementitious materials by the combination of microfibres and superabsorbent polymers. J Intell Mater Syst Struct. 2014;25:13–24.

26. ASTM Committee C09.48. ASTM C1679-14: Standard practice for measuring hydration kinetics of hydraulic cementitious mixtures using isothermal calorimetry. Annu B ASTM Stand Vol 0401. 2014.

27. Meiboom S, Gill D. Modified spin-echo method for measuring nuclear relaxation times. Rev Sci Instrum. 1958;29:688–91.

28. Box GE, Hunter JS, Hunter WG. Statistics for Experimenters. Hoboken, NJ, USA: Wiley; 2005.

29. Bentz DP, Peltz MA, Winpigler J. Early-age properties of cement-based materials. II: Influence of water-to-cement ratio. J Mater Civ Eng. 2009;21:512–7.

30. Hu J, Ge Z, Wang K. Influence of cement fineness and water-to-cement ratio on mortar early-age heat of hydration and set times. Constr Build Mater. 2014;50:657–63.

31. Scrivener K, Snellings R, Lothenbach B, editors. A practical guide to microstructural analysis of cementitious materials. CRC Press; 2018.

32. Muller ACA, Scrivener KL, Gajewicz AM, McDonald PJ. Use of bench-top NMR to measure the density, composition and desorption isotherm of C-S-H in cement paste. Microporous Mesoporous Mater. 2013;178:99–103.

33. Wyrzykowski M, Gajewicz-Jaromin AM, McDonald PJ, Dunstan DJ, Scrivener KL, Lura P. Water redistribution–microdiffusion in cement paste under mechanical loading evidenced by 1 H NMR. J Phys Chem C. 2019;123:16153–63.
34. Monteiro PJM, Geng G, Marchon D, Li J, Alapati P, Kurtis KE, et al. Advances in characterizing and understanding the microstructure of cementitious materials. Cem Concr Res. 2019;124:105806.
35. Mihaljevic SN, Chidiac SE, Krachkovskiy SA, Goward GR. Efficiency measure of SAP as IC material for cement using NMR-MRI. Manuscr Submitt Publ.
36. Powers TC. A discussion of cement hydration in relation to the curing of concrete. Proc Twenty-Seventh Annu Meet Highw Res Board. Washington, D.C.: Highway Research Board; 1948. p. 178–88.
37. Bažant ZP, Najjar LJ. Nonlinear water diffusion in nonsaturated concrete. Matériaux Constr. 1972;5:3–20.
38. Kim JK, Lee CS. Moisture diffusion of concrete considering self-desiccation at early ages. Cem Concr Res. 1999;29:1921–7.
39. van Breugel K. Numerical simulation of hydration and microstructural development in hardening cement paste (I): theory. Cem. Concr. Res. 1995.
40. Schindler AK, Folliard KJ. Heat of hydration models for cementitious materials. ACI Mater J. 2005;102:24–33.

4 Efficiency measure of SAP as internal curing for cement using NMR & MRI

Chidiac, S.E. , Mihaljevic, S.N., Krachkovskiy, S.A., & Goward, G.R. (2021). Efficiency measure of SAP as internal curing for cement using NMR & MRI, Construction and Building Materials, 278 122365, doi:10.1016/j.conbuildmat.2021.122365.

Abstract

Nuclear magnetic resonance and imaging was used to quantify the absorbed and desorbed water by superabsorbent polymers (SAP) and the efficiency of SAP as internal curing. SAP pore solution absorption and desorption are found, respectively, 25 g/g SAP, and inversely proportional to time and SAP content. Cement hydration rate of mixes without SAP is statistically equal to mixes with 0.2% SAP and different for 0.3% SAP. Estimated SAP spacing for mixes with 0.2% and 0.3% SAP is 0.78±0.03 and 0.67±0.05 mm, respectively. The corresponding SAP efficiency drops from 98±14% and 71±14% to 84% and 41% when accounting for particles agglomeration.

Keywords: internal curing; water movement; water absorption; water desorption; superabsorbent polymers; NMR- MRI; cement degree of hydration

4.1 Introduction

Concrete strength and durability, the two important design properties, increase by lowering the water to cement ratio (w/c) [1–3], but so does the occurrence of autogenous shrinkage due to self-desiccation [4–6]. For concrete mixtures with low w/c, a continuous supply of water is necessary to prevent self-desiccation. Internal curing (IC), using materials such as lightweight aggregate (LWA) [7–9] and superabsorbent polymers (SAP) [10–12], is the only viable option since external curing is ineffective because of densification of the concrete microstructure.

Self-desiccation which produces capillary tension is the basic mechanism driving autogenous shrinkage. The pores' internal pressure increases as the water in the capillary pores is consumed by the hydration reaction [13–15]. The corresponding capillary tension can be calculated using Young-Laplace equation, where

$$P_c = \frac{-2\gamma\cos(\theta)}{r} \tag{4.1}$$

in which P_c, P_v, γ, θ, and r are the capillary water pressure (Pa), the water vapour pressure (Pa), the surface tension of pore fluid (N/m), the liquid–solid contact angle (radians), and the meniscus radius of curvature (m), respectively. Alternatively, the capillary pressure is related to the internal equilibrium relative humidity (RH) represented by Kelvin's equation, where

$$P_c = \frac{\ln(RH)\,RT}{V_m} \tag{4.2}$$

in which R, T and V_m are respectively, the universal gas constant (8.314 J/mol K), the temperature (°K) and the molar volume of pore solution (~18×10^{-6} m^3/mol). The capillary pressure and corresponding autogenous shrinkage (ε) are correlated when assuming circular shape pores and applying Mackenzie's equation, where

$$\varepsilon = \frac{S\Delta P}{3}\left(\frac{1}{K} - \frac{1}{K_s}\right) \tag{4.3}$$

in which *S*, *K*, and K_s are the cement paste degree of saturation, the paste bulk modulus (Pa) and the bulk modulus of the solid skeleton of the cement paste (Pa), respectively [6]. Accordingly, autogenous shrinkage is inversely proportional to the pore size and directly proportional to ln(RH) [14]. Based on Richard's equation [16], the first pores to empty of water are the large ones [6,13,17], meanwhile pores are simultaneously becoming smaller as they are filled with hydration products and the RH decreases as the water in the pores is consumed by hydration [18,19]. Moreover, the cement degree of hydration, which is influenced by the cement content and type, temperature, and w/c, provides a measure of

the pore size, degree of saturation, and RH [14,15]. The presented technical brief, although well documented in the literature, is reproduced in this paper to highlight the correlation between autogenous shrinkage and pore size.

Internal curing mitigates autogenous shrinkage by supplying additional water to maintain a high RH in the paste [20] and to ensure that small pores remain saturated [6] as the degree of hydration increases [10,21]. According to Jensen and Hansen [10], theoretically a paste with w/c of 0.35 and w/c 0.30 plus an additional 0.05 of IC water should be identical in terms of degree of hydration, but are found to have a different microstructure. They attributed the discrepancy to the distribution of IC water [22,23]. This indicates that both the availability and distribution of IC water are important for developing a homogeneous dense concrete microstructure, and that the latter is a determining factor for the effectiveness of IC.

^{1}H NMR relaxometry is a non-destructive and non-invasive test method [24–26] that has been used to monitor the amount and movement of water in Portland cement paste [27,28]. The spin-spin relaxation time (T_2) provides a measure of the water phases and the corresponding signal intensity provides a measure of the amount of water [27]. For Portland cement, NMR signal is differentiated into four types of water: capillary water with $T_2 \cong 0.9$ ms, gel water with $T_2 \cong 0.25$ ms, interlayer water with $T_2 \cong 0.09$ ms, and CSH solid with $T_2 \cong 0.015$ ms [29]. When IC is added to the mixture, an additional signal was observed for the SAP water with T_2 ranging from 100 to 1000 ms [30]. Moreover, the magnetic resonance imaging (MRI) [31] is another test method that has been used to render the T_2 spatially dependent thus permitting the plotting of the water's spatial distribution with time [32].

Spatial and temporal monitoring of water movements in cement by means of NMR and MRI test methods have been well documented in the literature and this brief is to highlight relevant findings [30,33–37]. NMR relaxometry test results show a strong correlation

between the IC water released from the SAP and cement hydration and the IC water consumed within a period of approximately 2 days [27,33]. Another NMR study carried out on a large porous inclusion embedded in cement paste revealed that the inclusion absorbs water from the paste in the first 30 minutes after casting and desorbs water 5 hours later [34]. The effects of SAP addition methods on the SAP water absorption and desorption were investigated using NMR [30,35]. The results showed that pre-saturated SAP is the least effective addition method and that the dissolution of calcium ions in 0.5 w/c mixtures inhibits SAP ability to absorb water [30]. Another study using T_2 NMR found SAP absorbed more water than expected due to the low ion concentration initially in mixing water [38]. Analytically, the SAP water release kinetic was found to correlate with Powers' model [39], however the free water did not follow Powers' straight line [35].

The objectives of this study are fourfold: 1) to quantify the amount of water absorbed and desorbed by SAP; 2) to monitor the interaction of SAP water and added water and quantify their effect on the cement degree of hydration; 3) to analyze SAP spatial distribution and quantify the effects of percent SAP added on IC; and 4) to develop analytical models for determining the cement degree of hydration with and without SAP, and the efficiency of SAP. Accordingly, an experimental program was carried out to monitor the temporal and spatial distributions of water through cement paste with and without SAP using NMR and MRI. Thereafter, analytical models were derived.

4.2 Experimental program

The experimental program presents the materials, the protocol adopted for mixing, preparing, and testing the samples. The selection of cementitious material, and mixture design and proportions are first presented. The procedure set for mixing, sample preparation, and testing are then presented. This is followed by the test results.

4.2.1 Materials

White Portland cement CSA type GU-A3001 [40], SAP, and water were the materials used in this study. The low iron cement, manufactured by Federal White Cement Ltd., has a fineness of 400 m^2/kg and oxide composition listed in Table 4.1. The corresponding phases were calculated according to the Bogue equations [41]. The dry polyacrylate SAP, supplied by BASF Germany, has an average diameter of 126.5 μm ± 3.0 μm [42]. The SAP pore solution absorption of 25 g/g SAP was estimated using the simulated filtered cement slurry with a w/c of 10 and RILEM TC 260-RSC filtration method [43–45]. For reference, SAP absorption of distilled water was 120 g/g SAP.

Table 4.1 Oxide composition of Federal White Cement

Oxide	% Mass
CaO	65.10
SiO_2	21.39
Al_2O_3	6.32
Fe_2O_3	0.01
MgO	0.25
SO_3	3.25
Phase	**% Mass**
C_3S	59.93
C_2S	16.13
C_3A	16.73
C_4AF	0.03

Three cement paste mixes were developed for this study as given in Table 4.2. The amount of SAP as IC material for mixes SAP2 and SAP3 was determined using the cement slurry absorption of 25 g/g SAP. The addition of SAP content will provide the opportunity to investigate the effects of pore solution absorption and concentration of SAP on the amount of water and water distribution.

Table 4.2 Cement paste proportions

	Cement (g)	Water (g)	SAP (g/kg cement)	w/c
SAP0	750	262.5	0.0	0.35+0.00
SAP2	750	262.5	2.0	0.30+0.05
SAP3	750	262.5	3.0	0.27+0.08

4.2.2 Mixing and Testing Procedures

The materials were first proportioned according to the mix design and stored in the laboratory at 24±2°C for 24 h. The mixing was carried out using a Globe SP05 5-quart planetary mixer with the following sequences: For SAP0, 1) Mix water and cement for 3 min at 120 rpm; 2) Rest for 1 min; 3) Mix for 2 min at 120 rpm; For SAP2 and SAP3, 1) Mix the cement with 50% of the water for 1 min at 120 rpm; 2) Add SAP and mix for 1 min at 145 rpm; 3) Add remaining 50% of water and mix for 2 min at 145 rpm; 4) Rest for 1 min; 5) Mix for 1 min at 120 rpm. The edge of the bowl was scrapped at every "Rest" stage to minimize the loss of material. Immediately after mixing, the cement paste was placed in a glass vial that is 40 mm high and 13 mm inside diameter, sealed with parafilm tape to prevent water evaporation, then placed in the spectrometer. No segregation or bleeding was observed in the cement paste.

NMR experiments were carried out at 25°C using a Bruker Avance 300 NMR spectrometer equipped with a MicWB40 Probe in combination with the Micro2.5 Gradient System. A standard Carr-Purcell-Meiboom-Gill (CPMG) pulse sequence was used to measure the transverse relaxation time (T_2) of the bulk sample [46]. The excitation was achieved with a 44 μs 90-degree RF-pulse at 120 W. Up to 32 echos with echo delay of 300 μs were produced with signal intensities recorded after each echo. Eight scans were conducted each time with an inbetween relaxation delay of 2.5 s. CPMG pulse sequense was combined with phase encoding magnetic field gradient as described by Vashaee et al. [47] in order to map T_2 distribution within the sample along the vertical axis. Gradient pulses were 160 μs long and lineary increased in 32 steps from -7.2 to +7.2 G cm^{-1}, providing a 6.5 cm field of view with 0.2 cm resolution. Application of the magnetic field gradient introduces the

spatial variation of the spins Larmour frequency and allows to encode nucleus distribution in the sample through the phase shift of NMR signal at each pixel/slice gained during the gradient pulse. The end results were the identification and quantification of the water phase along the height of the sample. The test duration was approximately 48 h with a spectrum obtained every hour for the first 24 h and every 2 h for the remainder of the time.

Table 4.3 provides the limits adopted in this study for characterizing the gel water, capillary water, and entrained water. Accordingly, the water was classified using the T_2 time, which relates the interaction between the water molecules and the solid structure through the fast relaxation method [48]. The NMR data was then fitted using the three distinct relaxation times corresponding to three forms of water in the sample.

Table 4.3 Characterization of water phases and corresponding relaxation time

Water Phase	Diameter (nm) [36,49]	T_2 (ms)
Free water/SAP	> 50.0	> 6.700
Capillary Pores	50.0 to 10.0	6.700 to 1.340
Gel Pore	10.0 to 2.5	0.335 to 0.067
Micropores	< 2.5	undetectable by spectrometer

Isothermal calorimetry tests were performed on the cement paste mixes using an I-Cal 8000 HPC according to ASTM C1679 [50]. The mixes were tested at 20.1ºC for 90 h. Isothermal calorimetry tests were carried out to validate the NMR results [38].

4.2.3 Results

NMR results are first presented in the form of temporal average along the sample height with the corresponding standard deviation of the measured T_2 values and normalized signal intensity of the relative population of the corresponding types of water. Data points that deviated more than 3 standard deviations from the average were considered outliers and removed from the data set. Subsequently, the results were presented in the form of spatial average and standard deviation for each layer by means of the MRI technique. It should be noted that the monitored sample was 20 mm in height and that the sample was divided into 10 layers of equal thickness.

For SAP0, two distinct water signals corresponding to the capillary and gel waters were monitored. Fig. 4.1 displays the temporal variation of the average values and corresponding standard deviation for T_2 and corresponding normalized signal intensities along the sample height. The observed trend is as expected with the capillary water being consumed with time while the gel water shows an increase with time. These evidential observations are deduced from the decrease in the total signal intensity of capillary water due to its reaction with the cement particles to form the solid structure and from T_2 becoming shorter confirming the cement hydration and movement of capillary water to smaller pores. Furthermore, the low variability of the normalized signal intensity of the capillary and gel waters in the first 48 h indicates that the waters are statistically equally distributed across the sample height and that access to the capillary water have not yet been impacted by the hydration products reflected by the observed increase in the results variability thereafter.

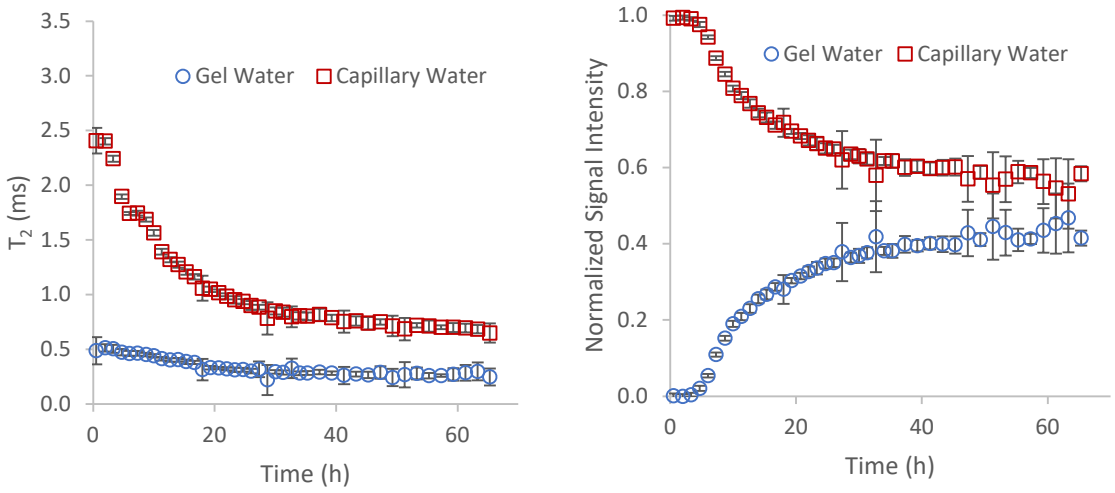

Fig. 4.1 Temporal distribution of capillary and gel waters in SAP0 by means of T_2 and normalized signal intensity

For SAP2 and SAP3, three distinct water signals were observed corresponding to the capillary, gel and SAP entrained water. Fig. 4.2 and Fig. 4.3 display the T_2 and normalized signal intensity for SAP2 and SAP3, respectively. SAP2 and SAP3's T_2 values show that the addition of SAP led to higher gel and capillary water values as reproduced in Table 4.4. Statistical analysis of the mean values to the 95% confidence level, given in Table 4.5, reveals that there is no statistical difference in the T_2 capillary water values after 2h of casting. T_2 values of SAP0 thereafter are statistically different from SAP2 and SAP3, and that the values for SAP2 and SAP3 become statistically different after 48h. This indicates that the capillary pore structure is statistically the same for all 3 mixes after 2h of casting and differs thereafter between mixes with and without SAP with the increase in cement hydration. After 48 h of casting, the capillary pore structure of SAP2 and SAP3 are also statistically different. From the gel water, the T_2 values show statistical difference when SAP is added even after 2h of casting and that the amount of SAP added, being 0.2% or 0.3% of cement content, is not statistically altering the gel pore structure up to the last measured time of 48h. These results concur with previously reported finding that the addition of SAP produces a different gel pore structure [10]. Statistical analysis of the

entrained water in the SAP reveals no statistical difference between SAP2 and SAP3 up to 48h after casting.

Capillary water results in Table 4.4 show a noticeable increase in the variation of T_2 when SAP is added to the mixture, which is indicative of varying number of SAP particles along the height of the sample. Of significance is the variation observed for T_2 corresponding to the gel water. The results show that the mixes containing SAP particles have higher variances in the first 24h after casting and lower variances at 48h when compared to SAP0. This signifies that the gel pores of the SAP mixes become more uniform across the height of the sample as more hydration products are formed. Another significant observation is the magnitude of T_2 gel water at 48h. These results indicate that SAP2 and SAP3 gel water is occupying larger size pores in comparison to SAP0 which is beneficial in reducing autogenous shrinkage [6].

Table 4.4 Comparison of T_2 values (ms)

	Gel Water			Capillary Water		
	2h	24h	48h	2h	24h	48h
SAP0	0.51±0.03	0.31±0.02	0.29±0.06	2.40±0.12	0.94±0.02	0.75±0.03
SAP2	0.76±0.12	0.42±0.05	0.39±0.04	2.69±0.44	1.33±0.28	1.35±0.25
SAP3	0.84±0.18	0.46±0.08	0.42±0.05	2.73±0.59	1.58±0.32	1.65±0.30

Table 4.5 T_2 P-values with 95% confidence level

	Time (h)	SAP0 to SAP2	SAP0 to SAP3	SAP2 to SAP3
Capillary Water	2	6.6E-02	0.16	0.87
	24	1.9E-03	3.7E-04	0.09
	48	3.7E-05	1.9E-05	0.03
Gel Water	2	7.9E-05	6.1E-04	0.25
	24	5.8E-05	1.6E-04	0.16
	48	1.2E-04	6.7E-05	0.27
SAP Water	2			0.57
	24			0.25
	48			0.35

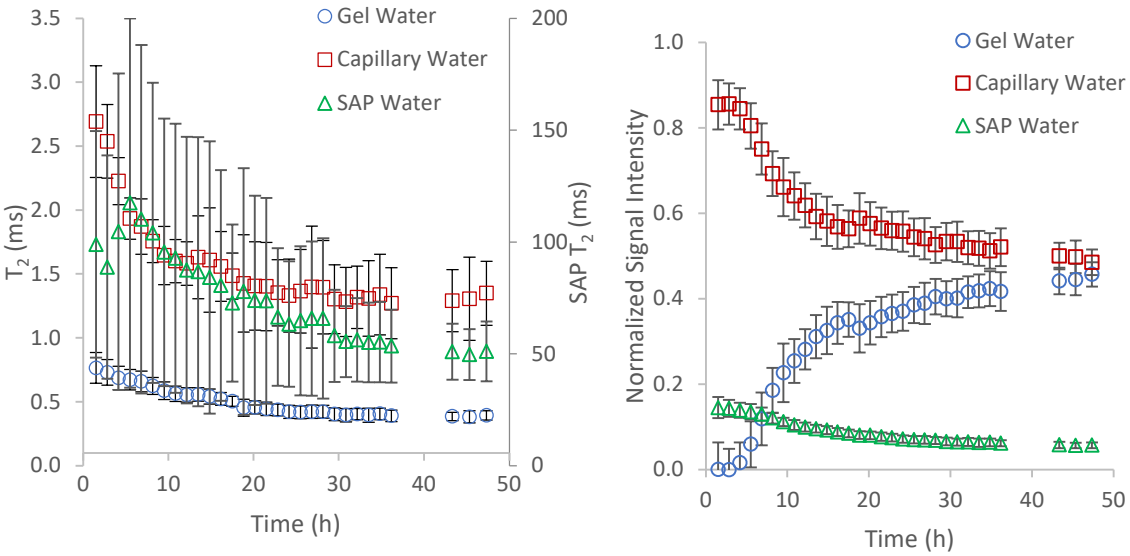

Fig. 4.2 Temporal distribution of gel, capillary, and SAP water in SAP2 by means of T_2 and normalized signal intensity

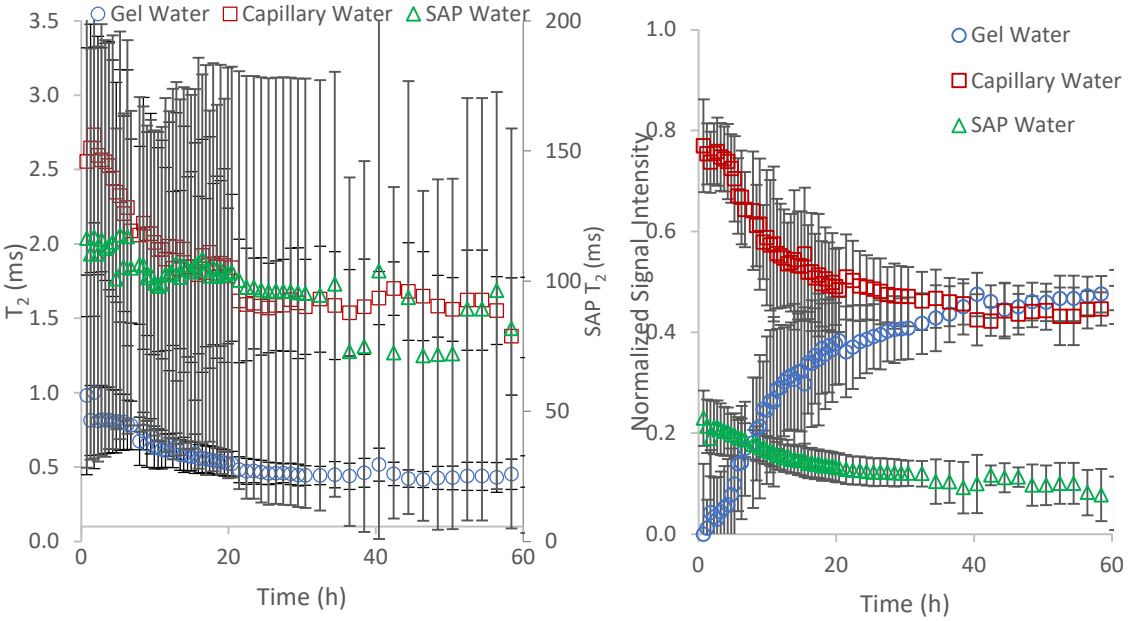

Fig. 4.3 Temporal distribution of gel, capillary, and SAP water in SAP3 by means of T_2 and normalized signal intensity

SAP water signal, observed in Fig. 4.2 and Fig. 4.3, reveals an increase when more SAP particles are added to the mix. Accordingly, 2h after casting the SAP water is found to account for 14.5% and 23.0% of the signal for SAP2 and SAP3, respectively. Therefore, the addition of 0.2% and 0.3% SAP has resulted respectively, 0.05 and 0.08 entrained water to cement content. These results confirm that 25 g/g SAP is a good estimate for the SAP water absorption in pore solution.

The effects of SAP on the rate of cement hydration, which controls concrete compressive strength development, were investigated by means of cement pore gel formation. Recognizing that cement hydration is best described mathematically by [51,52],

$$\alpha = \alpha_u exp\left[-\left(\frac{\tau}{t}\right)^{\beta}\right] \tag{4.4}$$

in which α_u, τ, and β are the ultimate degree of hydration, the hydration time parameter (h), and the hydration shape parameter, respectively. And, α_u can be quantified using the following relationship [51,53]

$$\alpha_u = \frac{1.031\, w/c}{0.194 + w/c} \tag{4.5}$$

Given that cement pore gel formation, I_{gel}, and cement degree of hydration are mutually dependent, Eq. (4.4) was adapted for this study as follows,

$$I_{gel} = I_{gel_u} exp\left[-\left(\frac{\tau}{t}\right)^{\beta}\right] \tag{4.6}$$

The fitted parameters τ and β were determined by regression analysis. The corresponding results presented in Fig. 4.4, yield a very good fit for I_{gel} with an R^2 value of 94%, 79%, and 68% for SAP0, SAP2, and SAP3, respectively. By analogy, the results reveal that the mixes with the highest amount of SAP has the highest α, and the hydration shape factor decreases with increasing amount of SAP. The former suggests that the addition of SAP affords the cement access to water for a longer period and the latter implies that the mixes with no entrained water have a faster cement reaction rate as visually displayed by Fig. 4.5. Statistical analysis by means of a t-test revealed that a significant difference between the

regression coefficients except the hydration shape factor of SAP0 and SAP2 with a P-value of 0.40. This implies that the cement hydration rate for SAP0 and SAP2 are statistically equal.

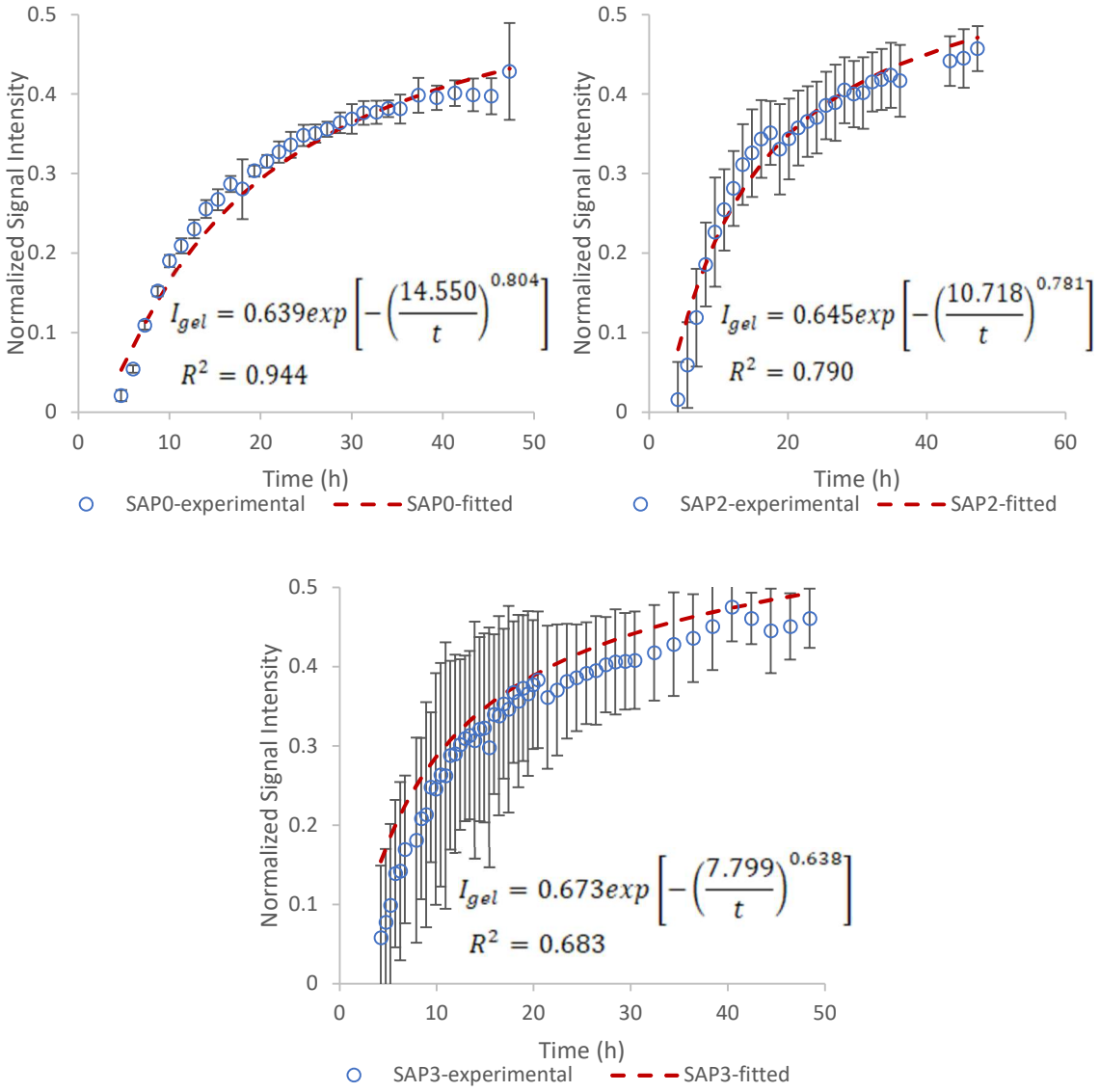

Fig. 4.4 Temporal distribution of measured and mathematically fitted gel water

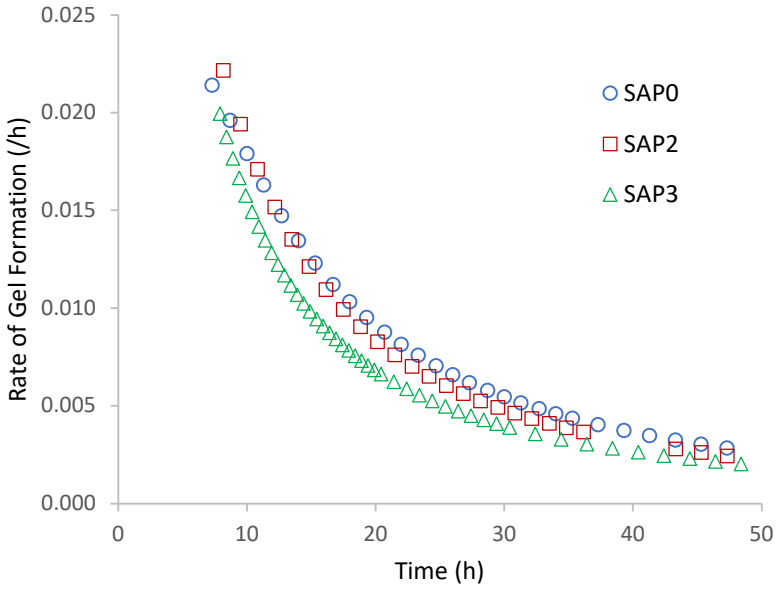

Fig. 4.5 Temporal rate distribution of mathematically fitted gel water

The desorption of SAP water was investigated to uncover any association between SAP content and the release of SAP water. Recognizing that water desorption in porous media obeys two mass transport phenomena, sorption and diffusion with the former occurring first and for a short period, whereas the latter is the most dominant and on-going process. Accordingly, the first 4 h data points are not considered as they are found to follow a different water movement pattern in comparison to the rest of the data. The natural logarithmic function given below is found to capture well the water content in SAP, I_{SAP}, and time relationship as shown in Fig. 4.6.

$$I_{SAP} = A\ln(t) + B \tag{4.7}$$

The corresponding coefficient of determination is 85% and 47% for SAP2 and SAP3. The kinetic relationship, which rewritten as

$$e^{I_{SAP}} = e^{B}t^{A} = Ct^{A} \tag{4.8}$$

reveals that the water desorption decreases with increasing SAP content. The water desorption rate, shown in Fig. 4.7, reveals that SAP2 has a slightly higher rate of

desorption. Statistically, there is a significant difference between the regression coefficients of SAP2 and SAP3. The rate of SAP desorption given by

$$\dot{I}_{SAP} = \frac{A}{t} \tag{4.9}$$

Statistically, there is a significant difference between SAP2 and SAP3 rate of desorption.

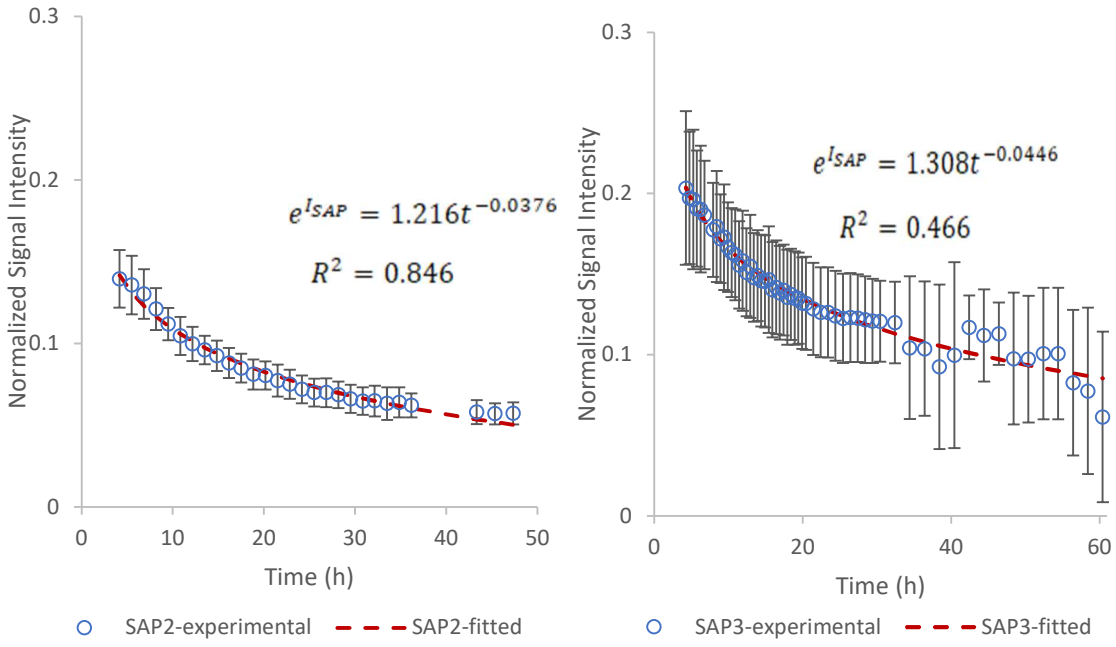

Fig. 4.6 Temporal distribution of measured and mathematically fitted SAP water desorption

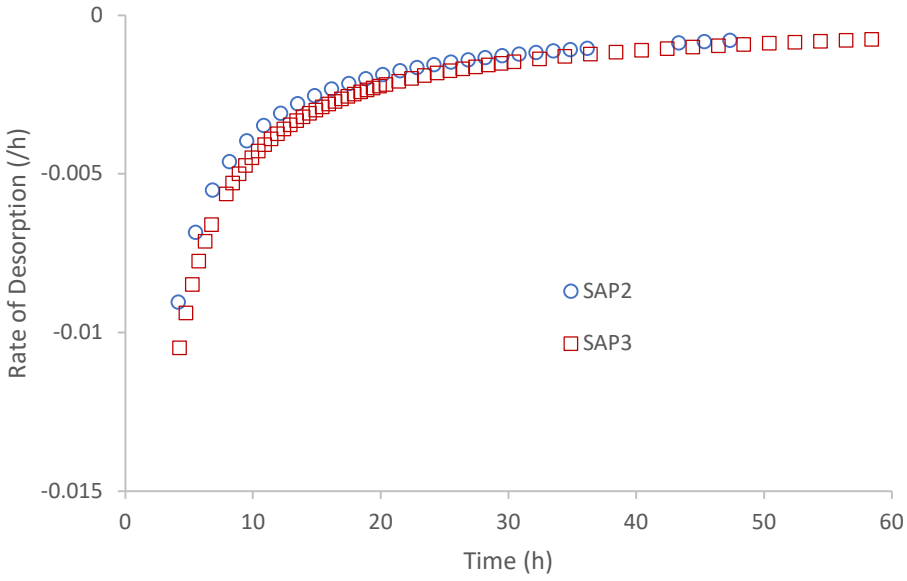

Fig. 4.7 Temporal rate distribution of mathematically fitted SAP water desorption

The water spatial distribution corresponding to the sample 10 vertical layers shown in Fig. 4.8, Fig. 4.9, and Fig. 4.10 for SAP0, SAP2, and SAP3, respectively, allows for a closer examination of the different water types and distribution. Results shown in Fig. 4.8 indicate a uniform and consistent capillary and gel water distribution across the layers and along the height represented by the standard deviation and straightness of the horizontal line, respectively. The capillary and gel water variances across the layer and along the height are found to slightly increase with time reflecting the incongruent dissolution of cement particles. The addition of SAP is found to increase the variances in the layer's capillary and gel water as well as their distribution along the height. SAP2 capillary and gel water are found to have slightly higher and inconsistent variances per layer in comparison to SAP3 as cement hydrates. However, SAP2 water distribution is more uniform when compared to SAP3. This suggests that increasing the SAP dosage has yielded a slight improvement for a consistent water sink and source per layer, but a much worse distribution system across the sample height. This finding is further supported by the SAP water variances. Increasing the SAP dosage has yielded higher variances per layer and along the sample height. Moreover, the results show that the amount of SAP water available for

cement hydration on average decrease by a factor of 3 and 2 for SAP2 and SAP3, respectively. This implies that the increase of SAP dosage can prolong the availability of SAP water but recognizing that its distribution and quantity are substantially inconsistent per layer and along the height of the sample. Accordingly, SAP water release rate depends not only on the SAP chemical composition but also on its dosage [33,35].

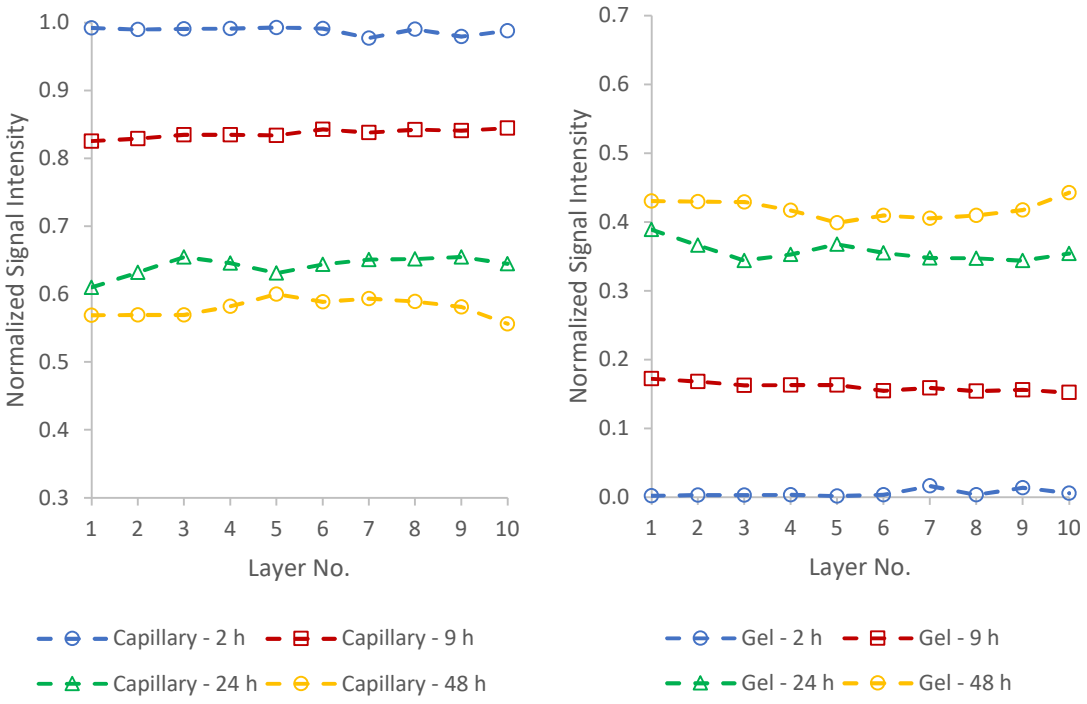

Fig. 4.8 MRI temporal and spatial water distribution of SAP0 paste

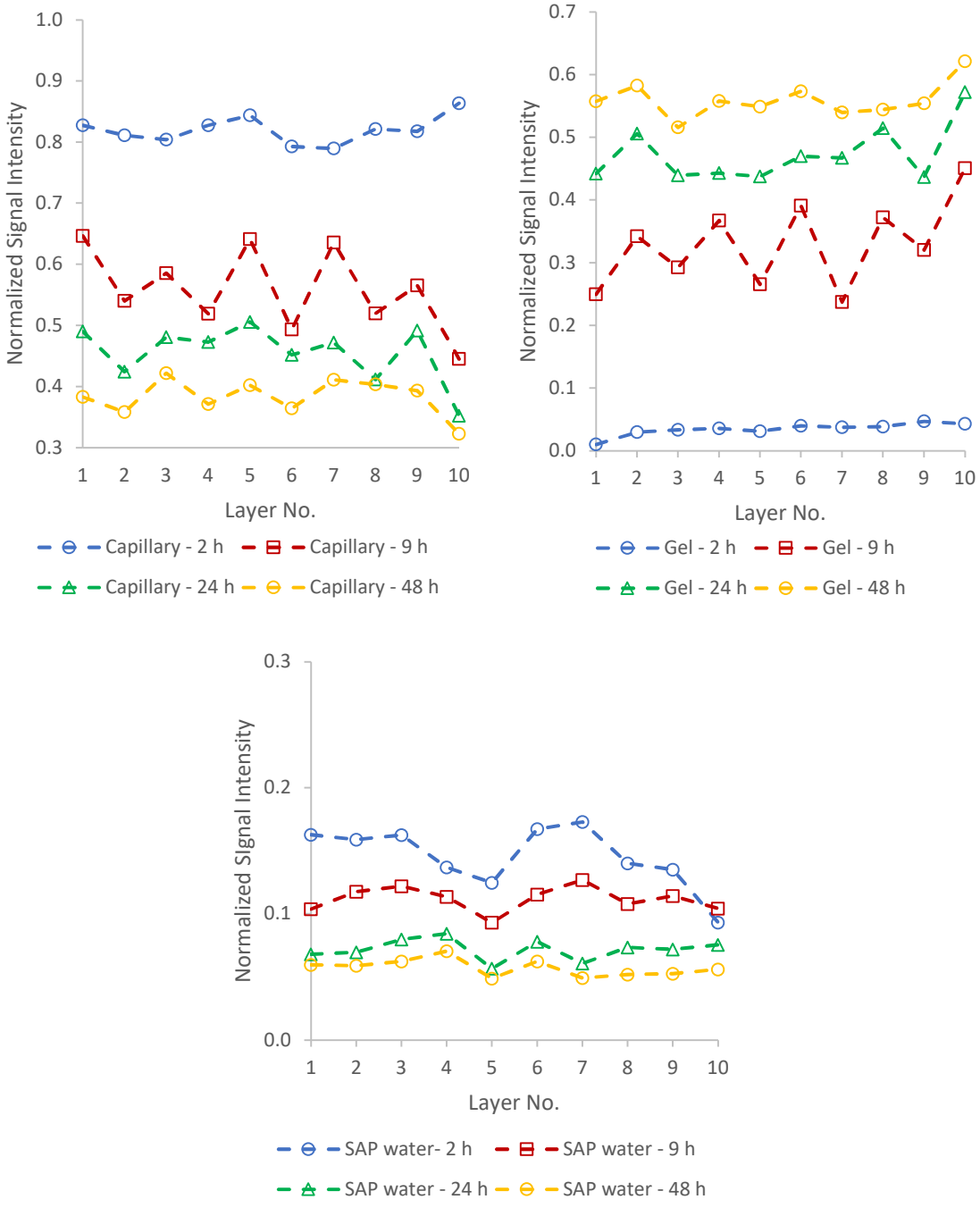

Fig. 4.9 MRI temporal and spatial water distribution of SAP2 paste

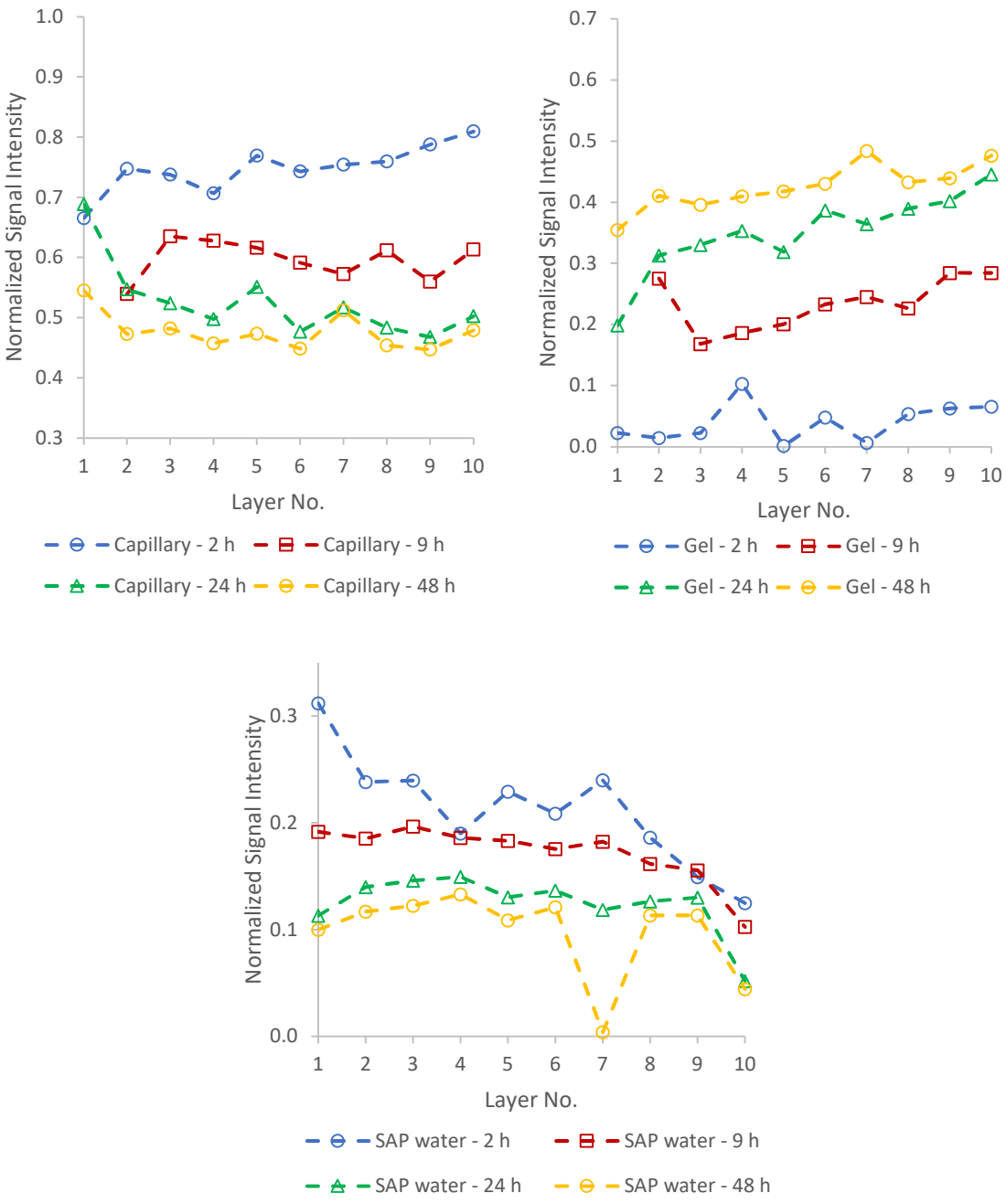

Fig. 4.10 MRI temporal and spatial water distribution of SAP3 paste

Based on the nature of the H^1 NMR testing, it can be stated that the signal detected is only from pores containing water, meaning the dry pores in the cement paste do not contribute to the signal [54]. Furthermore, based on the theory of drying [17], as water is consumed

by hydration or drying the water filled pores empty from largest to smallest. Previous work has shown that the pores in a cement paste can be estimated by NMR by applying the fast exchange model of relaxation as described by Valori et al. [24] and Halperin et al. [48]. An estimate of the average temporal pore size distribution of the water filled pores for the three cement pastes was then calculated while recognizing that the adsorbed water depends on the surface area (S) of the pores and the capillary water depends on the volume (V) of the pore. Assuming planar pores, the relaxation time can be related to the characteristic pore size (a) by the ratio of S/V and pore surface relaxivity (λ_2) using the following relationship [48]

$$\frac{1}{T_2} = \lambda_2 \frac{S}{V} = \frac{\lambda_2}{a} \tag{4.10}$$

in which λ_2 equals to 3.73×10^{-3} nm/μs [55]. Moreover, the fast relaxation method applicability condition of $6DT_2 \gg a^2$ in which $D \approx 2 \times 10^{-9}$ m^2/s for water is met in this study [24]. Accordingly, the average capillary pores, shown in Fig. 4.11, reveal that the addition of SAP to the mixture has led to a slower decrease in the size of water saturated capillary pores. After 48h, the characteristic size of the pores was approximately 5.6 ± 0.2, 10.1 ± 1.9 and 11.8 ± 1.6 nm for SAP0, SAP2 and SAP3, respectively. This shows that the water released from the SAP led to a larger saturated capillary pore size as well as larger pore size variance. By recognizing that the pressure in the capillary pores is inversely proportional to the largest water filled pore size, as shown by Eq. (4.1), and directly proportional to autogenous shrinkage, as shown by Eq. (4.2), these results show that the addition of SAP as IC reduces the effects of autogenous shrinkage as documented in the literature [6,20].

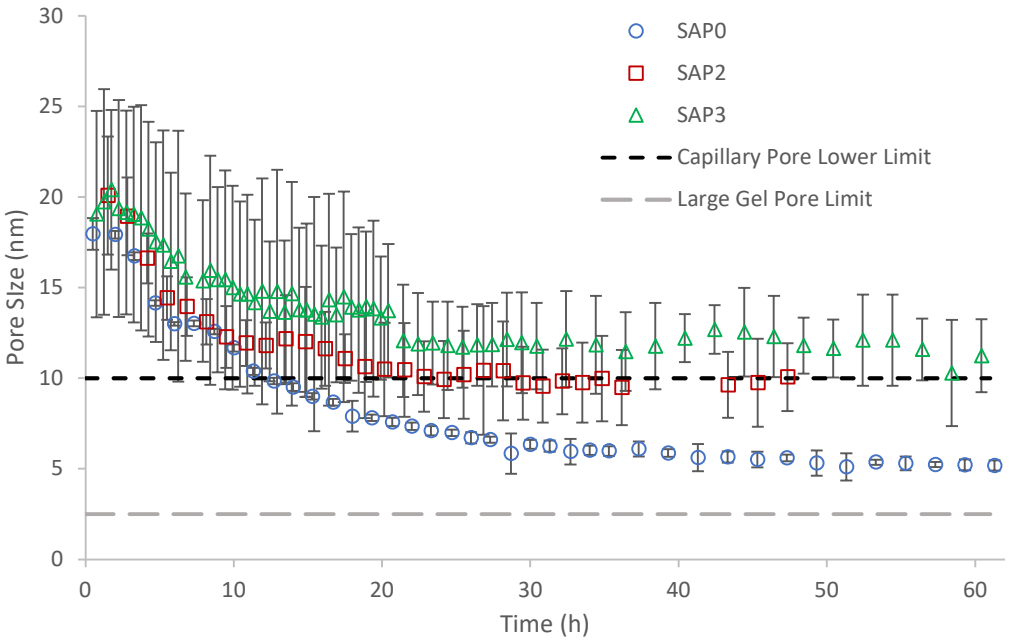

Fig. 4.11 Average characteristic capillary pore size

4.3 Data Analysis & Model development

The cement degree of hydration (α) can be determined from the NMR results with the use of Powers' model [10,39]. Accordingly, the initial porosity (p), capillary water (V_{cw}) and gel water (V_{gw}) are calculated using Eqs. (4.11), (4.12) and (4.13), respectively.

$$p = \frac{w/c}{w/c + \rho_w/\rho_c} \tag{4.11}$$

$$V_{cw} = p - 1.32(1-p)\alpha \tag{4.12}$$

$$V_{gw} = 0.60(1-p)\alpha \tag{4.13}$$

By equating the signal intensity from the normalized water signal to Powers' model normalized water volume, the gel water signal (I_{gw}) can be defined as follows,

$$I_{gw} = \frac{V_{gw}}{V_{gw} + V_{cw}} \tag{4.14}$$

Substituting Eqs. (4.12) and (4.13) into Eq. (4.14) and rearranging the terms, the cement degree of hydration is derived, where

$$\alpha = \frac{p}{\left(0.60/I_{gw} + 0.72\right)(1-p)} \tag{4.15}$$

To validate the adequacy of Eq. (4.9), the corresponding results were compared to the equivalent cement degree of hydration measured using isothermal calorimetry technique [56]. Since the NMR experiments were performed at 25.0ºC and the calorimetry experiments at 20.1ºC, the NMR times were converted to an equivalent calorimetry time as follows [57],

$$t_e = \sum_{0}^{t} \left(e^{-\frac{E}{R}\left(\frac{1}{T_r} - \frac{1}{T}\right)} \right) \Delta t \tag{4.16}$$

in which E, R, T and T_r are the activation energy (J/mol), the Universal gas constant, the curing temperature, the reference temperature of 239.15 K, respectively. SAP0 cement degree of hydration, shown in Fig. 4.12, shows excellent agreement between the two results. After about 40 h, the results begin to visually diverge slightly, with the calorimetry data predicting a slightly higher degree of hydration. However, statistically the results are found to be equal to the 95% confidence level.

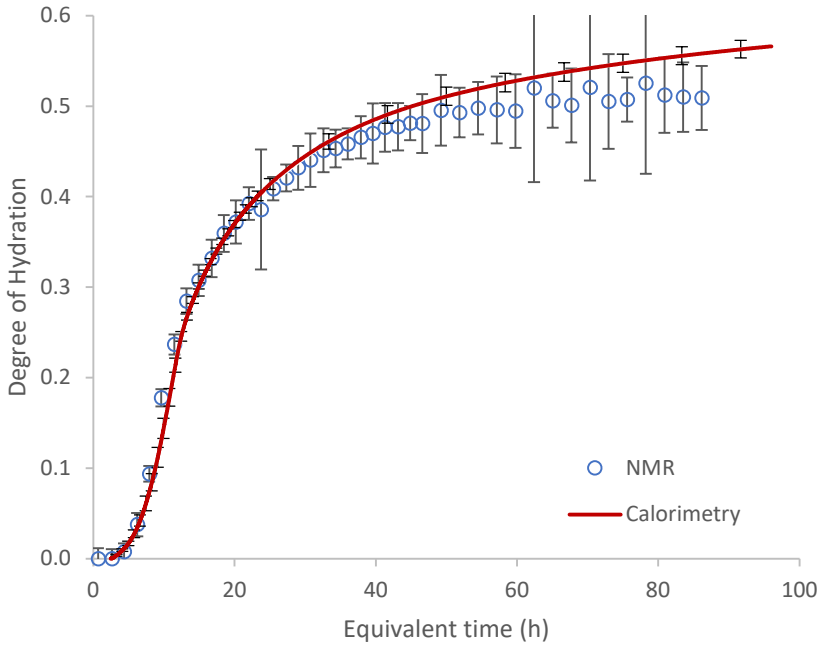

Fig. 4.12 Temporal distribution of SAP0 calorimetry and NMR cement degree of hydration

For the cement pastes containing SAP, the initial porosity model given in Eq. (4.6) was modified to account for the presence of SAP. Although we adopted Mönnig general methodology [58], the initial porosity of cement containing SAP was postulated to be additive consisting of the SAP porosity (p_{SAP}) and paste porosity (p_p) in comparison to a pooled porosity of the total paste proposed by Mönnig [58]. Accordingly, the w/c of the cement paste with SAP as IC, is calculated according to

$$w/c = (w/c)_p + (w/c)_{IC} \tag{4.17}$$

in which $(w/c)_p$ and $(w/c)_{IC}$ is the w/c components corresponding to the paste and IC, respectively. The porosity of the cement paste is first determined as follows,

$$p_p = \frac{(w/c)_p}{(w/c)_p + \rho_w/\rho_c} \tag{4.18}$$

The extra porosity from the space previously occupied by the IC material is accounted for as a space for the hydration product. The release of water from SAP results in shrinkage that leads to p_{SAP} porosity given by

$$p_{SAP} = \frac{V_{SAP-sat}}{V_T} \tag{4.19}$$

In which $V_{SAP-sat}$ and V_T are, respectively, the volume of the saturated SAP and the cement paste total volume. Using Eq. (4.14), the normalized gel water signal (I_{gw}) was then modified to account for the SAP content, where

$$I_{gw} = \frac{V_{gw}}{V_{gw} + V_{cw} + p_{SAP}} \tag{4.20}$$

Similarly, by substituting Equation (4.12) and (4.13) into (4.20) and rearranging the terms, a revised cement degree of hydration is obtained for a paste containing SAP, where

$$\alpha = \frac{p_p + p_{SAP}}{\left(0.60/I_{gw} + 0.72\right)(1 - p_p)} \tag{4.21}$$

Fig. 4.13 and Fig. 4.14 display the cement degree of hydration for SAP2 and SAP3, respectively. The plotted results correspond to Eqs. (4.9) and (4.16) and corresponding calorimetry. For the first 24 h, Eq. (4.9) appears to yield better estimates for SAP2 cement degree of hydration, although still slightly higher than the calorimetry. Subsequently, results of Eq. (4.16) are found to provide the better estimate although still slightly higher. Eq. (4.9) results are found to underestimate the degree of hydration. Similar trend is observed for SAP3. The initial estimate of $V_{SAP-sat}$ is most likely causing the higher predictions of α, and that the effect of the error diminishes with time. Statistically, Eq. (4.16) results are found equal to those obtained from calorimetry to the 95% confidence level at 24 and 48h. Whereas the results from Eq. (4.9) are not statistically equal to the calorimetry at 24h and 48h. For reference, Mönnig [58] suggestion of pooling p_{SAP} and p_p yields results that significantly underestimate the cement degree of hydration after 24 h.

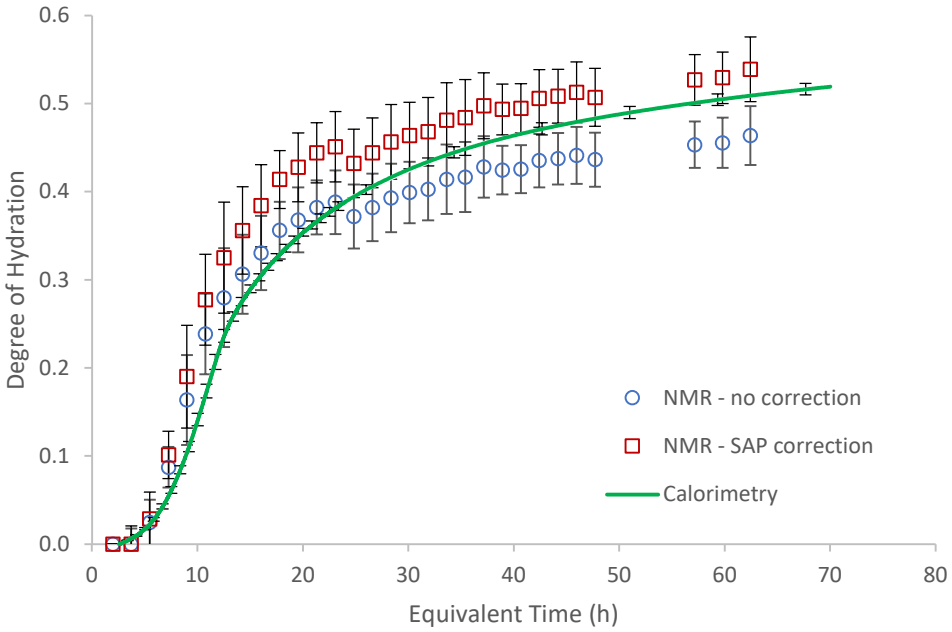

Fig. 4.13 Temporal distribution of SAP2 calorimetry, NMR, and SAP corrected NMR cement degree of hydration

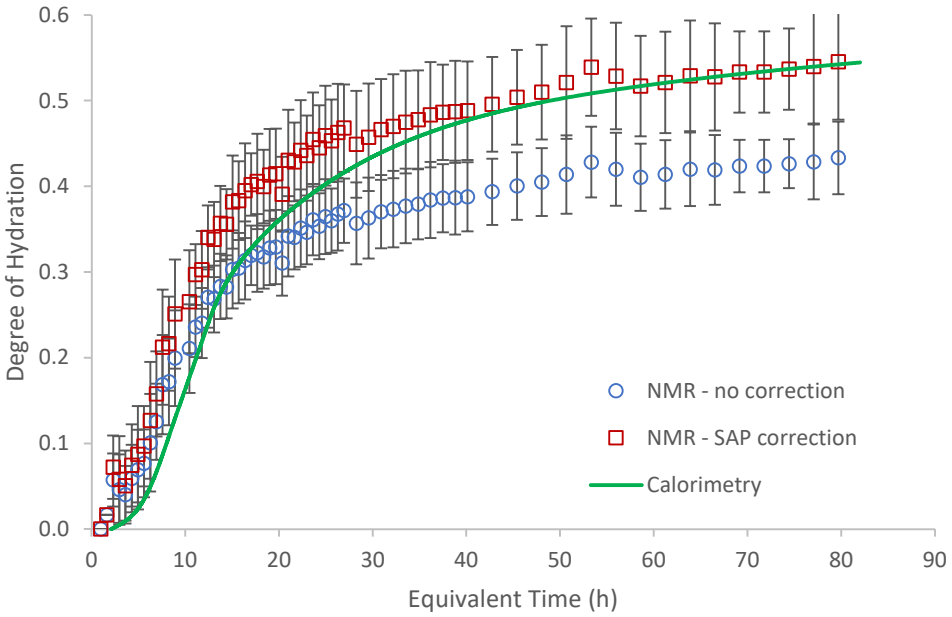

Fig. 4.14 Temporal distribution of SAP3 calorimetry, NMR, and SAP corrected NMR cement degree of hydration

For this study, a geometric model is developed to estimate the efficiency of SAP as IC in cement paste. The model assumes that the SAP particles are spherical, of equal diameter, and that every particle absorbs the same amount of solution in the cement paste environment. A dry SAP diameter, φ_{dry}, of 126.5 ± 3.0 µm was measured using the laser diffraction technique [42]. By acknowledging that the SAP absorption, K, is 25 g water/g SAP, and that the saturated SAP density can be estimated to be 1015 kg/m^3, the corresponding saturated SAP diameter, φ_{sat}, can be calculated using

$$\varphi_{sat} = \left(\frac{\rho_{SAP}}{\rho_{SAP-sat}} (1 + K) \right)^{1/3} \varphi_{dry} \tag{4.22}$$

Accordingly, a SAP particle is expected to swell to an average diameter of 416 µm which is a reasonable value when compared to the fully saturated diameter in distilled water of 655±20 µm measured using the laser diffraction technique. From the SAP saturated size and the SAP signal intensity (I_{SAP}), the number of particles for each layer (N_i) was estimated using

$$N_i = \frac{I_{SAP} V_{w_i} V_{layer}}{\frac{\pi}{6} {\varphi_{sat}}^3} \tag{4.23}$$

in which V_{layer} and V_{wi} are the volume of the layer and the initial volume of water in layer i, respectively. Knowing the total number of SAP per layer, an estimate for the particle spacing was then calculated by assuming that the particles are spaced at an equal distance (s_i) in each direction and in a cubic lattice structure, where

$$s_i = \sqrt[3]{\frac{V_{layer}}{N_i}} \tag{4.24}$$

Fig. 4.15 displays the distribution of the SAP along the sample height based on the initial signal measurement for SAP. For the ideal condition, a $(^{w}/_{c})_{IC}$ of 0.05 would be absorbed

by 536 SAP per layer at an equivalent spacing of 0.79 mm. For $(^{w}/_{c})_{IC}$ of 0.02 and 0.08, 225 and 820 particles per layer are needed at an equivalent spacing of 1.08 and 0.69 mm, respectively. Results plotted in Fig. 4.15 show that SAP2 has an average number of 563 particles with a standard deviation of 65 particles and SAP3 has 851±180 particles. The corresponding particles spacing for SAP2 and SAP3 are 0.78±0.03 mm and 0.67±0.05 mm. These results confirm that increasing the SAP dosage results in a significantly larger variance in the number of SAP and particles spacing in the paste.

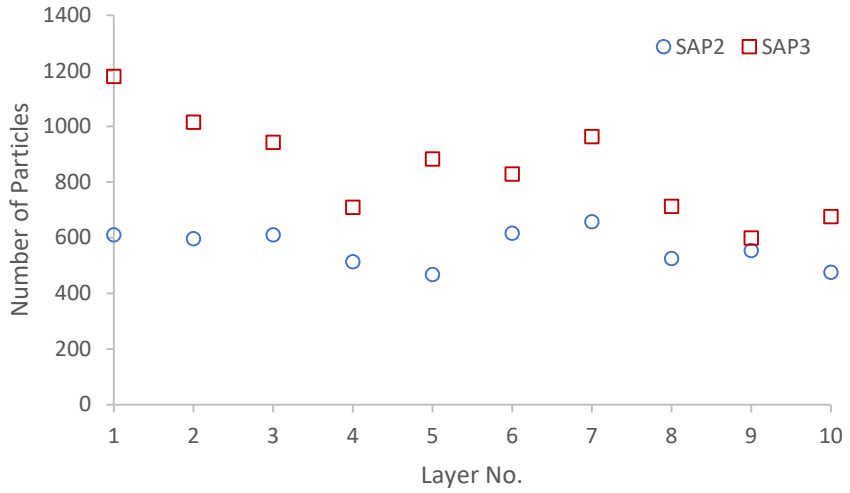

Fig. 4.15 Predicted SAP particles distribution

The calculated spacing for the SAP in each layer versus the predicted degree of hydration is presented in Fig. 4.16. Theoretically, as the distance between the SAP decreases, the degree of hydration increases as the cement particles will have a shorter access distance to the IC water. Results in Fig. 4.16 show the opposite for SAP3 where the layers with lower estimated SAP spacing have a lower degree of hydration. These results indicate that the SAPs were not equidistant and that some SAPs most likely agglomerated. Particles agglomeration results an increase in the spacing and consequently a reduction in the efficiency of the IC material. If the particles in SAP2 are equidistant and do not

agglomerate, they can provide water to a radial distance of 0.18 ± 0.02 mm as per assumed swollen radius of 87%.

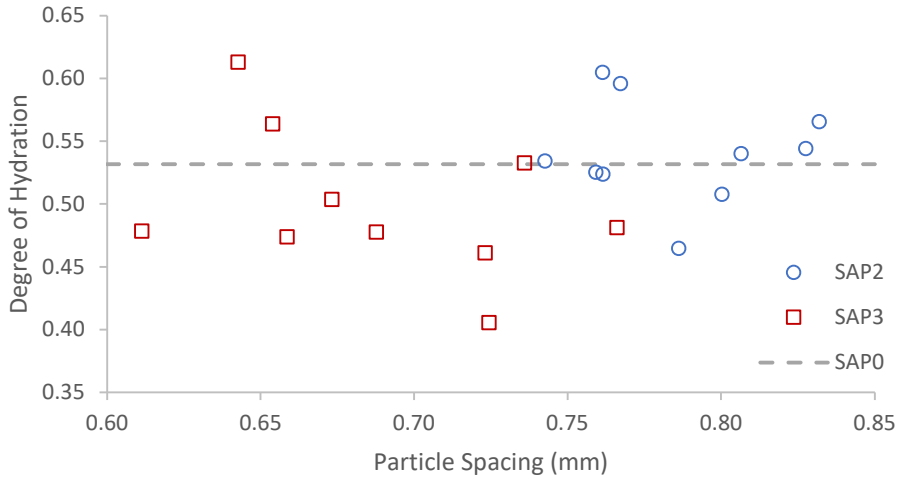

Fig. 4.16 Degree of hydration at 48 h versus SAP particle spacing

It is theorized that a paste with IC should have the same degree of hydration as a plain paste with the same total w/c [10]. Using this premise, the efficiency of the SAP as an IC material, η_{IC}, was calculated using

$$\eta_{IC} = \frac{{}^{\alpha_i}/_{N_i}}{{}^{\alpha_{ideal}}/_{N_{ideal}}} \tag{4.25}$$

The ideal number of SAP (N_{ideal}) is calculated by assuming that $({}^{w}/_{c})_{IC}$ of exactly 0.05 corresponds to 536 SAP particles per layer. The ideal degree of hydration (α_{ideal}) is taken equal to the degree of hydration of SAP0. The term ${}^{\alpha_i}/_{N_i}$ compares the degree of hydration of each layer to the number of SAP in the layer. The results, which are reproduced in Fig. 4.17, show that SAP2 and SAP3 have an efficiency of 98±14% and 71±14%, respectively. Statistical analysis reveals that the efficiency of SAP2 and SAP3 are not equal. Therefore, increasing the dosage can result in a decrease in the efficiency of SAP as an IC material when the amount of entrained water is kept constant.

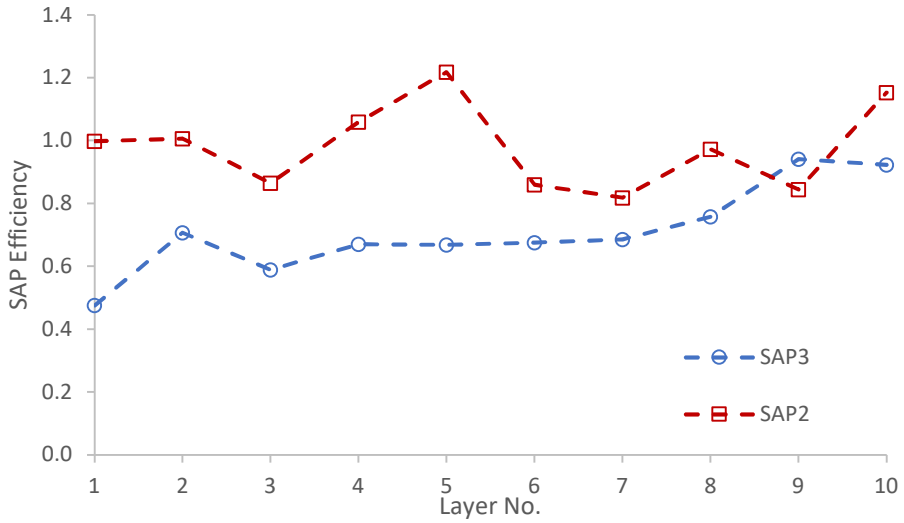

Fig. 4.17 SAP efficiency as IC based on cement degree of hydration

By comparing the mixes degree of hydration to an equivalent mix with ideal SAP spacing, the effective number of SAP, $N_{i_{effective}}$, can be estimated. When the degree of hydration is less than the equivalent mix, the spacing of the SAP is assumed to increase due to particles agglomeration as the effective number of SAP particles providing IC is reduced. Accordingly, a measure of agglomeration on the efficiency of SAP (η_{agg}) is proposed, where

$$\eta_{agg} = \frac{N_{i_{effective}}}{N_i} \tag{4.26}$$

The results, shown in Fig. 4.18, reveal a significant loss of efficiency with the increase of SAP content from 0.2% to 0.3%, highlighting the need to re-examine the amount SAP and entrained water. The average efficiency of SAP in SAP2 and SAP3 is 84% and 41%, respectively. By increasing the SAP content from 0.2 to 0.3%, the probability of particles agglomeration is found to increase. Therefore, a limit of 0.2% on the SAP content and corresponding entrained water of 0.05 may need to be set for the type and size of SAP used in this study to prevent the loss of SAP efficiency as IC due to particles agglomeration. It

should be noted that the limit on SAP content is specific to the mixture content and proportion, to the mixing protocol and equipment, and the type and size of SAP particles.

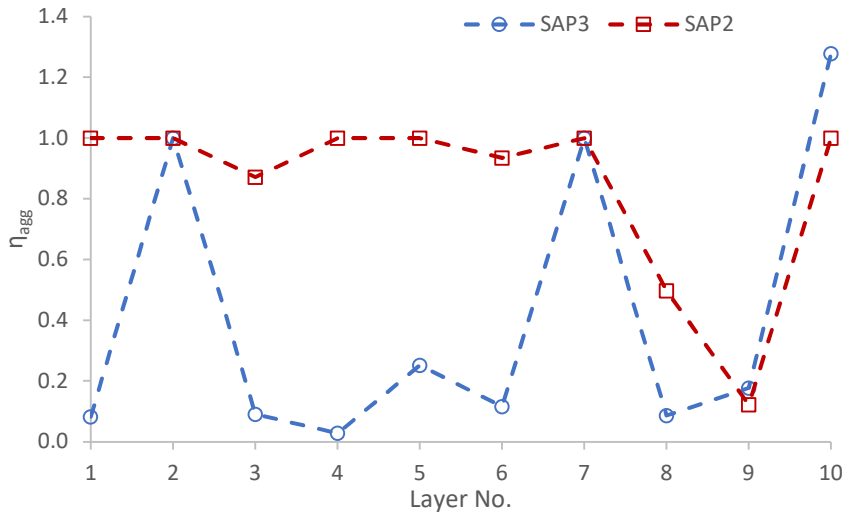

Fig. 4.18 Effect of particles agglomeration of the SAP efficiency as IC

4.4 Conclusions

From the NMR-MRI imaging of cement paste without and with SAP as IC, the following conclusions are drawn:

1. SAP used in this study have an approximated pore absorption of 25 g/g SAP, and a statistically decreasing desorption rate with increasing SAP content at constant w/c.
2. The rate of gel formation fits the well-known cement hydration rate equation.
3. Mixes with the highest amount of SAP have the highest cement degree of hydration whereas the hydration shape factor decreases with increasing amount of SAP.
4. After 48 h of casting, the capillary pore structure of mixes with SAP content are statistically different which confirms that SAP content affects the pore structure.
5. Gel pores of mixes with SAP become more uniform along the height of the sample as more hydration products are formed.

6. Increasing the amount of SAP while keeping the total w/c constant prolongs the availability of SAP water, however the distribution and quantity are substantially inconsistent per layer and along the height of the sample.
7. After 48 h, the characteristic pore size of the capillary pores of SAP0, SAP2, and SAP3 are 5.6 ± 0.2, 10.1 ± 1.9 and 11.8 ± 1.6 nm, respectively. This concludes that larger pores remained saturated with the addition of SAP.
8. The number of SAP and corresponding particles spacing for SAP2 and SAP3 are respectively, 0.78±0.03 mm and 0.67±0.05 mm, and 563±65 and 851±180 particles per layer.
9. Average efficiency of SAP2 and SAP3 as IC is 98±14% and 71±14%, respectively, and 84% and 41% when accounting for particle agglomeration.

The conclusions and observations made in this paper are specific to the type and size of SAP used in this study.

CRediT Authorship Contribution Statement

S.E. Chidiac: Conceptualization of study and models development; Methodology for experimental program and analytical investigation; Writing, reviewing & editing; Resources; Supervision. S.N. Mihaljevic: Conceptualization of study and Methodology; Carried out the experimental work and data analysis; Model development; Writing original draft and editing. S.A. Krachkovskiy: Designed and carried out the NMR and MRI portion of the experimental work including data generation and analysis; Reviewed manuscript. G.R. Goward: Contributed to the development of the project; Reviewed manuscript; Resources.

Acknowledgements

The authors would like to thank NSERC for funding this research and BASF Germany for providing the SAP material.

References

[1] S.E. Chidiac, F. Moutassem, F. Mahmoodzadeh, Compressive strength model for concrete, Mag. Concr. Res. 65 (2013) 557–572. doi:10.1680/macr.12.00167.

[2] S.E. Chidiac, M. Shafikhani, Phenomenological model for quantifying concrete chloride diffusion coefficient, Constr. Build. Mater. 224 (2019) 773–784. doi:10.1016/j.conbuildmat.2019.07.006.

[3] M. Shafikhani, S.E. Chidiac, A holistic model for cement paste and concrete chloride diffusion coefficient, Cem. Concr. Res. 133 (2020) 106049. doi:10.1016/j.cemconres.2020.106049.

[4] E. Tazawa, S. Miyazawa, Influence of cement and admixture on autogenous shrinkage of cement paste, Cem. Concr. Res. 25 (1995) 281–287. doi:10.1016/0008-8846(95)00010-0.

[5] B. Akcay, M.A. Tasdemir, Optimisation of using lightweight aggregates in mitigating autogenous deformation of concrete, Constr. Build. Mater. 23 (2009) 353–363. doi:10.1016/j.conbuildmat.2007.11.015.

[6] R. Henkensiefken, D. Bentz, T. Nantung, J. Weiss, Volume change and cracking in internally cured mixtures made with saturated lightweight aggregate under sealed and unsealed conditions, Cem. Concr. Compos. 31 (2009) 427–437. doi:10.1016/j.cemconcomp.2009.04.003.

[7] P. Lura, D.P. Bentz, D.A. Lange, K. Kovler, A. Bentur, Pumice aggregates for internal water curing, in: Int. RILEM Symp. Concr. Sci. Eng. A Tribut. to Arnon Bentur, 2004: pp. 137–151.

[8] D.P. Bentz, Internal curing of high-performance blended cement mortars, ACI Mater. J. 104 (2007) 408–414.

[9] S. Zhutovsky, K. Kovler, Effect of internal curing on durability-related properties of high performance concrete, Cem. Concr. Res. 42 (2012) 20–26. doi:10.1016/j.cemconres.2011.07.012.

[10] O.M. Jensen, P.F. Hansen, Water-entrained cement-based materials, Cem. Concr. Res. 31 (2001) 647–654. doi:10.1016/S0008-8846(01)00463-X.

[11] O.M. Jensen, P.F. Hansen, Water-entrained cement-based materials: II. Experimental observations, Cem. Concr. Res. 32 (2002) 973–978. doi:10.1016/S0008-8846(02)00737-8.

[12] M. Yamaguchi, H. Watamoto, M. Sakamoto, Water saturated super-absorbent polymers used in high strength concrete, Carbohydr. Polym. 7 (1987) 71–82.

[13] H. Ye, A. Radlińska, A Review and Comparative Study of Existing Shrinkage Prediction Models for Portland and Non-Portland Cementitious Materials, Adv. Mater. Sci. Eng. 2016 (2016) 1–13. doi:10.1155/2016/2418219.

[14] L. Wu, N. Farzadnia, C. Shi, Z. Zhang, H. Wang, Autogenous shrinkage of high performance concrete: A review, Constr. Build. Mater. 149 (2017) 62–75. doi:10.1016/j.conbuildmat.2017.05.064.

[15] P. Lura, O.M. Jensen, K. van Breugel, Autogenous shrinkage in high-performance cement paste: An evaluation of basic mechanisms, Cem. Concr. Res. 33 (2003) 223–232. doi:10.1016/S0008-8846(02)00890-6.

[16] L.A. Richards, Capillary conduction of liquids through porous mediums, Physics (College. Park. Md). 1 (1931) 318–333. doi:10.1063/1.1745010.

[17] G.W. Scherer, Theory of Drying, J. Am. Ceram. Soc. 73 (1990) 3–14. doi:10.1111/j.1151-2916.1990.tb05082.x.

[18] Z.C. Grasley, D.A. Lange, M.D. D'Ambrosia, Internal relative humidity and drying stress gradients in concrete, Mater. Struct. 39 (2006) 901–909. doi:10.1617/s11527-006-9090-3.

[19] J.K. Kim, C.S. Lee, Moisture diffusion of concrete considering self-desiccation at early ages, Cem. Concr. Res. 29 (1999) 1921–1927. doi:10.1016/S0008-8846(99)00192-1.

[20] L. Montanari, P. Suraneni, W.J. Weiss, Accounting for Water Stored in Superabsorbent Polymers in Increasing the Degree of Hydration and Reducing the Shrinkage of Internally Cured Cementitious Mixtures, Adv. Civ. Eng. Mater. 6 (2017) 20170098. doi:10.1520/ACEM20170098.

[21] P. Lura, O.M. Jensen, S.-I. Igarashi, Experimental observation of internal water

curing of concrete, Mater. Struct. 40 (2007) 211–220. doi:10.1617/s11527-006-9132-x.

[22] K. Farzanian, K. Pimenta Teixeira, I. Perdigão Rocha, L. De Sa Carneiro, A. Ghahremaninezhad, The mechanical strength, degree of hydration, and electrical resistivity of cement pastes modified with superabsorbent polymers, Constr. Build. Mater. 109 (2016) 156–165. doi:10.1016/j.conbuildmat.2015.12.082.

[23] M. Golias, J. Castro, J. Weiss, The influence of the initial moisture content of lightweight aggregate on internal curing, Constr. Build. Mater. 35 (2012) 52–62. doi:10.1016/j.conbuildmat.2012.02.074.

[24] A. Valori, P.J. McDonald, K.L. Scrivener, The morphology of C-S-H: Lessons from 1H nuclear magnetic resonance relaxometry, Cem. Concr. Res. 49 (2013) 65–81. doi:10.1016/j.cemconres.2013.03.011.

[25] V.I. Bakhmutov, NMR Spectroscopy in Liquids and Solids, CRC Press, 2015. doi:10.1201/b18341.

[26] T.C. Pochapsky, S.S. Pochapsky, Nuclear Magnetic Resonance Spectroscopy, in: Mol. Biophys. Life Sci., Springer New York, New York, NY, 2013: pp. 113–173. doi:10.1007/978-1-4614-8548-3_5.

[27] K. Friedemann, F. Stallmach, J. Kärger, NMR diffusion and relaxation studies during cement hydration-A non-destructive approach for clarification of the mechanism of internal post curing of cementitious materials, Cem. Concr. Res. 36 (2006) 817–826. doi:10.1016/j.cemconres.2005.12.007.

[28] M. Van Landeghem, J.B.D. De Lacaillerie, B. Blümich, J.P. Korb, B. Bresson, The roles of hydration and evaporation during the drying of a cement paste by localized NMR, Cem. Concr. Res. 48 (2013) 89–96. doi:10.1016/j.cemconres.2013.01.012.

[29] R. Holly, E.J. Reardon, C.M. Hansson, H. Peemoeller, Proton spin-spin relaxation study of the effect of temperature on white cement hydration, J. Am. Ceram. Soc. 90 (2007) 570–577. doi:10.1111/j.1551-2916.2006.01422.x.

[30] J. Yang, Z. Sun, Y. Zhao, Y. Ji, B. Li, The Water Absorption-release of Superabsorbent Polymers in Fresh Cement Paste: An NMR Study, J. Adv. Concr.

Technol. 18 (2020) 139–145. doi:10.3151/jact.18.139.

[31] T. Lazar, Basic One- and Two-Dimensional NMR Spectroscopy, 4th Edition, Synthesis (Stuttg). (2005). doi:10.1055/s-2005-867116.

[32] B.J. Balcom, J.C. Barrita, C. Choi, S.D. Beyea, D.J. Goodyear, T.W. Bremner, Single-point Magnetic Resonance Imaging (MRI) of cement based materials, Mater. Struct. Constr. 36 (2003) 166–182. doi:10.1617/14024.

[33] N. Nestle, A. Kühn, K. Friedemann, C. Horch, F. Stallmach, G. Herth, Water balance and pore structure development in cementitious materials in internal curing with modified superabsorbent polymer studied by NMR, Microporous Mesoporous Mater. 125 (2009) 51–57. doi:10.1016/j.micromeso.2009.02.024.

[34] M. Fourmentin, P. Faure, S. Rodts, U. Peter, D. Lesueur, D. Daviller, P. Coussot, NMR observation of water transfer between a cement paste and a porous medium, Cem. Concr. Res. 95 (2017) 56–64. doi:10.1016/j.cemconres.2017.02.027.

[35] D. Snoeck, L. Pel, N. De Belie, The water kinetics of superabsorbent polymers during cement hydration and internal curing visualized and studied by NMR., Sci. Rep. 7 (2017) 1–14. doi:10.1038/s41598-017-10306-0.

[36] M. Wyrzykowski, A.M. Gajewicz-Jaromin, P.J. McDonald, D.J. Dunstan, K.L. Scrivener, P. Lura, Water redistribution–microdiffusion in cement paste under mechanical loading evidenced by 1 H NMR, J. Phys. Chem. C. 123 (2019) 16153–16163. doi:10.1021/acs.jpcc.9b02436.

[37] Z. Hu, M. Wyrzykowski, K. Scrivener, P. Lura, A novel method to predict internal relative humidity in cementitious materials by 1 H NMR, Cem. Concr. Res. 104 (2018) 80–93. doi:10.1016/j.cemconres.2017.11.001.

[38] S.E. Chidiac, S.N. Mihaljevic, S.A. Krachkovskiy, G.R. Goward, Characterizing the effect of superabsorbent polymer content on internal curing process of cement paste using calorimetry and nuclear magnetic resonance methods, J. Therm. Anal. Calorim. (2020). doi:10.1007/s10973-020-09754-0.

[39] T.C. Powers, A discussion of cement hydration in relation to the curing of concrete, in: Proc. Twenty-Seventh Annu. Meet. Highw. Res. Board, Highway Research

Board, Washington, D.C., 1948: pp. 178–188.

[40] Canadian Standards Association, Cementitious materials compendium, CSA Group, Toronto, ON, 2018.

[41] H.F.W. Taylor, Cement chemistry. 2nd ed., London, 1997. doi:10.1016/S0958-9465(98)00023-7.

[42] L.P. Esteves, Recommended method for measurement of absorbency of superabsorbent polymers in cement-based materials, Mater. Struct. 48 (2015) 2397–2401. doi:10.1617/s11527-014-0324-5.

[43] C. Schröfl, D. Snoeck, V. Mechtcherine, A review of characterisation methods for superabsorbent polymer (SAP) samples to be used in cement-based construction materials: report of the RILEM TC 260-RSC, Mater. Struct. Constr. 50 (2017) 1–19.

[44] D. Snoeck, K. Van Tittelboom, S. Steuperaert, P. Dubruel, N. De Belie, Self-healing cementitious materials by the combination of microfibres and superabsorbent polymers, J. Intell. Mater. Syst. Struct. 25 (2014) 13–24. doi:10.1177/1045389X12438623.

[45] D. Snoeck, C. Schröfl, V. Mechtcherine, Recommendation of RILEM TC 260-RSC: testing sorption by superabsorbent polymers (SAP) prior to implementation in cement-based materials, Mater. Struct. 51 (2018) 116. doi:10.1617/s11527-018-1242-8.

[46] S. Meiboom, D. Gill, Modified spin-echo method for measuring nuclear relaxation times, Rev. Sci. Instrum. 29 (1958) 688–691. doi:10.1063/1.1716296.

[47] S. Vashaee, F. Marica, B. Newling, B.J. Balcom, A comparison of magnetic resonance methods for spatially resolved T2 distribution measurements in porous media, Meas. Sci. Technol. 26 (2015) 1–16. doi:10.1088/0957-0233/26/5/055601.

[48] W.P. Halperin, J.Y. Jehng, Y.Q. Song, Application of spin-spin relaxation to measurement of surface area and pore size distributions in a hydrating cement paste, Magn. Reson. Imaging. 12 (1994) 169–173. doi:10.1016/0730-725X(94)91509-1.

[49] A. Neville, Properties of Concrete - 5th Edition, London, 2012.

[50] ASTM Committee C09.48, ASTM C1679-14: Standard practice for measuring hydration kinetics of hydraulic cementitious mixtures using isothermal calorimetry, in: Annu. B. ASTM Stand. Vol. 04.01, 2014. doi:10.1520/C1679-13.2.

[51] A.K. Schindler, K.J. Folliard, Heat of hydration models for cementitious materials, ACI Mater. J. 102 (2005) 24–33.

[52] I. Pane, W. Hansen, Investigation of blended cement hydration by isothermal calorimetry and thermal analysis, Cem. Concr. Res. 35 (2005) 1155–1164. doi:10.1016/j.cemconres.2004.10.027.

[53] R. Mills, Factors influencing cessation of hydration in water-cured cement pastes, Symp. Struct. Portl. Cem. Paste Concr. Highw. Res. Board Spec. Rep. (1966).

[54] I. Maruyama, T. Ohkubo, T. Haji, R. Kurihara, Dynamic microstructural evolution of hardened cement paste during first drying monitored by 1H NMR relaxometry, Cem. Concr. Res. 122 (2019) 107–117. doi:10.1016/j.cemconres.2019.04.017.

[55] A.C.A. Muller, K.L. Scrivener, A.M. Gajewicz, P.J. McDonald, Densification of C-S-H measured by 1H NMR relaxometry, J. Phys. Chem. C. 117 (2013) 403–412. doi:10.1021/jp3102964.

[56] S.E. Chidiac, M. Shafikhani, Cement degree of hydration in mortar and concrete, J. Therm. Anal. Calorim. 138 (2019) 2305–2313. doi:10.1007/s10973-019-08800-w.

[57] P.F. Hansen, E.J. Pedersen, Maturity Computer for Controlled Curing and Hardening of Concrete, Nord. Betong. 1 (1977) 21–25.

[58] S. Mönnig, Superabsorbing additions in concrete: applications, modelling and comparison of different internal water sources, Institut für Werkstoffe im Bauwesen der Universität Stuttgart, 2009.

5 Effective free water diffusion coefficient of cement paste internally cured with superabsorbent polymers

Mihaljevic, S.N., & Chidiac, S.E. (2021). Effective free water diffusion coefficient of cement paste internally cured with superabsorbent polymers. Submitted to Journal of Building Engineering, Manuscript Number: JBE-D-21-02428

Abstract

A hybrid model, comprised of analytical and phenomenological models, was developed to quantify the effective free water diffusion coefficient of cement hydration with superabsorbent polymers (SAP) as internal curing. NMR/MRI measurements were used to estimate the water types and distribution, and the cement degree of hydration. Employing reverse engineering, the estimated temporal free water distribution in cement hydration with SAP was reproduced using 1-D finite element transient flow model and a tortuosity model. The computed free water diffusion coefficient and effective diffusion length of cement paste with 0.2% and 0.3% SAP is 5.48×10^{-12} m^2/s and 4.46×10^{-12} m^2/s, and 0.25 mm and 0.19 mm, respectively. The computed efficacy of SAP dropped by 8% and 27%, for 0.2% and 0.3% SAP content respectively, when accounting for particles agglomeration.

Keywords: Cement; Diffusion coefficient; Finite element model; Internal curing; NMR/MRI; Superabsorbent polymers

5.1 Introduction

Autogenous shrinkage due to self-desiccation is a primary cause of early-age cracking in high-strength, high-performance and ultra-high performance concrete [1–3]. Internal curing (IC), which is the supplier of water during cement hydration to mitigate self-desiccation [4–7], consists of adding water filled inclusions to the concrete constituents. As such, IC has afforded all the strength and durability benefits of low water to cement ratio (w/c) concrete without the adverse effect of autogenous shrinkage [8]. Not only does

IC design need to provide an adequate amount of water to compensate for autogenous shrinkage, but it also needs the IC water to be evenly and abundantly distributed over the whole paste [5,9,10]. Lightweight aggregate (LWA) [11–15] and superabsorbent polymers (SAP) [8,16–21] have been widely researched as IC materials because they have the capacity to store a large amount of water and to release the water as cement hydrates.

The effectiveness of IC depends on three factors: the amount of water available [21–23], the distribution of IC material [17,24], and the ability of water to move from the IC material to the hydrating cement paste [17,25,26]. The amount of IC water in SAP depends on the water absorption kinetics and efficiency, with the former depending on the SAP covalent crosslinking density and concentration of anionic functional groups [27], and the cement paste pore solution, especially the calcium ionic concentration, [28,29], and the latter on the SAP particle size [28,30,31]. Additionally, agglomeration of SAP particles greatly reduces the efficacy [17,24]. SAP water desorption is a function of the SAP anion concentration [29], the size and interconnectivity of the cement paste pore structure, and the interface between the SAP and cement paste [28]. Water desorption and water transport distance from SAP have not been fully quantified due to the challenge with continuously testing cement paste at early-age of cement hydration, which is the time when autogenous shrinkage is most damaging to concrete and IC is most essential [28].

Nuclear magnetic resonance (NMR), which is a nondestructive and noninvasive tool, has been employed to track type, amount, and movement of water in hydrating cement paste with IC [17,21,26,32–37]. The spin-spin relaxation time (T_2) of the H^1 atom is used to classify the phase of the water in the hydrating cement paste, and the signal intensity of T_2 times relates to the relative amount of water type [32]. When combining the NMR with magnetic resonance imaging technique (NMR-MRI), the temporal and spatial distribution of water can be estimated [17,38]. Moreover, NMR relaxometry has been used to study the effects of IC on cement degree of hydration [17,26,33], the uptake of water into the IC material [21,34], and the amount of water desorption from IC [17,26,32,33]. Chidiac et al.

[17] used NMR-MRI to determine the distribution of gel water, capillary water, and water inside SAP particles along a height of 20 mm for a period of 48 h. They developed an equation that relates the NMR intensity to the cement degree of hydration that considers the additional porosity due to SAP. The results showed that the efficiency of SAP as IC material, for a cement paste with 0.30 w/c and 0.05 IC water, drops from 98% to 71% when accounting for agglomeration. The adverse effect of agglomeration on the efficiency of SAP was reported to be more significant for the cement paste with 0.27 w/c and 0.08 IC water, where the efficiency dropped from 71% to 41% [17].

The distance that SAP water can transport, which has been estimated in a couple of studies, provides a measure of the IC effectiveness. Using an optical microscope and cement paste with 0.5 w/c, the water transport distance was reported to range between 0.05 and 0.06 mm from the surface of SAP [24]. Using Pulsed field gradient NMR, Friedemann et al. [32] found that the self-diffusion coefficient of cement paste with 0.3 w/c to be in the range of $1.25x10^{-10}$ to $1.5x10^{-10}$ m^2/s initially then decrease to $5x10^{-10}$ m^2/s after 10 h, which corresponds to an average diffusion length of 5 mm. They also reported that there was a small decrease in the self-diffusion coefficient as the w/c decreased. These studies reveal the significant discrepancy and challenge in measuring and predicting the water diffusion length. As such, this study aims to quantify the water effective diffusion coefficient for early age cement paste with SAP and the corresponding average diffusion length. Reverse engineering process, finite element modelling, and NMR-MRI experimental data were used to achieve the objectives.

This paper presents a hybrid diffusivity model developed for quantifying the water effective diffusion coefficient of hydrating cement paste containing SAP. The 1-D transient finite element model was re-arranged so that the model inputs are the free and chemically bound water content, and the output is the diffusion coefficient. The evolving cement gel is accounted for in the model through a tortuosity factor. The derivation of the hybrid model is first presented. NMR-MRI data reported in the literature is used to demonstrate the model

prediction of cement paste water diffusion coefficient. The effectiveness of SAP as IC material, specifically the effects of particle agglomeration, is then evaluated using average diffusion length measurements.

5.2 Mass Transport Model

The water transport model of a single SAP particle in cement paste is developed with the following assumptions:

1. SAP particle forms a perfect sphere.
2. Transport of water in the porous media is diffusion controlled.
3. Water diffusion from the SAP particle and across the cement paste is spherically symmetric.
4. Contact between the SAP particle and the cement paste is perfect.
5. Boundary mid-distance between the SAP particles is symmetric, i.e. no water moves across the boundary.
6. Water movement in the cement paste is being hindered by the ongoing formation of cement gel.

Accordingly, the differential equation that governs the 1-D mass transport, referred to as Fick's 2nd Law of diffusion, in spherical coordinates is given by,

$$D_w\left(\frac{1}{r^2}\frac{\partial}{\partial r}\left(r^2\frac{\partial c_w}{\partial r}\right)\right) - W = \frac{\partial c_w}{\partial t} \tag{5.1}$$

in which D_w, c_w, and W are respectively, the water diffusion coefficient, the concentration of free water, and the applied source or sink, and r and t are the space and time coordinates. Using the principle of virtual work and finite element discretization method [39], Eq. (5.1) can be written in matrix form as

$$[H]\{\dot{c}_w\} + [K]\{c_w\} = \{F\} \tag{5.2}$$

where $[H]$, $[K]$, and $\{F\}$ represent the storage matrix, conduction matrix, and load vector, respectively. The time derivatives in Eq. (5.2) are discretized according to Crank-Nicolson method [39], where

$$\{c_w\}^{t+\Delta t} = \{c_w\}^t + [(1-\theta)\{\dot{c}_w\}^t + \theta\{\dot{c}_w\}^{t+\Delta t}]\Delta t \tag{5.3}$$

where the unconditionally stable Crank-Nicolson method of $\theta = 0.5$ is used in this study. From Eqs. (5.2) and (5.3), the solution in time becomes

$$([H] + \theta\Delta t[K])\{c_w\}^{t+\Delta t} = ([H] - (1-\theta)\Delta t[K])\{c_w\}^{t} + (1-\theta)\Delta t\{F\}^{t} + \theta\Delta t\{F\}^{t+\Delta t} \tag{5.4}$$

Given $\{c_w\}^{t+\Delta t}$, $\{c_w\}^{t}$, $\{F\}^{t+\Delta t}$, and $\{F\}^{t}$ are known, the corresponding diffusion coefficient is calculated by re-arranging the terms in Eq. (5.4),

$$[K] = \frac{[H](\{c_w\}^{t} - \{c_w\}^{t+\Delta t}) + (1-\theta)\Delta t\{F\}^{t} + \theta\Delta t\{F\}^{t+\Delta t}}{\Delta t\left((1-\theta)\{\dot{c}_w\}^{t} + \theta\{\dot{c}_w\}^{t+\Delta t}\right)} \tag{5.5}$$

The corresponding element conduction matrix is given by

$$[K^e] = D_w \int_{V^e} [B]^T [B] dV \tag{5.6}$$

in which $[B]$ is the matrix for water concentration gradients interpolation.

With cement hydration, cement gel forms with time and the medium changes from an aqueous to solid state. That change, which results in an increase in the solid volume fraction, leads to a decrease in the porosity of the cement paste and an increase in the water path. Cement degree of hydration, α, defined as the fraction of Portland cement that has fully reacted with water, is used to quantify the formed solid volume fraction, V_s, by way of the model proposed in [40]:

$$V_s = \frac{0.63\alpha}{0.31\alpha + w/c} \tag{5.7}$$

The model, shown in Fig. 5.1, postulates that a 0.32 w/c results in a 100% cement hydration.

With the formation of cement gel, the tortuosity of the cement paste will increase and impede the water flow [41–43]. The increase in the diffusion length due to restrictions in the flow path is modelled according to Chidiac and Shafikhani [42]. Accordingly, the tortuosity factor, f_τ, is a function of V_s, where

$$f_\tau = \frac{3(1-V_s)^2}{3-V_s} \tag{5.8}$$

The model, shown in Fig. 5.1, postulates that f_τ is equal to 1 when V_s is zero representing no obstruction to the flow and f_τ is equal to zero when V_s is equal to 1 representing complete obstruction. Fig. 5.2 shows the increase in the length of the water path as the tortuosity increases with the degree of hydration. It is further postulated that the effective diffusion coefficient, D_w^e, can be computed using the following relationship,

$$D_w^e = \frac{3(1-V_s)^2}{3-V_s} D_o = f_\tau D_o \tag{5.9}$$

in which D_o is the free-water diffusion coefficient.

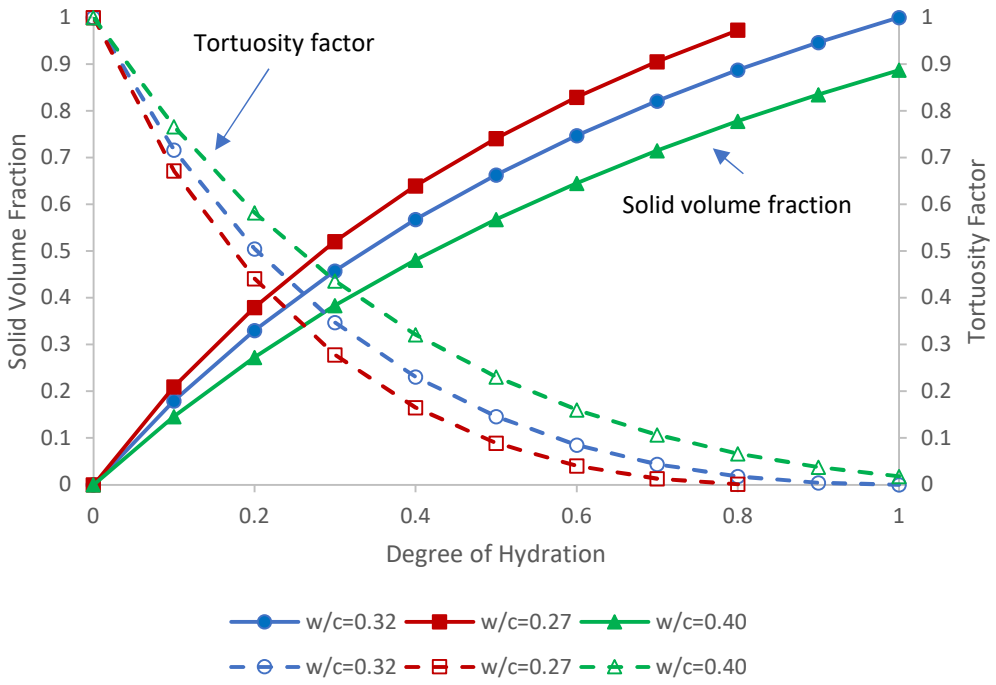

Fig. 5.1 Solid volume fraction and tortuosity factor versus degree of hydration.

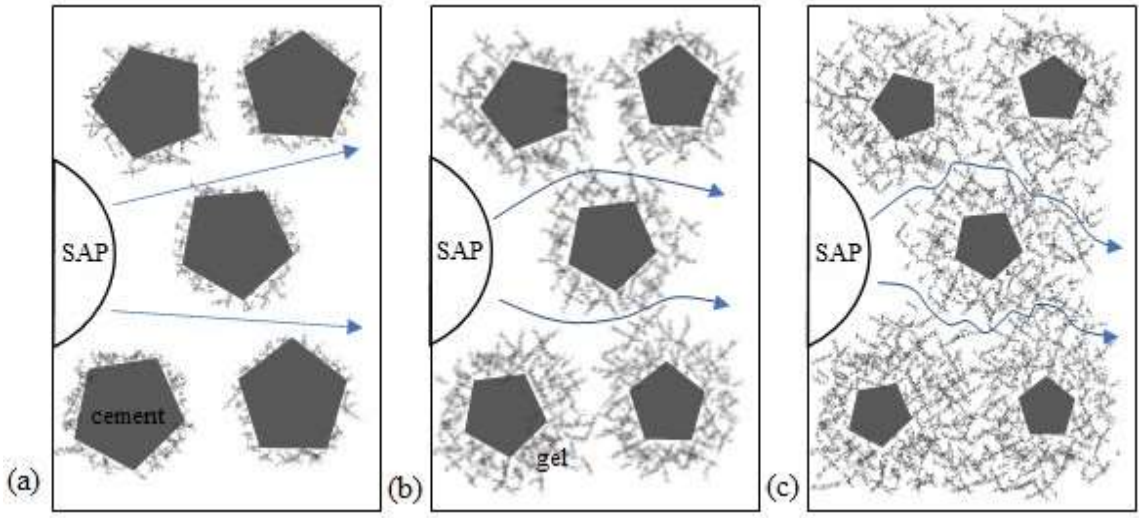

Fig. 5.2 Schematic illustration of tortuosity factor versus degree of hydration; (a) $\alpha << 20\%$, (b) $\alpha \approx 20\text{-}25\%$ - gel structure begins to connect, and (c) $\alpha > 40\%$.

5.3 NMR-MRI Experimental Program

The experimental program, presented in Chidiac et al. [17], is used in this study to quantify the effective water diffusion coefficient during cement hydration. As such, the details of the experimental program can be found in Chidiac et al. [17], and only the relevant information and experimental data are reproduced. The material consist of white Portland cement CSA type GU-A3001 [44], SAP, and water. The polyacrylate SAP has an average dry diameter of 126.5 μm ± 3.0 μm [45], and an average swollen diameter of 416 μm [17]. The program included three cement paste mixes as reproduced in Table 5.1.

Table 5.1 Cement paste proportions [17]

	Cement (g)	Water (g)	SAP (g/kg cement)	w/c
SAP0	750	262.5	0.0	0.35+0.00
SAP2	750	262.5	2.0	0.30+0.05
SAP3	750	262.5	3.0	0.27+0.08

The cement paste was mixed and molded into 40 mm high vials with inside diameter of 13 mm. The vials were immediately sealed, and within 30 min were placed in a Bruker Avance 300 NMR spectrometer equipped with a MicWB40 Probe in combination with the Micro2.5 Gradient System. Testing was performed for 48 h with measurments taken evey hour for the first 24 h then every 2 h for the rest of the test. Three distinct water relaxation times were obtained for the samples corresponding to gel, capillary, and SAP water. The relevant results, corresponding to the spatial and temporal distribution of the capillary, gel, and SAP water, are reproduced in Fig. 5.3, Fig. 5.4, and Fig. 5.5 for SAP0, SAP2, and SAP3, respectively. The water distribution is for a 20 mm long section corresponding to the middle section of the sample. The results were further refined by dividing the 20 mm sample into 10 equal size layers with layer 1 corresponding to the bottom of the sample and layer 10 to the top. Results of Fig. 5.3 show an almost uniform water distribution along the sample height for SAP0. As the SAP content increases, results of Fig. 5.4 and Fig. 5.5 reveal that the water distribution has more variation along the sample height, and that the variation is not influenced by the sample orientation.

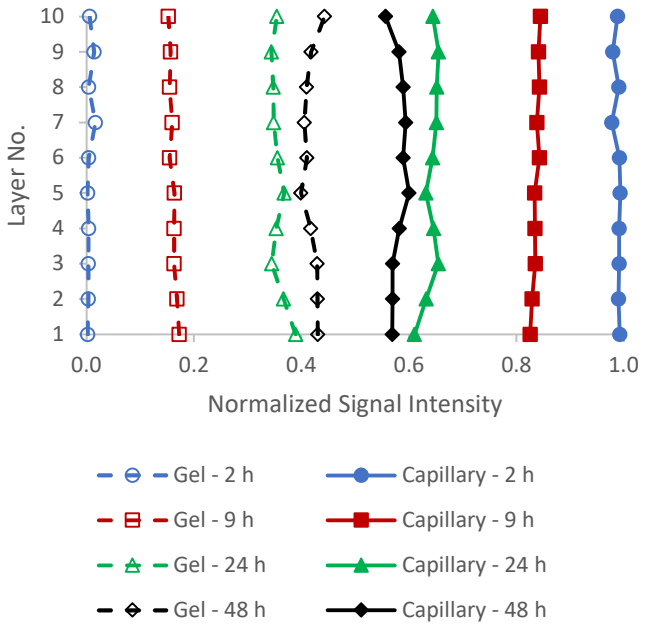

Fig. 5.3 MRI temporal and spatial water distribution along the sample height for SAP0 [17]

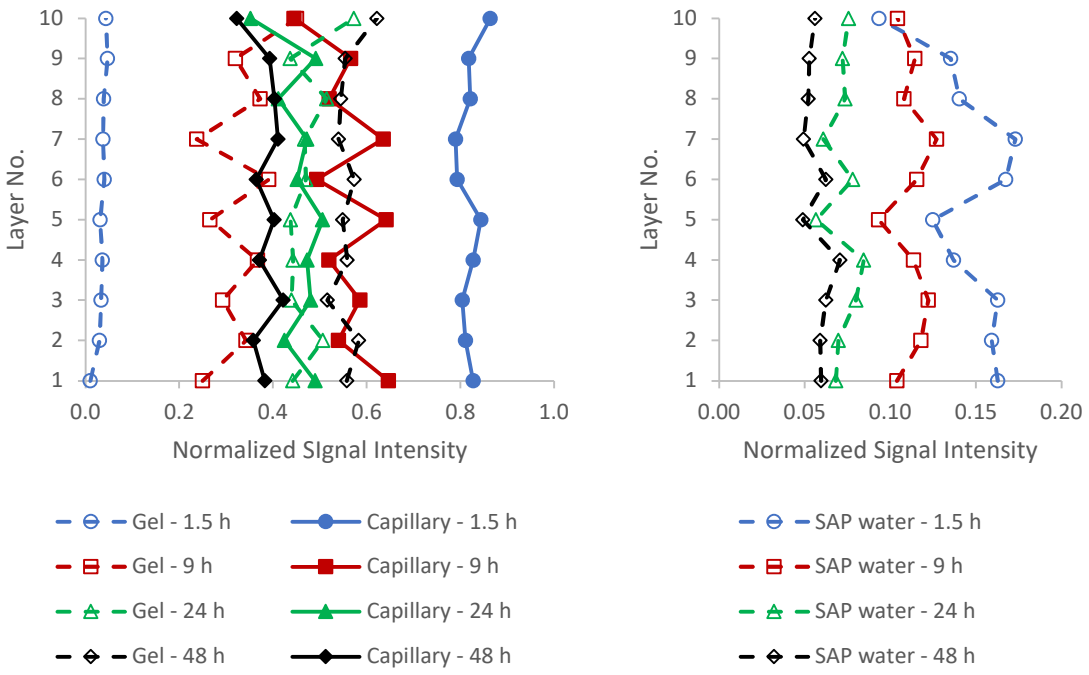

Fig. 5.4 MRI temporal and spatial water distribution along the sample height for SAP2 [17]

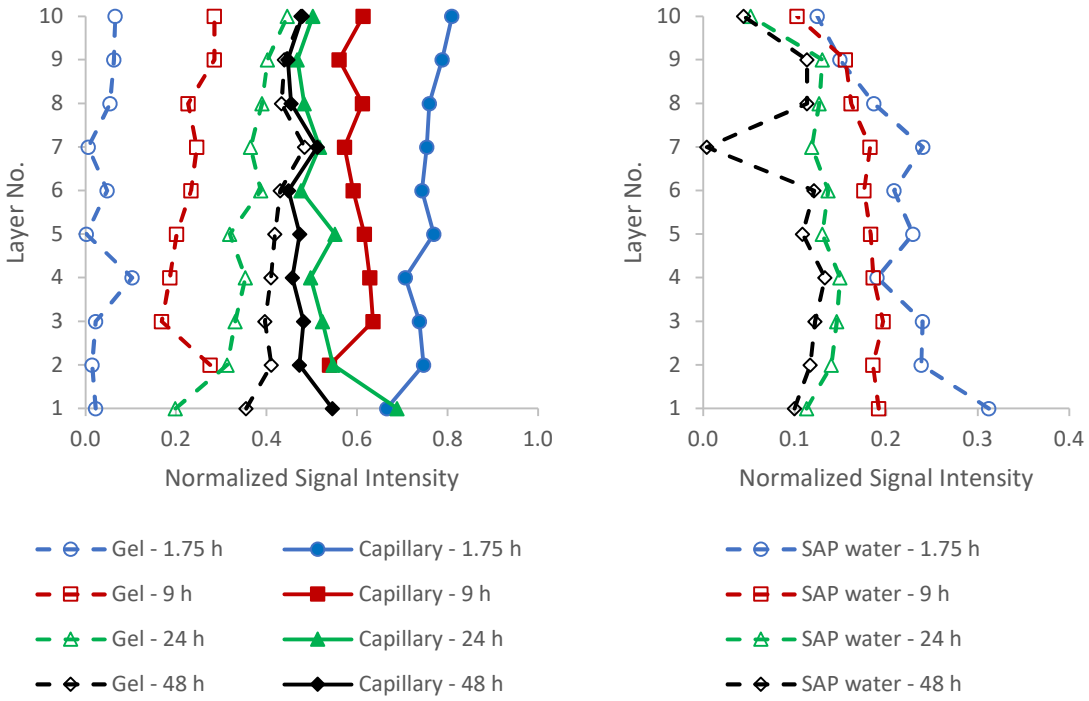

Fig. 5.5 MRI temporal and spatial water distribution along the sample height for SAP3 [17]

The cement degree of hydration, α, of mixes containing SAP was estimated using NMR results. The model proposed by Chidiac et al. [17] and validated via isothermal calorimetry, is as follows

$$\alpha = \frac{p_p + p_{SAP}}{\left(0.60/I_{gw} + 0.72\right)(1 - p_p)} \tag{5.10}$$

where I_{gw} is the normalized signal intensity of the gel water, p_p is the porosity of the paste, and p_{SAP} is the additional porosity provided by the SAP. Fig. 5.6 reproduces the calculated degree of hydration for the three cement pastes.

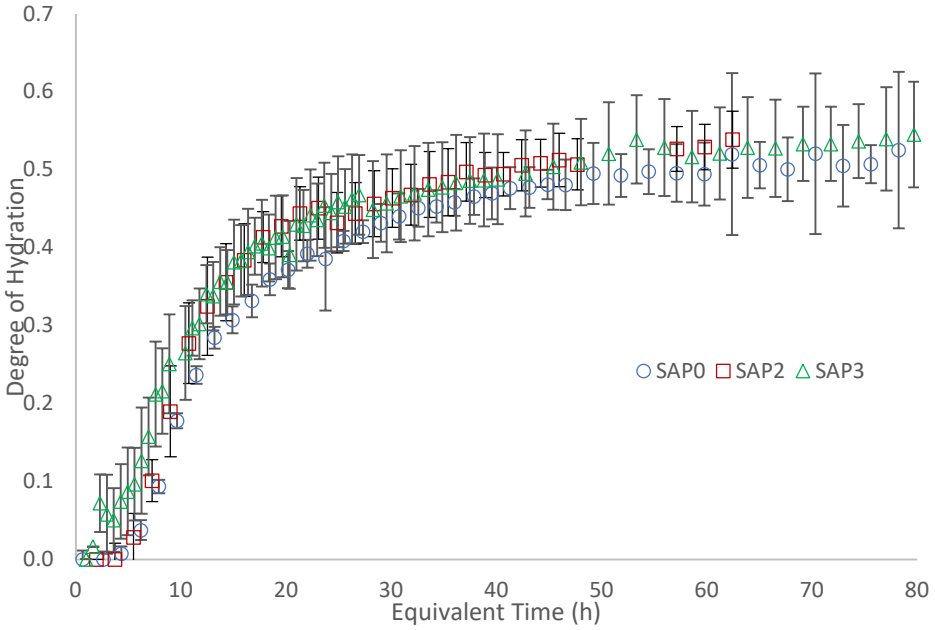

Fig. 5.6 Calculated degree of hydration [17]

By using the SAP saturated size and intensity of the SAP water signal, the SAP particle distribution per layer was determined as shown in Fig. 5.7. And, by assuming that the SAP particles form a cubic lattice structure with no particle agglomeration, the average SAP particle spacing was calculated, as reproduced in Fig. 5.7. The average number of particles for SAP2 is 563±65 spaced at 0.78±0.03 mm, and for SAP3 is 851±180 particles spaced at 0.67±0.05 mm.

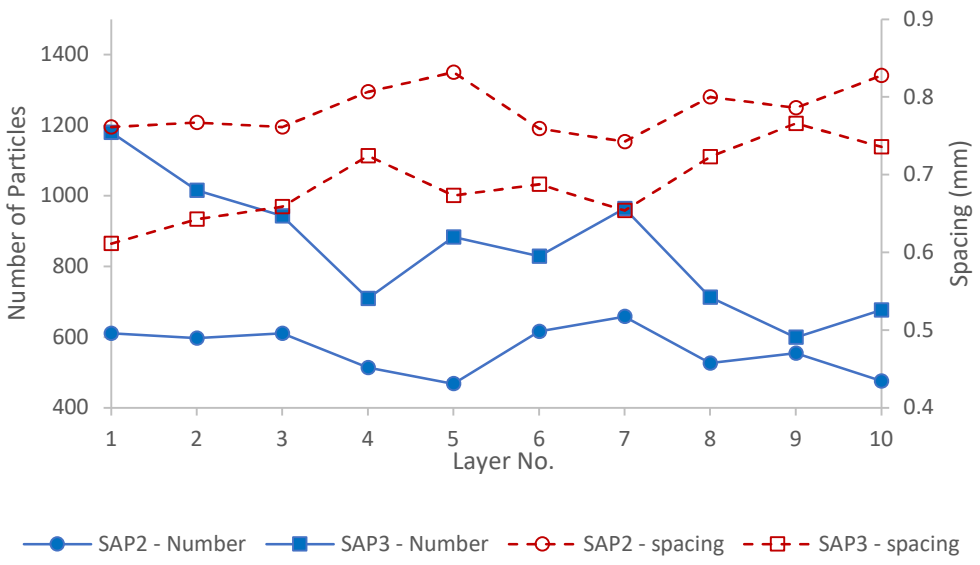

Fig. 5.7 Predicted SAP particles distribution and spacing [17]

5.4 Effective Water Diffusion Coefficient Model Validation

Water transport from the SAP particles to the cement paste is governed by the water concentration gradient between the SAP reservoir and the cement paste. To employ the NMR-MRI experimental results, the relative intensities of the water phases are converted to intensity concentrations. Accordingly, the governing equation, noted in Eq. (5.1), becomes

$$D_w^e\left(\frac{1}{r^2}\frac{\partial}{\partial r}\left(r^2\frac{\partial I_w}{\partial r}\right)\right) - I_{gel} = \frac{\partial I_w}{\partial t} \tag{5.11}$$

where D_w^e is the effective diffusion coefficient of water from SAP to cement paste, I_w is the concentration of the water signal, r is the radial distance from the surface of the SAP particle, and I_{gel} is the rate of water consumption by cement hydration. According to [17], I_{gel} was mathematically fitted to the following function

$$I_{gel} = {I_{gel}}_u exp\left[-\left(\frac{\tau}{t}\right)^{\beta}\right] \tag{5.12}$$

in which τ and β were fitting parameters.

Using the proposed diffusion model and the NMR-MRI experimental data, the free water diffusion coefficients were calculated, and the values are displayed in Fig. 5.8. The results show a common initial plateau for SAP2 and SAP3 in the diffusion coefficient up to about 20% degree of hydration, which corresponds to the time cement gel fractions start to connect [46]. From 20 to 60% degree of hydration, the average free water diffusion coefficient is 5.48×10^{-12} m^2/s and 4.46×10^{-12} m^2/s for SAP2 and SAP3, respectively. SAP3 diffusion coefficient is expected to be smaller than that of SAP2 since SAP3 mix has a lower w/c [32].

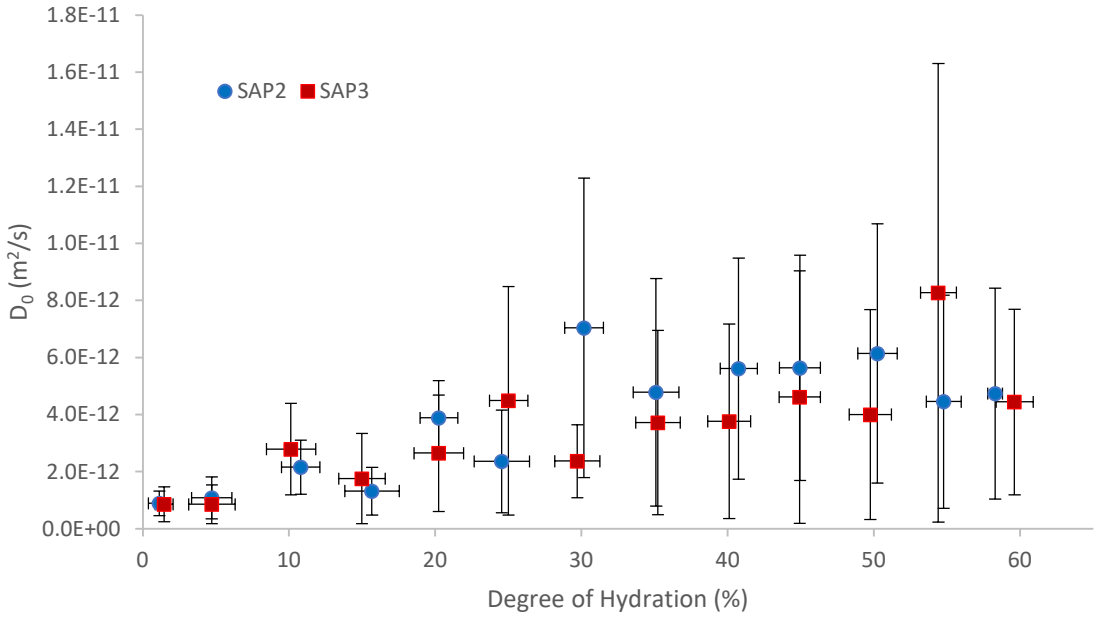

Fig. 5.8 Free water diffusion coefficient

To account for the formation of cement gel and corresponding tortuosity, the effective diffusion coefficients for SAP2 and SAP3 were calculated, and the results are displayed in Fig. 5.9. Similar to the free water diffusion coefficient, there are distinctions in the results before and after the 20% degree of hydration. Before the 20% degree of hydration, the effects of cement gel formation for both SAP2 and SAP3 are negligible as noted for the free water diffusion coefficient and are therefore ignored. After the 20% degree of

hydration, two distinct patterns can be observed for SAP2 and SAP3. As anticipated, SAP3, having a lower w/c, has a smaller effective diffusion coefficient than that of SAP2. The ability of water to flow from the SAP particles to the hydrating cement paste depends on the porosity and tortuosity of the paste. The predicted trends for the effective water diffusion coefficients, shown in Fig. 5.9 by the trend lines, are mathematically represented by Eq. (5.9), where D_w^e is equal to the free water diffusion coefficient multiplied by the tortuosity factor. The results show a good agreement between the two results with an R^2 value of 73% and 74% for SAP2 and SAP3, respectively. These results support the postulation that porosity and tortuosity of the paste are pivotal in quantifying the effective water diffusion coefficient of cement paste.

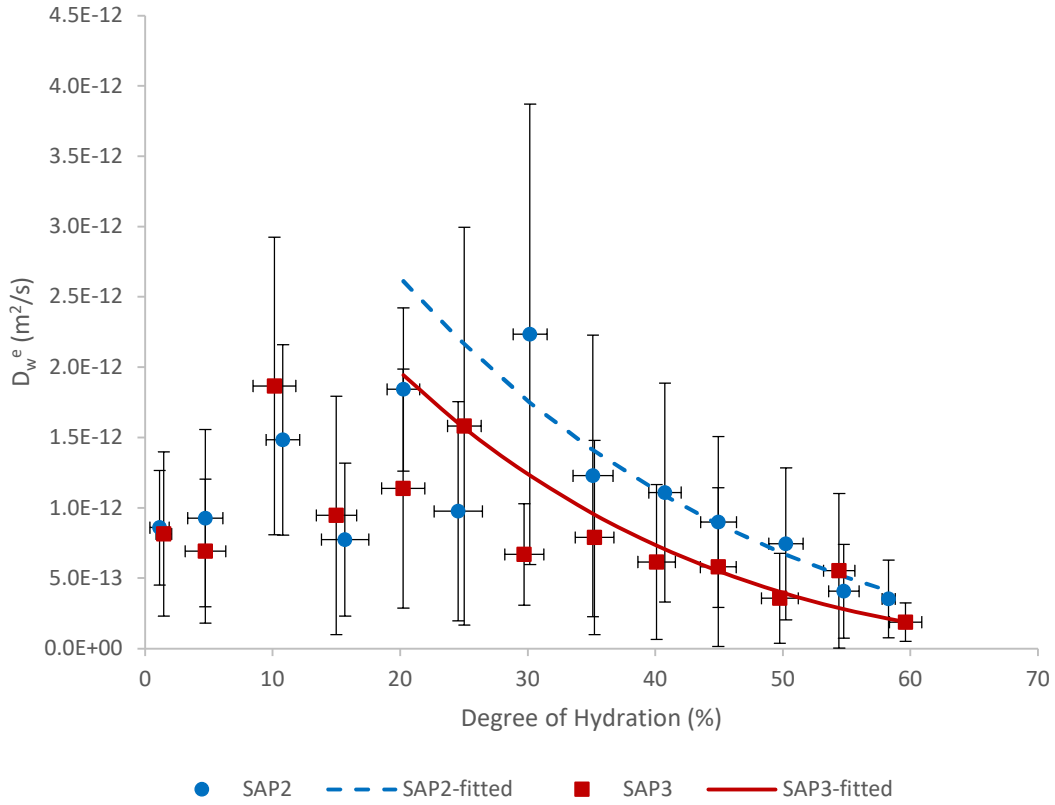

Fig. 5.9 Effective diffusion coefficient

The efficacy of the internal curing to provide water to the paste was calculated using the effective diffusion length, l_d, that was put forward by Friedemann et al. [32], where

$$l_d = \sqrt{D_w^e t} \tag{5.13}$$

where t corresponds to the time from the beginning of the experiment. The results, displayed in Fig. 5.10, reveal that the average effective diffusion length is 0.252 mm and 0.193 mm for SAP2 and SAP3, respectively, after about 8 h which corresponds to about 20% degree of hydration. These values are in the same range of the 0.5 mm protected paste distance observed for LWA [47,48]. The result shows that the SAP2 is more effective in providing water to the cement paste in comparison to SAP3, even though SAP2 has fewer SAP particles. This finding supports Powers' model that there is limit on the amount of water available for internal curing and that limit is governed by the porosity of the paste [8,49].

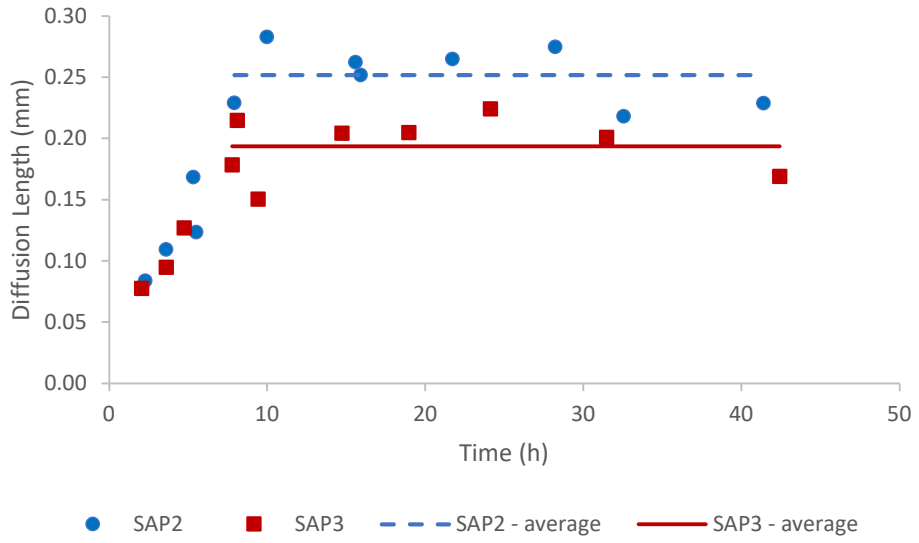

Fig. 5.10 Effective diffusion length

SAP particles tend to agglomerate in cement paste [17,24], therefore increasing the average spacing between the particles. Using the percent agglomeration and corresponding particle spacing reported in Chidiac et al. [17], the consequential effect of agglomeration on the

diffusion of water from SAP was evaluated. Accordingly, SAP2 had an average spacing of 0.78 mm without agglomeration and 0.89 mm when accounting for agglomeration. For SAP3, the average particle spacing was estimated to increase from 0.69 mm to 1.27 mm when accounting for agglomeration. Using the concept of effective diffusion length and the average spacing of the particles without agglomeration, the SAP in mixes SAP2 and SAP3 can provide water to 64% and 58% of the paste around an individual SAP particle, respectively. When accounting for particles agglomeration, the paste volume accessible to SAP water decreases to 57% and 32% for SAP2 and SAP3. The effect of agglomeration is found to be much more significant in the paste with a higher SAP content and lower w/c, where the efficacy of SAP2 is found to decrease by 8% whereas the efficacy of SAP3 decreases by 27%.

5.5 Conclusions

A hybrid model was developed to quantify the effective diffusion coefficient of cement pastes with SAP internal curing by way of NMR-MRI measurements. Accordingly, the following conclusions are drawn for this study:

1. The free water diffusion coefficient, D_o, depends on the w/c once the cement gel fractions start to connect, i.e., after 20% cement degree of hydration.
2. The calculated average D_o for SAP2 and SAP3 is 5.48x10^{-12} m^2/s and 4.46x10^{-12} m^2/s, respectively.
3. The effective water diffusion coefficient, D_w^e, depends on the w/c, cement gel volume fraction, and tortuosity once the cement gel fractions start to connect, i.e., after 20% cement degree of hydration.
4. The equation developed for SAP is given by $D_w^e = f_\tau D_o = [3(1 - V_s)^2/(3 - V_s)]D_o$.
5. Values of D_w^e confirm that the water ability to flow from the SAP particles to the cement paste depends on the porosity and tortuosity of the paste.
6. The SAP water diffusion length can be calculated from D_w^e. The average diffusion length of IC water for SAP2 and SAP3 was 0.252 mm and 0.193 mm, respectively.

7. SAP2 is more effective in providing IC water to the cement paste which supports Powers' model that the amount of water available for internal curing is limited by the porosity of the paste.
8. Particle agglomeration decreased the paste volume accessible to SAP water from 64% to 57% for SAP2 and from 58% to 32% for SAP3.

It should be noted that the experimental data and conclusions are specific to the type and size of SAP, as well to the cement paste mix composition.

Acknowledgements

The authors would like to thank NSERC for funding this research. The authors wish to express their gratitude to S.A. Krachkovskiy & G.R. Goward from the McMaster University Department of Chemistry and Chemical Biology for their assistance with the NMR-MRI experiments.

References

[1] L. Wu, N. Farzadnia, C. Shi, Z. Zhang, H. Wang, Autogenous shrinkage of high performance concrete: A review, Constr. Build. Mater. 149 (2017) 62–75. doi:10.1016/j.conbuildmat.2017.05.064.

[2] E. Tazawa, S. Miyazawa, Influence of cement and admixture on autogenous shrinkage of cement paste, Cem. Concr. Res. 25 (1995) 281–287. doi:10.1016/0008-8846(95)00010-0.

[3] R. Henkensiefken, D. Bentz, T. Nantung, J. Weiss, Volume change and cracking in internally cured mixtures made with saturated lightweight aggregate under sealed and unsealed conditions, Cem. Concr. Compos. 31 (2009) 427–437. doi:10.1016/j.cemconcomp.2009.04.003.

[4] D.M. Al Saffar, A.J.K. Al Saad, B.A. Tayeh, Effect of internal curing on behavior of high performance concrete: An overview, Case Stud. Constr. Mater. 10 (2019) e00229. doi:10.1016/j.cscm.2019.e00229.

[5] D.P. Bentz, W.J. Weiss, Internal Curing : A 2010 State-of-the- Art Review, Gaithersburg: US Department of Commerce. National Institute of Standards and Technology, 2011.

[6] P. Lura, D.P. Bentz, D.A. Lange, K. Kovler, A. Bentur, Pumice aggregates for internal water curing, in: Int. RILEM Symp. Concr. Sci. Eng. A Tribut. to Arnon Bentur, 2004: pp. 137–151.

[7] S. Zhutovsky, K. Kovler, Effect of internal curing on durability-related properties of high performance concrete, Cem. Concr. Res. 42 (2012) 20–26. doi:10.1016/j.cemconres.2011.07.012.

[8] O.M. Jensen, P.F. Hansen, Water-entrained cement-based materials: I. Principles and theoretical background, Cem. Concr. Res. 31 (2001) 647–654. doi:10.1016/S0008-8846(01)00463-X.

[9] M. Geiker, D. Bentz, O. Jensen, Mitigating autogenous shrinkage by internal curing, ACI Spec. Publ. (2004) 143–54.

[10] D.P. Bentz, P. Lura, J.W. Roberts, Mixture proportioning for internal curing, Concr. Int. 27 (2005) 35–40.

[11] B. Akcay, M.A. Tasdemir, Optimisation of using lightweight aggregates in mitigating autogenous deformation of concrete, Constr. Build. Mater. 23 (2009) 353–363. doi:10.1016/j.conbuildmat.2007.11.015.

[12] R. Henkensiefken, T. Nantung, J. Weiss, Saturated Lightweight Aggregate for Internal Curing in Low w/c Mixtures: Monitoring Water Movement Using X-ray Absorption, Strain. 47 (2011) e432–e441. doi:10.1111/j.1475-1305.2009.00626.x.

[13] M. Golias, J. Castro, J. Weiss, The influence of the initial moisture content of lightweight aggregate on internal curing, Constr. Build. Mater. 35 (2012) 52–62. doi:10.1016/j.conbuildmat.2012.02.074.

[14] J.T. Kevern, Q.C. Nowasell, Internal curing of pervious concrete using lightweight aggregates, Constr. Build. Mater. 161 (2018) 229–235. doi:10.1016/j.conbuildmat.2017.11.055.

[15] A. Paul, S. Murgadas, J. Delpiano, P.A. Moreno-Casas, M. Walczak, M. Lopez, The role of moisture transport mechanisms on the performance of lightweight aggregates in internal curing, Constr. Build. Mater. 268 (2021) 121191. doi:10.1016/j.conbuildmat.2020.121191.

[16] J. Liu, Z. Ou, J. Mo, Y. Wang, H. Wu, The effect of SCMs and SAP on the autogenous shrinkage and hydration process of RPC, Constr. Build. Mater. 155 (2017) 239–249. doi:10.1016/j.conbuildmat.2017.08.061.

[17] S.E. Chidiac, S.N. Mihaljevic, S.A. Krachkovskiy, G.R. Goward, Efficiency measure of SAP as internal curing for cement using NMR & MRI, Constr. Build. Mater. 278 (2021) 122365. doi:10.1016/j.conbuildmat.2021.122365.

[18] J. Justs, M. Wyrzykowski, F. Winnefeld, D. Bajare, P. Lura, Influence of superabsorbent polymers on hydration of cement pastes with low water-to-binder ratio, J. Therm. Anal. Calorim. 115 (2014) 425–432. doi:10.1007/s10973-013-3359-x.

[19] J. Justs, M. Wyrzykowski, D. Bajare, P. Lura, Internal curing by superabsorbent polymers in ultra-high performance concrete, Cem. Concr. Res. 76 (2015) 82–90. doi:10.1016/j.cemconres.2015.05.005.

[20] L. Montanari, P. Suraneni, M.T. Chang, C. Villani, J. Weiss, Absorption and Desorption of Superabsorbent Polymers for Use in Internally Cured Concrete, Adv. Civ. Eng. Mater. 7 (2018) 20180008. doi:10.1520/ACEM20180008.

[21] S.E. Chidiac, S.N. Mihaljevic, S.A. Krachkovskiy, G.R. Goward, Characterizing the effect of superabsorbent polymer content on internal curing process of cement paste using calorimetry and nuclear magnetic resonance methods, J. Therm. Anal. Calorim. (2020) 1–13. doi:10.1007/s10973-020-09754-0.

[22] L. Montanari, P. Suraneni, W.J. Weiss, Accounting for Water Stored in Superabsorbent Polymers in Increasing the Degree of Hydration and Reducing the Shrinkage of Internally Cured Cementitious Mixtures, Adv. Civ. Eng. Mater. 6 (2017) 20170098. doi:10.1520/ACEM20170098.

[23] S.-H.H. Kang, S.-G.G. Hong, J. Moon, Absorption kinetics of superabsorbent polymers (SAP) in various cement-based solutions, Cem. Concr. Res. 97 (2017) 73–83. doi:10.1016/j.cemconres.2017.03.009.

[24] S. Mönnig, Superabsorbing additions in concrete: applications, modelling and comparison of different internal water sources, Institut für Werkstoffe im Bauwesen der Universität Stuttgart, 2009.

[25] M. Wyrzykowski, P. Lura, F. Pesavento, D. Gawin, Modeling of Water Migration during Internal Curing with Superabsorbent Polymers, J. Mater. Civ. Eng. 24 (2012) 1006–1016. doi:10.1061/(ASCE)MT.1943-5533.0000448.

[26] D. Snoeck, L. Pel, N. De Belie, The water kinetics of superabsorbent polymers during cement hydration and internal curing visualized and studied by NMR, Sci. Rep. 7 (2017) 1–14. doi:10.1038/s41598-017-10306-0.

[27] Q. Zhu, C.W. Barney, K.A. Erk, Effect of ionic crosslinking on the swelling and mechanical response of model superabsorbent polymer hydrogels for internally cured concrete, Mater. Struct. 48 (2015) 2261–2276. doi:10.1617/s11527-014-0308-5.

[28] P. Lura, K. Friedemann, F. Stallmach, S. Mönnig, M. Wyrzykowski, L.P. Esteves, Kinetics of Water Migration in Cement-Based Systems Containing Superabsobent Polymers, in: Appl. Super Absorbent Polym. Concr. Constr., Springer Netherlands, Dordrecht, 2012: pp. 21–37. doi:10.1007/978-94-007-2733-5_4.

[29] C. Schröfl, V. Mechtcherine, M. Gorges, Relation between the molecular structure and the efficiency of superabsorbent polymers (SAP) as concrete admixture to mitigate autogenous shrinkage, Cem. Concr. Res. 42 (2012) 865–873. doi:10.1016/j.cemconres.2012.03.011.

[30] O.M. Jensen, P.F. Hansen, Water-entrained cement-based materials: II. Experimental observations, Cem. Concr. Res. 32 (2002) 973–978. doi:10.1016/S0008-8846(02)00737-8.

[31] L.P. Esteves, On the absorption kinetics of superabsorbent polymers, in: Int. RILEM Conf. Use Superabsorbent Polym. Other New Addit. Concr. 15-18 August, RILEM publications SARL, 2010: pp. 77–84.

[32] K. Friedemann, F. Stallmach, J. Kärger, NMR diffusion and relaxation studies during cement hydration-A non-destructive approach for clarification of the mechanism of internal post curing of cementitious materials, Cem. Concr. Res. 36 (2006) 817–826. doi:10.1016/j.cemconres.2005.12.007.

[33] N. Nestle, A. Kühn, K. Friedemann, C. Horch, F. Stallmach, G. Herth, Water balance and pore structure development in cementitious materials in internal curing with modified superabsorbent polymer studied by NMR, Microporous Mesoporous Mater. 125 (2009) 51–57. doi:10.1016/j.micromeso.2009.02.024.

[34] J. Yang, Z. Sun, Y. Zhao, Y. Ji, B. Li, The Water Absorption-release of Superabsorbent Polymers in Fresh Cement Paste: An NMR Study, J. Adv. Concr. Technol. 18 (2020) 139–145. doi:10.3151/jact.18.139.

[35] Z. Hu, M. Wyrzykowski, K. Scrivener, P. Lura, A novel method to predict internal relative humidity in cementitious materials by 1 H NMR, Cem. Concr. Res. 104 (2018) 80–93. doi:10.1016/j.cemconres.2017.11.001.

[36] M. Wyrzykowski, A.M. Gajewicz-Jaromin, P.J. McDonald, D.J. Dunstan, K.L. Scrivener, P. Lura, Water redistribution–microdiffusion in cement paste under mechanical loading evidenced by 1 H NMR, J. Phys. Chem. C. 123 (2019) 16153–16163. doi:10.1021/acs.jpcc.9b02436.

[37] M. Fourmentin, P. Faure, S. Rodts, U. Peter, D. Lesueur, D. Daviller, P. Coussot, NMR observation of water transfer between a cement paste and a porous medium, Cem. Concr. Res. 95 (2017) 56–64. doi:10.1016/j.cemconres.2017.02.027.

[38] B.J. Balcom, J.C. Barrita, C. Choi, S.D. Beyea, D.J. Goodyear, T.W. Bremner, Single-point Magnetic Resonance Imaging (MRI) of cement based materials, Mater. Struct. Constr. 36 (2003) 166–182. doi:10.1617/14024.

[39] R. Cook, D. Malkus, M. Plesha, Concepts and applications of finite element analysis, Wiley, New York :, 1989.

[40] I. Odler, M. Rößler, Investigations on the relationship between porosity, structure and strength of hydrated Portland cement pastes. II. Effect of pore structure and of degree of hydration, Cem. Concr. Res. 15 (1985) 401–410. doi:10.1016/0008-8846(85)90113-9.

[41] K.P. Saripalli, R.J. Serne, P.D. Meyer, B.P. McGrail, Prediction of Diffusion Coefficients in Porous Media Using Tortuosity Factors Based on Interfacial Areas, Ground Water. 40 (2002) 346–352. doi:10.1111/j.1745-6584.2002.tb02512.x.

[42] S.E.E. Chidiac, M. Shafikhani, Phenomenological model for quantifying concrete chloride diffusion coefficient, Constr. Build. Mater. 224 (2019) 773–784. doi:10.1016/j.conbuildmat.2019.07.006.

[43] J. Bear, Dynamics of Fluids in Porous Media, Soil Sci. 120 (1975) 162–163. doi:10.1097/00010694-197508000-00022.

[44] Canadian Standards Association, Cementitious materials compendium, CSA Group, Toronto, ON, 2018.

[45] L.P. Esteves, Recommended method for measurement of absorbency of superabsorbent polymers in cement-based materials, Mater. Struct. 48 (2015) 2397–2401. doi:10.1617/s11527-014-0324-5.

[46] D.P. Bentz, E.J. Garboczi, Percolation of phases in a three-dimensional cement paste microstructural model, Cem. Concr. Res. 21 (1991) 325–344. doi:10.1016/0008-8846(91)90014-9.

[47] M. Li, J. Liu, Q. Tian, Y. Wang, W. Xu, Efficacy of internal curing combined with expansive agent in mitigating shrinkage deformation of concrete under variable temperature condition, Constr. Build. Mater. 145 (2017) 354–360. doi:10.1016/j.conbuildmat.2017.04.021.

[48] D.P. Bentz, K.A. Snyder, Protected paste volume in concrete, Cem. Concr. Res. 29 (1999) 1863–1867. doi:10.1016/S0008-8846(99)00178-7.

[49] T.C. Powers, A discussion of cement hydration in relation to the curing of concrete, in: Proc. Twenty-Seventh Annu. Meet. Highw. Res. Board, Highway Research Board, Washington, D.C., 1948: pp. 178–188.